

UCSF

UC San Francisco Electronic Theses and Dissertations

Title

Structure and Assembly Properties of a Conserved C-terminal Domain in Kv7 Channels

Permalink

<https://escholarship.org/uc/item/31b0m3d2>

Author

Howard, Rebecca Joy

Publication Date

2008-01-07

Peer reviewed|Thesis/dissertation

**Structure and Assembly Properties of a Conserved C-terminal
Domain in Kv7 Channels**

by

Rebecca Joy Howard

DISSERTATION

Submitted in partial satisfaction of the requirements for the degree of

DOCTOR OF PHILOSOPHY

in

CHEMISTRY AND CHEMICAL BIOLOGY

in the

GRADUATE DIVISION

of the

ACKNOWLEDGEMENTS

The work in this thesis would not have been possible without my PhD advisor, Professor Daniel L. Minor, Jr., who has been generous with his time and attention beyond the scale of most major professors since the day I began working as a rotation student in his lab. In addition to providing access to unparalleled technical resources, working in Professor Minor's lab has given me the opportunity to participate in group meetings, journal clubs, book clubs, and lab interactions that have been consistently challenging, insightful, and inspirational. Professor Minor has been thoroughly dedicated to my personal progress in his lab, giving me detailed advice on successful grant applications and manuscript submissions. He has entrusted me with equipment, techniques, and student mentorship, providing me with invaluable experience, opportunities to collaborate and publish with members of other labs, and lasting confidence to move into the next stage of my science career.

I owe significant thanks to my faculty mentors at the University of California, San Francisco. Professor Lily Jan served on both my PhD candidacy qualification committee and my thesis committee, and her commanding expertise in potassium channel molecular biology and physiology provided invaluable insight and guidance for my own work. Professor David Julius hosted me in his lab as a rotation student in addition to serving on both my PhD committees; his generosity with lab resources and insight into other areas of ion channel research shaped my technical training and future career interests. Furthermore, the close relationships between the members of my lab and those of Professors Jan and Julius have been consistently informative and enjoyable. I am grateful to Professor Robert Stroud, whose reputation I revered prior to entering graduate school, for serving on my PhD candidacy committee, providing much of my

theoretical background in protein crystallography, and serving as a distinguished role model in science. Professor Pam England also hosted me as a rotation student and served on my candidacy committee, and gave me more focused attention and advice in those roles than any other mentor in my graduate experience. My annual meetings with my academic advisor, Professor Sue Miller, were also informative and supportive.

I owe a deep debt of gratitude to Chris Olson, Graduate Program Administrator for Chemistry and Chemical Biology. Chris has taken every opportunity to nurture and support each graduate student in the program well beyond the call of duty. She has counseled me through academic and personal challenges and celebrated every milestone in my graduate career path. Her patient work for the program and the individuals enrolled in it goes largely uncredited, yet most of us can trace what success we've enjoyed directly back to her. I am also grateful to Professor Charley Craik, my Graduate Program Director, for bringing me into the program (even though I applied to a different one!) and believing in my potential throughout.

My work in Professor Minor's lab has been supported and accompanied by a remarkable group of fellow lab members. I owe an incalculable debt to Camellia Asgarian, Joanne Chan, Joy Chen, May Cho, Libby Cooley, Courtney Domigan, Karl Duderstadt, Yui Fujiwara, Justus Hammon, Yuni Jung, Eun Young Kim, Sebila Kratovac, Angie Marson, Madina Mohammedi, Simone Mueller, Dinesh Palanivelu, Christine Rumpf, Lara Tully, Serenity Wang, and every member of the Minor lab, past and present, for creating and maintaining a positive and stimulating environment. In particular, former postdoctoral fellow Filip van Petegem and research technician Raika Pancaroglu were, and continue to be, infinitely patient and generous advisors, colleagues, and friends. Former technician Franck Chatelain established the social and professional atmosphere

of the lab and has been unflinching in his technical and personal encouragement. My lab manager and benchmate Kim Clark has been a constant resource, confidant, and collaborator since I began as a rotation student; I owe both my publication and my enjoyment of more than 5 years of lab work to her companionship. Postdoc Marta Pioletti has been an indomitable scientific and personal resource ever since I joined the lab. Postdocs Qiang Xu and Wes McDermott have accompanied my work on Kv7 channels; I wish them success in their coming ventures. I am grateful to Chris Bohlen and Sam Pfaff for being gracious and attentive advisees. Finally, postdoc Felix Findeisen is simply one of the dearest men in my life, and has taught me more about crystallography, electrophysiology, classical music, and social grace than any other single person.

I am grateful to the many members of other labs who have made UCSF a remarkably rich place to work, learn and live. In particular, Pam Tsuruda was my partner in studying coiled coils and ion channels, down to the level of learning specialized techniques and battling specific challenges; her spirit and capability are unstoppable. Ben Myers was patient and generous in teaching me almost all I know about cell culture, enabling me to set up our own cell culture facility. Diana Bautista, Zach Newby, and Jan Siemens have been colleagues of the highest caliber in my collaborations with the Julius lab. James Holton, Beamline Scientist at the Advanced Light Source, is an unmatched technical and scientific resource, and provided crucial input to my own education and publication. Danny Hatters was an energetic and well-informed colleague in learning the “ins and outs” of analytical ultracentrifugation. Beyond those mentioned here, it is to a phenomenal community of UCSF scholars that I owe the breadth as well as the depth of my training.

My graduate experience has also benefited significantly from career mentors outside the lab, to whom I am deeply thankful. I have been fortunate to participate in the founding and Executive Board of the SF Association for Women in Science; in particular, fellow AWIS members Edi Alvarez, Paola Dozzo, Melissa Rice, Joleen White, and Melissa Woodrow have been role models of unmatched professionalism and dedication. I have enjoyed sustaining support from my peers in the former Women in Life Sciences student organization, particularly the talented and insightful members of my Group, Jennifer Garrison, Temina Madon, Keiko Petrosky, Jennifer Shen, and above all Dani Behonick, who has also been a dearly inspiring friend. Morgan Royce-Tolland has been my most valued combination of scientific colleague, activity partner, and companion. Finally, my longtime advocate and friend Nicki Taylor Moore has taken an hour out of every week for the past two years to keep me to my personal and career goals; her positivity and moral constancy continue to motivate and inspire.

I want to recognize the patience and support of those individuals who have shared their homes with me through the irregular schedules and moods of my graduate career. I am especially grateful to Andy Shirey, Maxime Beauchemin, and Shannon Stevens, who have withstood the last two years with friendly tolerance. Thanks also to past roommates Matt Gray, Laura McVittie, Kevin Packard, Wendy Ostroff, Rob Genova, Hannah Lingrell, Reid Spice, Ron Ricci, Charlie Sheldon, Ryan Manley, Steve Steele, and Nura and Pietro Belluschi for making it a continually interesting time. Though not officially roommates, the individuals that have made my San Francisco experience memorable and unique deserve special thanks, especially the ever-inspiring Quintin Mecke, infinitely spirited Megan Hall, Damon Magnuski, Marie McCarthy, Geoff Sturm, and other part-time residents of 1091 York St. I am grateful for my lasting

relationships with members of the Pomona College community, for whom I feel indissoluble love and respect, especially Marissa Carlson, Anita Kapoor, Joanna Takagi, and Matthew Zay; my mentors, especially Professors Donna Di Grazia, Daniel O’Leary, and Cynthia Selassie; and my former sponsees, especially Anna Bell-Hibbs, Jessica Drenk, Emily Curran, and Vanessa Tamas. Thanks to the members of the SF Concert Chorale and Creative Voices, who provided nourishing expressive outlets from my earliest days in San Francisco. Thanks also to the members of the Lorax Lounge for taking expressive outlets to the next level. And thanks always to Rachael Feigenbaum, whose jovial motivation, friendly instigation, and intelligent celebration of all our community has to offer have transformed my experience of science, art, and human possibility.

Finally, I am uniquely fortunate in the family members who have supported my scientific and personal goals unquestioningly for as long as I can remember. My mother and father are striking exceptions to the PhD student rule that “my parents don’t know (or care) what I do”; on the contrary, they are insightful and well-informed professionals in their own rights, yet have taken the time and attention to follow every step of my training with love and encouragement. Thanks to my sister Faith for modeling honesty and creativity in all our lives. Thanks to my Uncle John for taking me under his wing in the strange new world of San Francisco and showing me how to live it better. Thanks to my Grandfather Jack and my Aunt Melissa for their long-distance support, and to my Grandmother Georgia, who I wish could have seen me graduate. I am grateful to my new family, especially Nick Gray and Veronica and Dieter Soell, for their unquestioning hospitality. Not every graduate student has one, let alone two, fathers to provide critical and experienced input on her work. My confidence and enthusiasm for engaging future

scientific challenges stem in no small part from the consummate support my family brings close to hand.

To my fiancée Oliver, you know I am better for being with you, and that I owe almost all I have enjoyed and accomplished to your undemanding love. I look forward to taking our next steps together.

CO-AUTHOR ACKNOWLEDGEMENT

Daniel L. Minor, Jr., a co-author for Chapter 2, directed and supervised the research that forms the basis for this dissertation. Kimberly A. Clark expressed and purified some of the HMT fusion proteins used in Figures 4 and 5 of Chapter 2. James M. Holton assisted with crystallographic data collection and generation of molecular replacement search models to solve the structure in Figure 1 of Chapter 2. Rebecca Howard performed all other experiments and analyses. This work is comparable to work for a standard thesis awarded by the University of California, San Francisco.

- Daniel L. Minor, Jr.

ABSTRACT

Potassium (K^+) channels are membrane-embedded proteins that selectively pass K^+ ions in or out of cells in response to a variety of signals, such as membrane potential changes or binding of ligands. In an excitable cell, such as a neuron or cardiac muscle cell, delayed rectifier voltage-gated K^+ channels respond to changes in membrane potential to restore the cell membrane to its resting state after an action potential.

In vertebrates, voltage-gated K^+ (K_v) channels are tetramers of similar or identical subunits arranged around a central conducting pore. While these channels are primarily gated by membrane potential, their biophysical properties are set by the type of subunits in each tetramer and by interactions with other effector molecules, such as membrane phospholipids, calcium-binding proteins, kinases, and scaffolding proteins. In some cases, discrete intracellular domains control the specific assembly of pore-forming and accessory proteins. However, the molecular mechanisms that direct specific assembly of this wide range of components into a functional K channel complex are incompletely understood.

Chapter 2 of this thesis establishes the atomic-resolution structure of one such assembly domain from a K_v7 family channel ($K_v7.4$). This study suggests the structural basis for specific assembly properties and binding of scaffolding proteins by other members of the K_v7 channel family. Additional studies in Chapter 3 explore implications of the $K_v7.4$ assembly domain structure for oligomerization in other subtypes. The biochemical and functional effects of K_v7 mutations designed to disrupt or enhance assembly domain oligomerization further support the critical role for this domain in specific assembly of these channels.

TABLE OF CONTENTS

Title page	i
Acknowledgements	iii
Co-Author Acknowledgement	viii
Abstract	ix
Table of Contents	x
List of Figures	xii
List of Tables	xiii

CHAPTER I. INTRODUCTION TO Kv7 CHANNEL ASSEMBLY

A. Structure and Assembly of Voltage-Gated K ⁺ Channels	
i. A variety of selective ion channels regulates membrane potential and disease in excitable cells.	1
ii. K ⁺ channels share structural features critical to specific assembly and function.	5
iii. The T1 Domain is a model K channel assembly module.	9
iv. Coiled coils are alternative assembly motifs that may drive tetramerization in K ⁺ channels.	11
v. Coiled coils can determine specific assembly properties.	16
B. Structure and Assembly of Kv7 Channels	22
i. Unique structural and functional profiles facilitate critical physiological roles of Kv7 channels.	23
ii. Pharmacological tools aid in research and therapy of Kv7 channels.	26
iii. A variety of factors regulates trafficking and modulation of Kv7 channels.	29
iv. Kv7 channels exhibit specific assembly properties mediated by C-terminal modular domains.	34
v. The Kv7 A-domain consists of distinct subdomains with different structural and functional properties.	38
C. References	43
D. Figures	60

CHAPTER 2. STRUCTURAL INSIGHT INTO KCNQ (Kv7) CHANNEL ASSEMBLY AND CHANNELOPATHY

A. Summary	64
B. Introduction	64
C. Results	
i. Structure of the Kv7 Assembly Specificity Domain	67
ii. Kv7.4 is a Stable Tetramer in Solution	70
iii. Biochemical and Structural Comparisons of Kv7 A-Domain Tails	72
iv. Structural Insight into Cardiac Arrhythmia Mutations	74
D. Discussion	75
i. Kv7 A-Domain Tails and Assembly Specificity	77
ii. Structural Consequences for Kv7.1 Arrhythmia Mutations and Implications for Coiled Coils as Sites of Ion Channel Regulatory Complex Assembly	79
E. Experimental Procedures	
i. Protein Cloning, Expression, and Purification	81
ii. Crystallization and Data Collection	83

iii. Structure Determination	83
iv. CD Spectroscopy	84
v. Size Exclusion Chromatography.....	85
vi. Equilibrium Sedimentation.....	86
F. Acknowledgements	86
G. References	87
H. Figures	92

CHAPTER 3. CRITICAL AMINO ACID INTERACTIONS IN Kv7 COILED-COIL ASSEMBLY

A. Results	
i. A-domain Tails from different subtypes have varying propensities to form coiled-coil oligomers.	102
ii. Mutations at predicted interfaces modify oligomerization of Kv7 coiled coils.	104
iii. Long QT syndrome mutations do not abolish oligomerization of Kv7.1 A-domain Tails.	108
iv. Mutations that promote oligomerization also increase currents of chimeric channels containing Kv7.3 coiled coils.	110
B. Discussion	112
C. Experimental Procedures	
i. Sequence Analysis	119
ii. DNA Constructs	119
iii. Protein Expression and Lysis	120
iv. HMT Fusion Protein Purification	121
v. Size Exclusion Chromatography.....	121
vi. Equilibrium Sedimentation.....	122
vii. Affinity Copurification.....	122
viii. Electrophysiology	123
D. References	123
E. Figures	126

CHAPTER 4. CONCLUSIONS AND FUTURE DIRECTIONS

A. The Kv7 A-domain Tail in Context	133
B. References	135

LIST OF FIGURES

CHAPTER 1

<i>Figure 1. Architecture of voltage-gated K⁺ channels</i>	60
<i>Figure 2. Geometric properties of coiled coils</i>	61
<i>Figure 3. Architecture of Kv7 channels</i>	62

CHAPTER 2

<i>Figure 1. Structure of the Kv7 Coiled-Coil Assembly Domain</i>	92
<i>Figure 2. Hydrophobic and Electrostatic Contacts in the Kv7.4 Coiled-Coil Domain</i>	94
<i>Figure 3. Solution Properties of the Kv7.4 A-Domain Tail</i>	95
<i>Figure 4. Comparing Interactions in Alternative Kv7 Subtypes</i>	96
<i>Figure 5. Mapping of Long-QT Syndrome Mutations</i>	98
<i>Figure 6. Model of a Kv7 Channel Regulatory Complex</i>	99

CHAPTER 3

<i>Figure 1. Assembly Properties of Kv7 A-Domain Tails</i>	126
<i>Figure 2. Effect of Predicted Interface Mutations on Kv7 A-Domain Tail Oligomerization</i> ..	127
<i>Figure 3. Sedimentation Equilibrium of Kv7.1 Wild-Type and Interface Mutant Proteins</i> ..	128
<i>Figure 4. Effect of Interface Mutations on Pull-Down of Isolated Kv7.1 A-Domain Tails</i> ..	129
<i>Figure 5. Effect of Kv7.1 LQTS Mutations on A-domain Tail Oligomerization</i>	130
<i>Figure 6. Sedimentation Equilibrium of Kv7.1 A-Domain Tails with LQTS Mutations</i>	131
<i>Figure 7. Effect of Interface Mutations on Kv7.2, Kv7.3, and Kv7.2_{3T} Chimera Currents</i> ..	132

CHAPTER 4

No Figures

LIST OF TABLES

CHAPTER 1

No Tables

CHAPTER 2

Table 1. Data Collection and Refinement Statistics 100

Table 2. Coiled-Coil Parameters 101

CHAPTER 3

No Tables

CHAPTER 4

No Tables

CHAPTER I

INTRODUCTION TO Kv7 CHANNEL ASSEMBLY

A. Structure and Assembly of Voltage-Gated K⁺ Channels

i. A variety of selective ion channels regulates membrane potential and disease in excitable cells.

The evolution of diverse, selective, precisely regulated ion channels has allowed organisms from bacteria to humans to harness the power of electrical signaling with exquisite control. To appreciate the significance of these molecules, consider that the lipid membrane surrounding every cell regulates, among other things, the electrochemical characteristics of the intracellular environment. A polar solute, such as a charged ion, faces a major energetic obstacle in crossing the bilayer: it must shed its hydration shell of water molecules in favor of the hydrocarbon tails of the bilayer core. Passage of a hydrated ion is similarly disfavored due to the energetic barrier to burying polar moieties, including water, in the hydrophobic membrane core. The exchange of polar for nonpolar solvation is so thermodynamically unfavorable that membranes made purely of phospholipids are virtually impermeable to charged ions (Parsegian, 1969).

Cells have capitalized on the restricted permeability of lipid membranes by evolving membrane-embedded proteins that allow selected charged particles to pass. Ion exchange proteins drive ion transfer either actively by the hydrolysis of ATP, or passively in response to electrochemical gradients. If the passage of ions results in uneven charge distribution, it creates a potential difference across the membrane. Specialized cell types, called *excitable cells*, use a variety of ion-conducting proteins to modulate and propagate potentials across their membranes, allowing them to conduct information several orders of magnitude faster than would be possible via chemical

signals alone. Most excitable cells—such as neuronal, cardiac, and skeletal muscle cells in humans—maintain precise negative resting potentials across their membranes. This resting state is primarily established by membrane-integral Na^+/K^+ ATPases, which harness energy from the hydrolysis of ATP to transport out Na^+ ions and pump in K^+ ions. For each molecule of ATP, exchangers move 3 Na^+ ions out of and 2 K^+ ions into the cell. This uneven charge exchange, along with the slow passive diffusion of K^+ ions through K^+ leak channels, creates a negative resting potential near the equilibrium potential of K^+ , around -50 to -90 mV (Lieberman and Skulachev, 1970).

Most dynamic signaling events in excitable cells arise from the interplay between passive, selective, voltage-sensitive ion exchange proteins called ion channels. The classic example of controlled electrical signaling is the *action potential*, an electrical current that propagates rapidly along a neuronal axon or the surface of a muscle or glandular cell. In a single cell, an action potential is recorded as a rapid spike and recovery of membrane potential mediated by voltage-gated ion channels. When a local excitatory stimulus depolarizes the cell membrane above a threshold voltage, nearby channels selective for Na^+ activate rapidly. Sodium flows into the cell down its electrochemical gradient. This process further depolarizes the membrane, causing more Na^+ channels to activate; the inward flow of positive ions rapidly overtakes the outward flow through K^+ leak channels, establishing a positive membrane potential around +50 mV. As membrane potential peaks, the Na^+ channels begin to inactivate in a time-dependent manner. Delayed-rectifier K^+ channels also respond to depolarization, but only after a delay, such that K^+ begins to flow just as Na^+ flow ceases. Due to the positive membrane potential and the high intracellular concentration of K^+ , K^+ flows out of the cell until the equilibrium potential for K^+ is re-established. Inactivation of voltage-

gated Na^+ channels combined with the slow responsiveness of delayed rectifier K^+ channels leads to a hyperpolarization of the cell, called the undershoot. After a brief refractory period, active transport by the Na^+/K^+ ATPase restores the membrane to its initial resting potential (Baranauskas, 2007).

Of course, this simple schema describes only a fraction of the voltage-sensitive ion transport events that influence electrical signaling in an excitable cell. For example, in a cardiac myocyte action potential, the initial influx of Na^+ ions (I_{Na}) during depolarization is followed by a transient outward current carried by K^+ channels (I_{to1} , passing K^+ ions out) and anion channels (I_{to2} , passing Cl^- ions in). These channels inactivate long before repolarizing the cell membrane; at this point, Ca^{2+} influx ($I_{\text{Ca(L)}}$) through voltage-gated Ca^{2+} channels begins to predominate, while another species of delayed rectifier K^+ channels maintains the membrane potential by passing K^+ ions out (I_{Ks}). When the Ca^{2+} channels inactivate, K^+ channels return the membrane to its resting potential (I_{Ks} , I_{Kr} , I_{Kl}) (Nerbonne and Kass, 2005). A variety of other currents mediate both excitatory and inhibitory variations in membrane potential. For example, stimulation of sensory transduction channels evokes adaptive, graded receptor potentials (Hille, 2001). Conversely, sub-threshold depolarizations in neurons elicit inhibitory M-currents that stabilize membrane potentials and prevent overexcitability (Cooper and Jan, 2003). In sum, a wide range of ion channels mediates an equal range of functions to control membrane potential precisely.

The critical role of ion channels in normal physiology is underscored by a growing catalog of channelopathies, that is, disorders arising from mutations in ion channel genes. Mutations in over 60 ion channels have been linked to human disease. In many cases, even minor gain-of-function mutations in Na^+ channels or loss-of-function

mutations in K^+ channels induce hyperexcitability, causing epilepsy in neuronal channels, arrhythmias in cardiac channels, or contractile disorders in skeletal muscle channels.

The inverse—diminished Na^+ or enhanced K^+ channel function—can also cause disease, generally due to reduced excitability. Channelopathies are not restricted to the brain, heart, and skeletal muscle: mutations in epithelial channels affect salt and water balance in various tissues, including the inner ear, kidneys, and airways. Intracellular ion channel mutations may severely affect pH or other ion gradients in organelles, including synaptic vesicles, mitochondria, and the endoplasmic reticulum (ER) (Ashcroft, 2006).

The impact of ion channel mutations on health may be minor to severe. In some cases, disease mutations affect the gating or conductance of a channel: channels are present but respond inappropriately to stimuli, leading to disease. More often, disease mutations cause defects in synthesis or trafficking of channels to the cell surface; the remaining channels function properly, but the overall response of the cell is decreased. In recessive channelopathies, one mutant copy of an ion channel gene can be compensated by the presence of a wild-type copy from the other parent. This inherent redundancy may arise from the multimeric nature of many ion channels, especially K^+ channels, which are usually tetramers of identical or similar gene products (MacKinnon, 1991). If a binding site in one subunit is disrupted by mutation, other subunits may be able to compensate. In dominant channelopathies, even one mutant channel gene is sufficient to disrupt normal function. However, since heterozygous individuals usually retain a small population of wild-type channels, dominant channelopathies are often less severe than recessive forms. The severity of a channelopathy is related to the multimeric state of the channel it affects, and the ability of normal subunits to compensate for mutant binding partners (Ashcroft, 2006).

ii. K^+ channels share structural features critical to specific assembly and function.

Due to their prominence in maintaining membrane potential and recovering the cell from excitation, K^+ channels have been major targets of functional and structural study. This field is made both richer and more challenging by the remarkable diversity of K^+ channels. Channels selective for K^+ are found in bacteria, archaeobacteria, eukaryotes, and some viruses, and over 75 distinct K^+ channel genes have been cloned in mammals alone. Based on sequence homology, functional characteristics, and low- and high-resolution structural data, all K^+ channels appear to exist as tetramers of identical or similar subunits, each containing 2-8 helical transmembrane segments around a central conductive pore (Tempel *et al.*, 1987; MacKinnon, 1991; MacKinnon *et al.*, 1993; Li *et al.*, 1994; Schulteis *et al.*, 1996; Spencer *et al.*, 1997; Doyle *et al.*, 1998; Jiang *et al.*, 2002; Kuo *et al.*, 2003; Jiang *et al.*, 2003; Long *et al.*, 2005). Additional K^+ channel diversity arises from alternative RNA splicing, heteromeric assembly of subunits, and coassembly with accessory proteins. Thus, cells have a remarkably broad repertoire of K^+ channel complexes with various functional profiles at their disposal (Jenkinson, 2006). Despite their diversity, K^+ channels share some general features in terms of selectivity, kinetics, modulation, and selectivity. Relative to other voltage-gated channels, K^+ channels tend to activate slowly; once open, however, they can conduct more than 10^6 ions per second—near the diffusion-limited rate (Hille, 2001). The conductive and kinetic properties of K^+ channels respond to numerous signals, including pharmacological agents, intracellular Ca^{2+} , phosphorylation, and binding of accessory proteins. Finally, K^+ channels are more than 100-fold selective for K^+ over Na^+ ions; this selectivity is key to controlling a precise interplay between ion permeabilities, for example in successive phases of the action potential (Hille, 2001).

A handful of high-resolution structures reveals conserved features of K⁺ channel architecture (Figure 1). As predicted, all known K⁺ channel structures are complexes of four subunits (Doyle *et al.*, 1998; Jiang *et al.*, 2002; Kuo *et al.*, 2003; Jiang *et al.*, 2003; Long *et al.*, 2005); in some cases, this feature has provided noncrystallographic symmetry operators essential to solving the structure (Doyle *et al.*, 1998). Unlike previously characterized membrane pores, which are bundles of β -sheets (Schulz, 1996), K⁺ channels comprise a novel fold based on membrane-embedded α -helices. The K⁺ channel conduction pathway is defined by two central helices, called “outer” and “inner” helices in the bacterial channels Kcsa (Doyle *et al.*, 1998), MthK (Jiang *et al.*, 2002), and KirBac1.1 (Kuo *et al.*, 2003), or S5 and S6 in the voltage-gated channels KvAP (Jiang *et al.*, 2003) and Kv1.2 (Long *et al.*, 2005). Beginning at the N-terminus, each outer helix (one from each subunit) crosses from the intra- to extracellular sides of the membrane, paralleling the ion pathway and interacting significantly with lipids. As each polypeptide exits the membrane, the first few residues of the pore domain form an extracellular “turret.” The polypeptides then reenter the membrane as short *pore helices*, angled with their negative dipole moments towards the center of the pore. The next dozen residues extend back towards the extracellular side to form the *selectivity filter*, the narrowest part of the conduction pathway; this subdomain is characterized by a consensus sequence T/S-x-x-T-x-G-Y-G (Heginbotham *et al.*, 1992). Finally, the inner helices pass to the intracellular side, nested inside the outer helices and surrounding the pore (Doyle *et al.*, 1998).

The K⁺ ion conduction path is conserved in all known K⁺ channel structures (Figure 1A). A K⁺ ion enters the channel via a constricted opening at the intracellular

end of the inner helices; this region is thought to play a role in activation gating (Kuo *et al.*, 2003). The ion then passes into a large, solvent-filled cavity lined with nonpolar residues. The hydrophobic nature of this inner vestibule facilitates rapid transport by preventing charged ions or their solvating water molecules from interacting strongly with the channel (Zhou *et al.*, 2001). The pore helices converge at the extracellular end of the vestibule. Although early work proposed the pore helix dipole might stabilize ions in the pore, its role is controversial (Chatelain *et al.*, 2005). Having passed through the inner vestibule, ions exchange their solvating waters for the backbone carbonyls of residues in the selectivity filter. The geometry of the selectivity filter perfectly coordinates K^+ but not Na^+ , Rb^+ , or other ions. Neighboring residues in the filter form a chain of equivalent binding sites, such that K^+ ions pass in a single-file column. The filter collapses to a nonconducting conformation when the concentration of K^+ is low (Zhou *et al.*, 2001); the conformation of this domain may play a major role in inactivation (Cordero-Morales *et al.*, 2006). The extracellular entryway of the channel is negatively charged, forming a binding site for extracellular blockers (Doyle *et al.*, 1998). These results largely agree with previous electrophysiological data, which predicts that ions should pass single-file through a selective pore sensitive to extracellular blockers (Hodgkin and Keynes, 1955; Begenisich and De Weer, 1977; Hille and Schwarz, 1978).

The structural basis for voltage sensitivity in K^+ channels also appears to be conserved. A voltage-gated K^+ (Kv) channel generally displays strong outward rectification: at highly negative potentials the channel is “closed”; depolarization alters the electromagnetic field in the membrane, causing a conformational change that opens the channel. The steep voltage-dependence of Kv channel opening implies it is coupled to the movement of several charges through the membrane electric field. Indeed, tiny

gating currents can be measured during the lag before channel opening, representing the movement of around 12-16 positive charges, or 3-4 per subunit, toward the extracellular solution prior to activation (Schoppa *et al.*, 1992; Aggarwal and MacKinnon, 1996; Zagotta *et al.*, 1994). X-ray crystallographic structures of Kv channels from archaeobacteria (Jiang *et al.*, 2003) and rat (Long *et al.*, 2005; Long *et al.*, 2007) include a conserved voltage-sensing domain (VSD) consisting of four transmembrane helices S1-S4. The S4 helix contains multiple conserved Arg and Lys residues likely to carry positive charges. It has been proposed that a helix-turn-helix motif comprising S4 and the C-terminal half of S3 translocates in response to changes in the membrane electromagnetic field, altering a gate at the intracellular side of the S6 inner helices. Notably, the Kv1.2 VSD is a discrete modular domain, associating only loosely with the S5-S6 pore-forming helices (Figure 1B). The VSD moves freely in the lipid membrane and interacts cooperatively with different subunits in the K⁺ channel complex (Alabi *et al.*, 2007). Furthermore, the Kv VSD is structurally homologous to voltage sensors in the proton channel Hv1 (Sasaki *et al.*, 2006) and the soluble phosphatase Ci-VSP (Murata *et al.*, 2005), supporting the theory that this motif is a self-contained domain that can be implemented in diverse contexts.

Structural data on K⁺ channels confirms the hypothesis that membrane proteins, like soluble proteins, implement modular domains to carry out critical regulatory functions. As described above, even voltage sensing, a defining feature of Kv channels, is attributed to a domain with remarkable independence from the rest of the channel (Figure 1B) (Long *et al.*, 2005). The implementation of modular domains by K⁺ channels is an important experimental insight. Isolated domains may be tractable to biochemical

and structural analysis, and can subsequently be useful in solving the structures of full-length complexes: high-resolution structures of isolated RCK and T1 domains provided molecular replacement search models that were instrumental in solving the structures of MthK (Jiang *et al.*, 2002) and Kv1.2 (Long *et al.*, 2005), respectively. In addition, modular domains may operate independently to regulate function and assembly. Because a given cell may express a wide range of homologous K⁺ channels simultaneously, all K⁺ channels face a common problem of selecting appropriate partners for assembly (Papazian, 1999; Deutsch, 2003). K⁺ channels fine-tune their properties by permitting only one or a few combinations of subtypes to interact. Specific assembly of tetramers also adds to the great diversity of channels, as functional heteromers often have different properties from either of their parent homomers. Although the membrane helices of a K⁺ channel make sufficient intersubunit contacts to stabilize a tetrameric complex even in the presence of SDS (Heginbotham *et al.*, 1997; Schrempf *et al.*, 1995), these regions are relatively conserved between families, and cannot account for the highly specific nature of K⁺ channel assembly. In most cases it appears that specific K⁺ channel assembly is determined by interaction of intracellular motifs. Chapters 2 and 3 of this thesis will consider an informative case of Kv channel assembly determined by a modular intracellular motif, and its implications for assembly specificity.

iii. The T1 Domain is a model K channel assembly module.

Little is known about the structure of K⁺ channel intracellular domains. One of the few well-characterized examples is the T1 domain, found in the N-terminus of many Kv channels. T1 domains are independent tetramerizing motifs: they interact with one another and form tetramers even when isolated from full-length K⁺ channels (Li *et al.*,

1992; Shen *et al.*, 1993). According to most evidence, deleting the T1 domain prevents the channel from assembling and reaching the cell surface (Shen *et al.*, 1993; Schulteis *et al.*, 1998; Papazian *et al.*, 1999; Isacoff *et al.*, 1990; Minor *et al.*, 2000). Replacing the domain with an alternative tetrameric motif restores functional channels, albeit with modified properties (Minor *et al.*, 2000; Zerangue *et al.*, 2000). T1 domain tetramerization appears to be the earliest event in channel assembly, taking place while the channel polypeptide is still bound to the ribosome (Lu *et al.*, 2001).

In addition to driving tetramerization, the T1 domain plays a major role in selecting specific partners to bind to the channel. Despite the similarity of their transmembrane domains, voltage-gated K⁺ channels generally do not coassemble between families: for example, Kv1 family channel subunits will not form tetramers with Kv2 subunits. This subtype specificity is encoded by the T1 domain. Yeast 2-hybrid experiments show the Kv1 T1 domain binds only Kv1 channels, T1 from Kv2 binds only Kv2 channels, and so on (Xu *et al.* 1995). Substituting the Kv1 T1 domain into Kv2 allows the chimeric channel to assemble with Kv1 subunits (Li *et al.*, 1992). Beyond the pore-forming complex, T1 domains also form docking platforms for accessory proteins such as β subunits (Yu *et al.*, 1996; Gulbis *et al.*, 2000) and calcium-binding proteins (Scannevin *et al.*, 2004; Pioletti *et al.*, 2006). Residues on the membrane-proximal surface of T1 may also interact with inactivating factors (Kreusch *et al.*, 1998; Gulbis *et al.*, 2000). Thus, the T1 domain is a nexus for specific assembly of pore-forming and accessory proteins.

X-ray crystallographic data on T1 domains indicate a structural basis for K⁺ channel subunit interaction. The T1 domain is a novel protein fold, consisting of mixed

α -helical and β -sheet subunits arranged symmetrically around a four-fold axis (Kreusch *et al.*, 1998). The hydrophobic core residues of each subunit are fairly conserved across K^+ channel families, suggesting the overall fold is also conserved. Residues at subunit interfaces vary more between families, presumably allowing TI to recognize appropriate assembly partners (Kreusch *et al.*, 1998). Notably, the TI domain subunit interface consists primarily of polar residues, which form salt bridges and hydrogen bonds between subunits (Kreusch *et al.*, 1998; Minor *et al.*, 2000).

The polarity of the TI interface is unexpected, since most constitutively bound proteins interact via nonpolar residues (Janin *et al.*, 1988) and polar amino acids tend to destabilize protein-protein interactions (Hendsch and Tidor, 1994). Indeed, the TI interface is not optimized for stability of binding, as mutating any of several polar residues on the interaction surface to Ala stabilizes the TI tetramer and shifts the channel's activation voltage to a more positive potential (Minor *et al.*, 2000). These results suggest the TI domain may not only act to nucleate the channel complex, but may also undergo conformational changes in the course of normal channel function. The effect of such conformational changes on the channel pore would most likely be indirect, since TI associates with the transmembrane domains at a distance—about 50 Å from the pore, according to the structure of full-length Kv1.2 (Long *et al.*, 2005).

iv. Coiled coils are alternative assembly motifs that may drive tetramerization in K^+ channels.

TI domains are not ubiquitous; some K^+ channels must find alternative solutions to the problem of efficient, specific assembly. One likely alternative approach is the use of *coiled coils*, common protein motifs that occur in as many as 5% of all open reading

frames (Newman *et al.*, 2000). Coiled coils have been identified in the intracellular domains of over thirty ion channels (Jenke *et al.*, 2003), and there is experimental evidence in several channels that coiled coils play roles in assembly. For example, a coiled coil in the C-terminus of intermediate conductance Ca^{2+} -activated K^+ channels is necessary for assembly of the C-terminal domains and for trafficking of channels to the cell surface (Syme *et al.*, 2003). Cyclic nucleotide-gated channels can form homotetramers of A subunits, or asymmetric heterotetramers of one B and three A subunits; a three-stranded coiled coil in the A subunit C-terminus is required to selectively assemble the heteromeric form (Zhong *et al.*, 2003). In several transient receptor potential channels, a C-terminal coiled coil is necessary for channel assembly, maturation, and trafficking, and is sufficient for tetramer formation (Tsuruda *et al.*, 2006). Coiled coils from the C-termini of two ether-a-go-go superfamily channels, EagI and ErgI, assemble independently as multimers, and disrupting these domains in either channel leads to loss of function (Jenke *et al.*, 2003). In terms of specificity, neither the EagI subunit nor its coiled-coil domain coassembles with ErgI; however, transplanting the coiled coil from EagI into ErgI rescues function, and allows the chimeric protein to form EagI heteromultimers (Jenke *et al.*, 2003). The Kv7 channel contains a C-terminal motif, called the A-domain, that is important in channel assembly; this domain contains a coiled coil that supports multimerization, trafficking, and binding of accessory proteins (Kanki *et al.*, 2004, Schwake *et al.*, 2006). We will consider the Kv7 example in detail in the second half of this chapter and the investigations in Chapters 2 and 3. In general, the coiled-coil motif seems to represent a common strategy for directing assembly in a variety of channels.

Coiled coils comprise one of the most widespread and versatile classes of protein-protein interaction domains. They play structural roles in skeletal proteins such as α -keratin (Crick, 1952), molecular stalks such as influenza hemagglutinin (HA) (Wilson *et al.*, 1981), and the lever domains of molecular motors such as myosin (Kavinsky *et al.*, 1983). Coiled coils are also the basis for a variety of interactive scaffolds, such as the muscle regulatory protein tropomyosin (Sodek *et al.*, 1972), the bacterial cell wall spacer Omp α (Engel *et al.*, 1992), and the “fuzzy coat” M proteins of streptococci (Phillips *et al.*, 1981). In some families of transcription factors, specific dimerization mediated by coiled coils is required for DNA binding (Baxevanis and Vinson, 1993). Specific interaction between coiled coils also mediates the fusion of synaptic vesicles to neuron membranes during neurotransmitter release. Vesicle fusion requires formation of complexes between soluble NSF attachment receptors (SNAREs) on the vesicle and target membranes, where NSF is N-ethylmaleimide sensitive fusion protein, an ATPase that dissociates SNAREs. The fusion and recycling of presynaptic vesicles involves the dynamic assembly and dissociation of SNARE coiled-coil domains (Sutton *et al.*, 1998).

Coiled coils are superhelical bundles of 2-5 α -helices. Long before any relevant structure was solved at high resolution, Crick predicted the detailed geometry of a left-handed coiled coil as a function solely of superhelical *pitch* (ω_0), *radius* (R_0), and “*a*”-*position orientation* (ϕ) (Figure 2A, 2B) (Crick, 1953a). Other authors have derived alternative notations, but the same general principles apply (Nishikawa and Scheraga, 1976; Busson and Doucet, 1999). In the Crick parameterization, the radius R is the average distance between the helix axis and any atom. The subscripts 1 and 0 are used

to denote values for α -helices and superhelices, respectively. The value of R_1 is generally 2.2 Å – 2.3 Å; R_0 can vary between 4 Å and 8 Å. Typically, steric hindrance enforces a larger R_0 for higher order complexes. The “ a ”-position orientation ϕ is the angle by which the first residue in each repeating heptad rotates away from the superhelix axis. In a left-handed coiled coil, ϕ falls between 0° and 40°, usually around 20°. The pitch is the distance required to complete a full turn of the supercoil, generally on the order of 100 Å – 300 Å (Seo & Cohen, 1993). While R_0 and ϕ are relatively consistent, the local pitch is sensitive to interactions in the coiled coil interface, varying as much as twofold over the length of a single domain (Offer & Sessions, 1995). Helix pitch can also be expressed in terms of ω , the number of residues required to complete a turn. For a single α -helix, ω_1 is 3.6 residues/turn; for the supercoil, ω_0 is around 100 residues/turn. A right-handed coiled coil can be described by the same parameters, but the values of ϕ and ω are negative (Harbury *et al.*, 1995).

The parameters of coiled-coil geometry arise from the repeating properties of component α -helices. If the value ω_1 for a straight α -helix were 3.5 residues/turn, seven residues “ $a-b-c-d-e-f-g$ ” would complete 2 full turns: every seventh residue “ a ” would occupy exactly the same position, displaced along the helical axis. If every “ a ”-position residue were a colored knob, the knobs would form a stripe parallel to the helical axis. However, since peptide backbone geometry constrains ω_1 around 3.6 residues/turn, every “ a ” residue in a heptad repeat lags 2 full turns by about 20°. Thus, a series of “ a ”-position knobs would form a stripe at a 20° angle to the rising helix. Conversely, twisting the α -helix uniformly 20° to the left for every 7 residues would allow every knob to face into the superhelical axis (Harbury *et al.*, 1998). If two such twisted helices

were paired with their knobs facing one another, the “a”-position side chains would clash. However, if the helices were paired with their “a”-positions rotated away from the superhelical axis by an angle ϕ of about 20° , each “a” knob would point obliquely between the “a” and “g” residues of the neighboring helix (Figure 2). Rotating the “a” residues away would also rotate the “d” residues toward the superhelical axis, such that each “d”-position points between the “d” and “e” residues of the neighboring coil (Figure 2C). Crick termed this geometry “knobs-into-holes” packing and demonstrated that it explains the X-ray diffraction patterns of α -keratin (Crick, 1953b).

The repeating nature of the coiled-coil scaffold is reflected in repeating patterns of residues at key positions of the heptad repeat. Residues at “a”- and “d”-positions tend to be hydrophobic, since they are buried at the interface between coils. Residues at “e”- and “g”-positions are at least partially exposed to solvent, but are also in close proximity to one another, with each “e”-position of one coil approaching a “g”-position of its neighbor. Therefore, polar or charged residues capable of forming hydrogen bonds or salt bridges often occupy complimentary “e”- and “g”-positions in the heptad repeat (Marti *et al.*, 2003). Residues at “b”-, “c”-, and “f”-positions are on the surface of the coiled-coil complex. It is considered favorable for these residues to be polar to increase solubility, but uncharged to avoid electrostatic interactions with neighboring “e” and “g” residues (O’Shea *et al.*, 1993). The propensity of a novel amino acid sequence for forming a coiled coil can be calculated from the statistical probability of each amino acid occurring at a given heptad position in known coiled coils (Lupas *et al.*, 1991). The accuracy of these prediction algorithms has been improved by incorporating pairwise residue correlations (Berger *et al.*, 1995), higher-order coiled coils (Wolf *et al.*,

1997), and hidden Markov models (Delorenzi and Speed, 2002), and by explicitly searching for favorable “a/d”- and “e/g”-position interactions (Walshaw *et al.*, 2001).

v. *Coiled coils can determine specific assembly properties.*

Despite the conserved nature of coiled-coil sequences, these domains are capable of selecting binding partners with remarkable specificity. In most cases, even relatively similar coiled coils segregate as homomeric complexes. Some coiled-coil sequences are able or even prefer to assemble as heteromers, but only a limited range of partners is typically allowed: exhaustive screening of all coiled-coil motifs in the genome of the prototypic yeast *Saccharomyces cerevisiae* identifies only one interaction for every ~100 pairwise combinations (Newman *et al.*, 2000). Similarly, fewer than 6% of all human basic leucine zipper (bZip) domains interact strongly in a microscale protein array (Newman and Keating, 2003). Coiled-coil specificity is partly influenced by long-range interactions. Polar or charged interface residues have a strong effect on superhelical pitch, influencing the proximity of interacting residue pairs (Seo and Cohen, 1993). Also, many coiled coils appear to depend on the presence of stable “trigger sequences” in order to fold. Although a wide variety of trigger sequences has been identified, each has a high propensity for α -helix formation, forming a nucleation site from which interacting chains can “zip up” in the intended register (Steinmetz *et al.*, 2007). Trigger sequences have been shown to play a role in specificity: exchanging the native trigger sequence of GCN4 for that of an unrelated coiled coil abolishes chain association (Kammerer *et al.*, 1998).

In addition to long-range influences such as trigger sequences, extensive research has identified a consistent set of interfacial residue interactions that tune the specificity of coiled coils for binding partners. A primary target for understanding assembly specificity has been the pattern of core “a/d”-position residues. The core positions are generally occupied by mid-sized hydrophobic residues such as Ile, Leu, or Val, whose side chains are small enough to allow close packing but large enough to fill the interhelical gap (Woolfson and Alber, 1995). However, many coiled coils in the leucine zipper family occupy a single “a” layer with polar residues, usually Asn, which can form buried hydrogen bonds with one another (O’Shea *et al.*, 1991; Junius *et al.*, 1995). By including an Asn layer, GCN4 sacrifices some stability but gains specificity for binding partners with complementary “a”-position Asn residues (Acharya *et al.*, 2002; Arndt *et al.*, 2000). Cavities at the coiled-coil interface can also cause marginal destabilization while dictating specificity. In general, small residues such as Ala at “a”- and “d”-positions are considered destabilizing (Hodges *et al.*, 1981; Liu *et al.*, 2002), but in some cases they can be accommodated by tight coiled-coil packing geometry or offset antiparallel orientation (Shu *et al.*, 2000; Gernert *et al.*, 1995). The cavity created by an “a”- or “d”-position Ala can also drive specificity by allowing heterotypic interaction with unusually bulky residues (Schnarr and Kennan, 2002). In general, variability at the core positions of a coiled coil plays a major role in specifying binding partners as well as determining overall stability.

The pattern of electrostatic interactions between “e”-and “g”-position residues plays a controversial role in specificity. Generally, assembly of heteromers is preferred if it abolishes “e/g”-position interactions that are unfavorable in homomers of either protein (Vinson *et al.*, 1993; O’Shea *et al.*, 1993; Pelletier *et al.*, 1999). In one classic

example, homodimers of the transcription factor Fos assemble weakly due to unfavorable negative charge interactions between their “e”- and “g”-positions. Several corresponding “e”- and “g”-positions in the homologous coiled-coil protein Jun are either neutral or positively charged. Thus, when Fos and Jun are mixed, heterodimers assemble in preference to either homomeric form (O’Shea *et al.*, 1989); the same specificity can be conferred on an unrelated coiled coil by transferring just the “e” and “g” residues (O’Shea *et al.*, 1992). Nonetheless, stabilization of coiled coils by favorable charge pairs is inconsistent, perhaps due to complex interactions of “e”- and “g”-position residues with solvent as well as protein atoms (Matousek *et al.*, 2007). Structural and thermodynamic studies indicate “e/g” ion pairs in the transcription factor GCN4 do not stabilize the complex significantly (O’Shea *et al.*, 1993; Krylov *et al.*, 1998). Furthermore, peptides derived from a genetic screen for stable heteromeric coiled coils include some with “e/g” pairs predicted to be repulsive, but which mediate dimerization *in vivo* more efficiently than rationally designed homologs with fully complementary “e/g” residue pairs (Arndt *et al.*, 2000; Arndt *et al.*, 2002). Thus, although peripheral charge pairing does play some role in selecting specific binding partners, its overall impact on coiled-coil stability and assembly remains unclear.

Coiled coils achieve additional diversity and specificity by occupying a variety of oligomerization states. Although two-stranded coiled coils are the best characterized, three-stranded complexes are also widespread, particularly in membrane fusion proteins (Wolf *et al.*, 1997). Four-stranded coiled coils also occur in nature in both parallel and antiparallel orientations (Antonin *et al.*, 2002), and at least one naturally occurring five-stranded coiled coil has been observed, though it may only assemble in hydrophobic

environments (Cornea *et al.*, 2000). Synthetic coiled coils with as many as seven strands have been reported (Liu *et al.*, 2006).

Seemingly minor deviations from interface residue rules can modify the stoichiometry as well as the subtype specificity of coiled-coil assemblies. For example, replacing the native “*a*”-position Asn of GCN4 with Val or Leu stabilizes the complex but converts it into a trimer or tetramer, respectively (Potekhin *et al.*, 1994; Lumb and Kim, 1995). This result has been generalized by statistical analysis, which indicates that Asn or positively charged (Lys or Arg) residues at “*a*”-positions are accommodated better by two-stranded than by three-stranded coiled coils (Woolfson and Alber, 1995). Similarly, exhaustive screening of “*d*”-position residues in a model coiled coil shows all charged residues (Lys, Arg, Glu, Asp) at this position induce the two-stranded state (Tripet *et al.*, 2000). These preferences probably arise from the diminished shielding of core residues in two-stranded complexes, such that polar core residues can be partially solvated. This model also predicts that nonpolar residues at peripheral “*e*”- and “*g*”-positions would give rise to higher-order complexes, in which they are more shielded from solvent. Indeed, replacing an “*e*”-position residue with Ala in a two-stranded leucine zipper creates a four-stranded complex (Krylov *et al.*, 1994); more dramatically, replacing all eight “*e*”- and “*g*”-positions of GCN4 with Ala yields a seven-helix coiled coil (Liu *et al.*, 2006). Our investigations in Chapter 3 of this thesis probe the consequences of some noncanonical coiled-coil interaction residues in the case of the Kv7 channel assembly domain.

A structural model for specific oligomerization has also been proposed for coiled coils with canonical interface residues. A mutant GCN4 construct containing only Ile at four “*a*”-positions and only Leu at four “*d*”-positions assembles as a parallel dimer, like

the native peptide. A mutant containing Ile at all eight “a”- and “d”-positions assembles as a parallel trimer; Leu at all “a”-positions with Ile at all “d”-positions yields a parallel tetramer (Harbury *et al.*, 1993). Comparing the structures of two-, three-, and four-stranded complexes suggests their oligomerization preferences arise from conserved knobs-into-holes geometry. Interface packing in a three-stranded coiled coil accommodates Ile in its preferred rotamer at both “a”- and “d”-positions (Harbury *et al.*, 1994). Thus, the three-stranded conformation may be a default oligomerization state, favored by a random distribution of hydrophobic core residues (Woolfson and Alber, 1995). Two- and four-stranded coiled coils have opposite interface geometries: an “a”-position residue in a two-stranded coiled coil adopts an orientation similar to that of a “d” residue in a four-stranded coiled coil, and a two-stranded “d” residue is orientated similarly to a four-stranded “a” residue. Thermodynamic measurements indicate Ile is strongly favored over Leu in the two-stranded “a”/four-stranded “d” orientation, while Leu is favored in the two-stranded “d”/four-stranded “a” geometry (Zhu *et al.*, 1993; Harbury *et al.*, 1993). In Chapter 3 of this thesis, we apply some of these preferences to the coiled coil stoichiometry of the Kv7 channel assembly domain.

More generally, molecular modeling suggests “a”-position Ile and “d”-position Leu residues have strong packing energies in the dimer structure, but that relatively weak interactions between “a”-position Leu and “d”-position Ile residues lead to the looser tetramer structure (DeLano and Brünger, 1994). Although these generalizations are based on synthetic peptides with unnaturally conserved “a” and “d” residues, they reflect the bias of leucine zippers—in which most or all “d”-positions are occupied by Leu—for forming two-stranded complexes. Statistical analysis of “a” and “d” residue occurrences in various orders of coiled coils also supports the residue preferences

above. Based on these findings, two- versus three-stranded stoichiometries can now be predicted with relative accuracy (Wolf *et al.*, 1997). Finally, it is informative that discontinuities in coiled coils—especially stutters in the heptad repeat—are found more often in tetramers than in dimers; the larger gap between helices in a four-stranded coiled coil can tolerate more variations in core side chain orientation (Lupas, 1996). It should be noted that switches between oligomerization states can be very sensitive. Multiple crystal structures have been reported in which identical sequences give rise to different stoichiometries, depending on the conditions of crystal growth (Gonzalez *et al.*, 1996a; Gonzalez *et al.*, 1996b). Further structural information on multi-stranded coiled coils will be required for accurate structure prediction and characterization of coiled-coil assemblies.

A largely unexpected characteristic of coiled coils has been their ability to mediate dynamic as well as constitutively bound interactions (Burkhard *et al.*, 2001). In many cases, the dynamic nature of coiled-coil domains presents a challenge to solving their structures by static techniques such as X-ray crystallography (Schnell *et al.*, 2005). Biological examples of inherently dynamic complexes include the motor proteins myosin II and dynein, in which bending or unwinding of coiled coil domains is critical for coordinating motion of their active head domains (Hawkins *et al.*, 2006; Lauzon *et al.*, 2001; Li *et al.*, 2003). Similarly, membrane fusion of synaptic vesicles involves rapid association and dissociation of coiled-coil domains in SNARE proteins (Yan *et al.*, 2004; Sollner *et al.*, 1993). Dynamic changes in coiled-coil assembly can arise from environmental signals such as pH. For example, exposure to the acidic endosome interior triggers extension of coiled-coil domains in both viral hemagglutinin (HA) and the macrophage scavenger receptor, leading to vesicular fusion and ligand dissociation,

respectively (Huang *et al.*, 2003; Suzuki *et al.*, 1997). Phosphorylation has also been shown to influence the stability of coiled coils. Phosphorylation of interface Thr residues in the dimeric tail of myosin II promotes formation of a nonfunctional intramolecular four-stranded coiled coil (Liang *et al.* 1999). Similarly, stabilization of coiled-coil domains in vitellogenin binding protein (VBP) and other transcription factors may account for phosphorylation-enhanced DNA binding *in vivo* (Szilák *et al.*, 1997b; Xiao *et al.*, 2002; Pan *et al.*, 2002). Conversely, phosphorylation of specific residues in the coiled-coil domains of VBP and the acid-sensing ion channel (ASIC1) can destabilize assembly (Leonard *et al.* 2003). The capacity of coiled coils to undergo structural modification by various intracellular signals suggests this motif, like the T1 domain, can support specific modulation as well as coordinate assembly. If coiled coils are, as we describe in Chapters 2 and 3 of this thesis, common assembly determinants for ion channels, it is likely that they could support the dynamic properties of T1 domains.

B. Structure and assembly of Kv7 channels

The Kv7 or KCNQ family of voltage-gated K⁺ channels is of particular interest in terms of both physiology and structure. Each of the five subtypes of Kv7 channels has one or more correlates in human physiology, including some common genetic diseases. Several pharmacological targets have been found to be effective and specific for Kv7 channels, opening the door to significant research and treatment possibilities. Different Kv7 channel subtypes display different electrophysiological profiles, depending on the specific assembly of pore-forming subunits into homo- or heterotetramers and on modulation by membrane and intracellular factors. In terms of structure, while the transmembrane architecture of Kv7 channels is likely to be similar to that of other

voltage-gated K⁺ channels, the intracellular domains are unique. The specific assembly properties of Kv7 channels are determined by a conserved C-terminal region, which we characterize in some detail in Chapters 2 and 3 of this thesis.

i. Unique structural and functional profiles facilitate critical physiological roles of Kv7 channels.

Kv7 channels are qualitatively similar to other Kv channels in function and structure, but have several unique properties. In general, Kv7 channels pass outwardly rectifying K⁺ currents at voltages positive to -60 mV (Figure 3A). Although Kv7 channels are now classified with other six-transmembrane/one-pore voltage-gated K⁺ channels, they occupy an independent phylogenetic lineage (Gutman *et al.*, 2003), and upon initial characterization were sufficiently dissimilar to other Kv channels that they were considered in a separate class (Hille, 2001). In particular, the kinetics of Kv7 activation and deactivation tend to be slower than those of other Kv channels, taking on the order of a second to reach full activation in heterologous expression systems (Robbins, 2001). Some subtypes, particularly Kv7.1, Kv7.4, and Kv7.5, display limited time- and voltage-dependent inactivation, but their inactivation is on the order of seconds and may be removed entirely by interaction with accessory subunits (Jensen *et al.*, 2007).

In terms of structure, residues from S5 to S6 in Kv7 channels are thought to form the pore, including the activation gate, pore helices, and selectivity filter (Figure 3B). Voltage sensitivity depends on the movement of conserved positive charges on the S4 transmembrane subunit (Robbins, 2001). As in most Kv channels, the N- and C-termini are intracellular; however, the intracellular N-terminus of Kv7 channels is short (~100 amino acids) and contains no T1 domain or other conserved motifs. Conversely,

the Kv7 C-terminus is relatively long (~320-580 amino acids) and contains several conserved regions involved in subunit assembly and channel modulation. As discussed later in this chapter, Kv7 channels are regulated directly and indirectly by unique membrane and intracellular factors, particularly via their C-terminal domains (Delmas and Brown, 2005; Jespersen *et al.*, 2005).

The cloning of the first Kv7 channel highlighted the importance of this channel family in human physiology. Kv7.1 was cloned by linkage analysis of patients suffering from long QT syndrome (LQTS), a cardiac disorder leading to arrhythmia, ventricular fibrillation, and cardiac arrest (Wang *et al.*, 1996b). This discovery has been identified as the first direct correlation between a K⁺ channel mutation and human disease (Busch, 1999). The Kv7.1 channel, in association with the membrane-spanning accessory subunit KCNE1, was soon found to constitute the slowly activating voltage-gated cardiac I_{Ks} current (Barhanin *et al.*, 1996; Sanguinetti *et al.*, 1996). The Kv7.1/KCNE1 current, like the experimentally measured I_{Ks} current, activates at potentials positive to -20 mV with extremely slow activation and deactivation and no appreciable inactivation. The slow kinetics of this current facilitate the prolonged cardiac action potential; the current is also upregulated by sympathetic stimulation to mediate variations in heartbeat (Jespersen *et al.*, 2005). Although other K⁺ currents also contribute to cardiac repolarization, the process is initiated and regulated by I_{Ks}; Kv7.1/KCNE1 is the only channel upregulated in fast heartbeats. It follows that numerous mutations in Kv7.1 as well as KCNE1 are associated with mild to severe cardiac arrhythmias (Schwartz *et al.*, 2001). Chapters 2 and 3 of this thesis investigate one possible mechanism for disease arising from a cluster of naturally occurring C-terminal Kv7.1 mutations.

Whereas Kv7.1 channels are primarily associated with cardiac repolarization, other members of the Kv7 channel family characterize the neuronal *M-current*. All Kv7 channels are relatively slow to activate and therefore are unlikely to play a major role in repolarizing the rapid neuronal action potential. Instead, various combinations of Kv7.2 – Kv7.5 subunits form *M channels*, molecular correlates of an additional, slow K⁺ current that functions as a “brake” on repetitive action potential discharges (Cooper and Jan, 2003). When exposed to an excitatory stimulus, this M-current opposes the influx or efflux of small currents by other channels, effectively clamping the membrane at a sub-threshold potential (Delmas and Brown, 2005). The M-current “brake” is released when ligands such as acetylcholine, angiotensin, substance P, and bradykinin stimulate G-protein coupled receptors (GPCRs) (Marrion, 1997). The native M-current is primarily associated with heteromers of Kv7.2 and Kv7.3 subunits (Roche *et al*, 2002), though the pharmacological, kinetic, and regulatory profiles of all five Kv7 subtypes are consistent with M channel behavior (Selyanko *et al*, 2000) (Kv7.1 channels are typically not classified as M channels on account of the absence of Kv7.1 in neurons). Mutations in Kv7.2 and Kv7.3 cause benign epilepsies (Rogawski, 2000), underlining the significance of these channels in suppressing neuronal excitability via the M-current. However, the activation kinetics of Kv7.4 and Kv7.5 channels are even more characteristic of classic M-currents than those of Kv7.2/Kv7.3 heteromers (Lerche *et al.*, 2000); Kv7.5 in particular is expressed in areas of the central nervous system where significant M-currents are observed (Schroeder *et al.*, 2000). The precise contribution of each Kv7 subtype to M channels *in vivo* remains to be elucidated.

Kv7 channels also play critical roles the auditory system. Kv7.1 channels are essential for secretory function in the inner ear, as well as other epithelial cells including

the linings of the airways, stomach, colon, and kidneys. In the inner ear, Kv7.1/KCNE1 channels in marginal cells of the stria vascularis control K^+ secretion into to the endolymph of the scala media, which is essential for hearing (Wangemann *et al.*, 1995). Accordingly, homozygous recessive mutations in Kv7.1 channels lead to deafness as well as severe cardiac disorders (Neyroud *et al.*, 1997). Conversely, Kv7.4 channels are expressed in inner ear *hair cells* that transduce auditory vibrations into membrane potential and neurotransmitter release. Tissue distribution and pharmacology suggest that Kv7.4 channels underlie the $I_{K,n}$ current, which tunes the input resistance of hair cells and recycles K^+ from mechano-electrical transduction channels back to the stria vascularis (Wong *et al.*, 2004b). This finding is supported by mutations in Kv7.4, which cause a nonsyndromic autosomal dominant deafness disorder (Kubisch *et al.*, 1999). It has also been suggested that Kv7.4 channels account for the large $I_{K,L}$ current, which tunes the input resistance of Type I vestibular hair cells to detect motion and equilibrium (Kharkovets *et al.*, 2000). Finally, although no disease has been linked to Kv7.5, recent work identifies these channels in the dendritic nerve endings of auditory neurons (Caminos *et al.*, 2007), suggesting this subtype may also play a role in auditory signaling.

ii. Pharmacological tools aid in research and therapy of Kv7 channels.

The development of pharmacological agents has allowed detailed characterization of Kv7 channel properties. Compared to other ion channel targets, such as $GABA_A$ receptors, K^+ channels have relatively small extracellular domains, making the development of potent small molecule inhibitors more challenging (Cooper, 2006). Fortunately, early screens for compounds to treat Alzheimer's Disease led to the identification of linopirdine (3,3-bis(4-pyridinylmethyl)-1-phenylindolin-2-one) (Earl *et*

al., 1998) and its derivatives (Zaczek *et al.*, 1998), which specifically block Kv7 channels from the extracellular side (Costa and Brown, 1997). High-affinity inhibition by these agents is a hallmark of Kv7 channels, used to identify Kv7-mediated currents in novel tissues and organisms. Other Kv7 blockers display subtype-specific inhibition: some chromanols (Lerche *et al.*, 2007) and benzodiazepines (Seebohm *et al.*, 2003a) bind at residues unique to the Kv7.1 selectivity filter and inner vestibule, whereas tetraethylammonium (TEA) binds preferentially to a Tyr residue proximal to the selectivity filter in Kv7.2. The differential sensitivity of Kv7 channels to TEA allows pharmacological distinction of subtype expression (Hadley *et al.*, 2000).

The therapeutic potential of Kv7 channel blockers is significant but problematic. Blocking Kv7.1 channels prolongs the cardiac action potential duration and can suppress reentrant arrhythmias; however, it may also delay repolarization, inducing LQTS. Volatile anesthetics such as isoflurane inhibit Kv7.1/KCNE1 channels, prolonging QT intervals, and must therefore be used with caution in patients with cardiac disorders (Chen *et al.*, 2002). Still, the particular kinetic properties of Kv7.1/KCNE1 channels are thought to ameliorate the arrhythmogenic effects of inhibition compared to other cardiac K⁺ channels (Varro, 2000). Blocking M channels causes a similar mix of desirable and undesirable effects. Linopirdine and its derivatives enhance cognition in animal models (Brioni *et al.*, 1993) and are neuroprotective in the absence of crucial growth factors (Xia *et al.*, 2002). However, these and other M channel blockers have not proved effective in Phase III clinical trials for Alzheimer's disease (Börjesson *et al.*, 1999), and may induce epilepsy at high doses (Zhu *et al.*, 2000). Cross-reactivity between the diverse physiological roles of Kv7 channels is another significant concern: for example, the antiarrhythmic drug clofilium blocks Kv7.1 channels but also Kv7.3 (Yang *et al.*, 1998)

and Kv7.5 (Lerche *et al.*, 2000), and could cause undesired enhancement of neuronal excitability.

Due in part to these challenges, increasing attention has been focused on developing selective Kv7 channel activators, particularly for neuronal Kv7 subtypes (Munro and Dalby-Brown, 2007). The best characterized Kv7 activator is retigabine (N-(2-amino-4-(fluorobenzylamino)-phenyl) carbamic acid), which shifts the voltage-dependence of Kv7.2-Kv7.5 channels to more negative voltages (Wickenden *et al.*, 2000). Retigabine binds a hydrophobic pocket formed near the intracellular activation gate in its open state (Wuttke *et al.*, 2005). The acrylamide compound (S)-1 ((S)-N-(1-(3-morpholin-4-yl-phenyl)-ethyl)-3-phenyl-acrylamide) blocks Kv7.1 but activates Kv7.2-Kv7.5 channels, presumably by a mechanism similar to that of retigabine, as both compounds require a common Trp in the cytoplasmic end of S5 (Bentzen *et al.*, 2006). Other neuronal Kv7 channel activators include N-ethylmaleimide, which alkylates a C-terminal Cys conserved in Kv7.2, Kv7.4, and Kv7.5 channels, increasing their open probability (Li *et al.*, 2004a). Some selective Kv7.1 activators are derived from inhibitors: for example, the benzodiazepine R-L3 ((3-R)-1,3-dihydro-5-(2-fluorophenyl)-3-(1H-indol-3-ylmethyl)-1-methyl-2H-1,4-benzodiazepin-2-one) activates Kv7.1 channels at low concentrations by stabilizing the S6 inner helix in an open state (Seeböhm *et al.*, 2003b). Fenamates activate either cardiac or neuronal Kv7 channels, depending on the derivative: mefenamic acid (2-(2,3-dimethylphenyl)aminobenzoic acid) and diclofenac (2-(2-(2,6-dichlorophenyl)aminophenyl)ethanoic acid) activate Kv7.1/KCNE1 and Kv7.2/Kv7.3 channels, respectively, probably by a conserved mechanism (Abitbol *et al.*, 1999; Peretz *et al.*, 2005).

In therapeutic terms, whereas K⁺ channel blockers increase cellular excitability, K⁺ channel activators dampen excitability. Kv7 enhancement could counteract prolonged QT intervals in the heart or convulsive activity in the brain. Indeed, some fenamate derivatives rescue the function of mutant Kv7.1 channels associated with LQTS (Abitbol *et al.*, 1999); related compounds specific for Kv7.2/Kv7.3 channels have been proposed as antiepileptic drugs (Peretz *et al.*, 2005). Retigabine originated from the NIH Antiepileptic Drug Development Program (Rostock *et al.*, 1996) and is currently in stage III clinical trials for adult partial epilepsy (Plosker *et al.*, 2006). Neuronal Kv7 channel openers are also effective treatments for neuropathic pain, as they reduce the excitability of nociceptors (Passmore *et al.*, 2003). Significant interest from the pharmaceutical industry has yielded a growing family of neuronal Kv7 openers, including acrylamides (Bentzen *et al.*, 2006), benzanilides (Wickenden *et al.*, 2005), and the compound MaxiPost ((5-chloro-2-methoxyphenyl)-1,3-dihydro-3-fluoro-6-(trifluoromethyl)-2H-indol-2-one), which has an even higher efficacy for Kv7.5 than that of retigabine (Dupuis *et al.*, 2002). The wide range of pharmacological applications for Kv7 modulators underscores the importance of these channels in human physiology.

iii. A variety of factors regulates trafficking and modulation of Kv7 channels.

The Kv7 channel complex is not limited to the pore-forming subunits. For most subtypes, physiological channel function is only recapitulated in the presence of accessory proteins and signaling molecules. Signals that dynamically regulate Kv7 channels include pH (Freeman *et al.*, 2000), oxidation (Gamper *et al.*, 2006), ubiquitination (Jespersen *et al.*, 2007), membrane swelling (Hougaard *et al.*, 2004), and binding of scaffolding (Wong and Scott, 2004a) and ankyrin proteins (Chung *et al.*, 2006).

The roles of four critical regulatory elements—accessory KCNE subunits, phosphoinositide (PI) abundance, intracellular Ca^{2+} /CaM, and phosphorylation—are described below (Figure 3B).

Perhaps the most significant regulatory element of cardiac Kv7 channels is the KCNE family of membrane proteins. The five KCNE subtypes are single-pass helical transmembrane proteins with extracellular N-termini (Tian *et al.*, 2007). Functional studies indicate that two KCNE subunits assemble intimately with four Kv7.1 subunits (Chen *et al.*, 2003), close enough that some KCNE residues are exposed to the outer pore vestibule (Figure 3B) (Wang *et al.*, 1996a; Melman *et al.*, 2004). However, recent evidence suggests KCNE1 expression may be transient, exerting reversible modulation on Kv7.1 channels (Poulsen *et al.*, 2007). Coassembly with KCNE1 increases Kv7.1 currents, shifts activation voltage to more positive potentials, slows activation and deactivation, and removes inactivation (Splawski *et al.*, 1997), giving rise to currents very similar to the recorded cardiac I_{Ks} . Conversely, Kv7.1/KCNE2 channels are constitutively open (Dedek *et al.*, 2001) and may be prominent in stomach and intestinal epithelia (Jespersen *et al.*, 2004). KCNE3 accelerates activation and deactivation of Kv7.1 (Mazhari *et al.*, 2002), while KCNE4 and KCNE5 inhibit Kv7.1 altogether at physiological potentials (Bendahhou *et al.*, 2005). Although KCNE1 is the predominant subtype expressed in human heart, most KCNE's are expressed to some extent, such that cardiac function probably arises from a mixed population of channels with different properties (Lundquist *et al.*, 2005). Notably, KCNE5 is located on the X chromosome, and may be linked to gender differences in atrial fibrillation due to overactivation of Kv7.1 channels (Ravn *et al.*, 2007). KCNE subunits have been shown to modulate Kv7

subtypes other than Kv7.1, but the physiological relevance of these interactions is unclear (Tinel *et al.*, 2000; Strutz-Seebohm *et al.*, 2006).

Recent studies have revealed numerous ion channels, including all Kv7 subtypes, to be directly modulated by membrane phosphoinositides. Kv7 channels are upregulated by phosphatidylinositol bisphosphates (PIP₂), a general term for phospholipids derived from the double phosphorylation of membrane PI stores. PIP₂ is recycled between the membrane and the intracellular environments as a signaling molecule in the course of cell metabolism and lipase cascades; it also is a convenient effector of ion channel modulation, as it can be rapidly cycled in response to other cell signals, and is concentrated near membrane-bound proteins (Gamper and Shapiro, 2007). PIP₂ increases amplitude, slows deactivation, and shifts activation voltages of I_{Ks} currents by binding to the Kv7.1 C-terminus (Loussouarn *et al.*, 2003; Park *et al.*, 2005). The physiological role of PIP₂ in dynamic regulation of Kv7.1 channels is currently unclear, although at least one study suggests activation of phospholipase C (PLC), which cleaves PIP₂, inhibits I_{Ks} in vestibular dark cells of the inner ear (Marcus *et al.*, 1997). PIP₂ sensitivity has been more thoroughly characterized in M channels, where it underlies inhibition by muscarinic acetylcholine (M1) and angiotensin II (AT1) receptors. M channels take their name from their characteristic inhibition by M1 receptors, and were among the first ion channels known to be modulated by GPCRs (Brown and Adams, 1980). In the absence of GPCR stimulation, PIP₂ interacts with the C-termini of Kv7.2-Kv7.5 channels to increase their open probability (Li *et al.*, 2005). GPCR stimulation activates PLC to cleave PIP₂, removing it from Kv7 channels and inhibiting channel function (Horowitz *et al.*, 2005; Zaika *et al.*, 2006). Differential sensitivity of Kv7 subtypes to PIP₂ depletion allows fine-tuning of M channel inhibition by expression of

specific homo- or heteromeric Kv7 complexes (Li *et al.*, 2005). PIP₂ is thought to interact with the proximal end of the Kv7 C-terminus, near or overlapping binding sites for calmodulin (CaM) and A-kinase anchoring proteins (AKAPs) (Figure 3B) (Zhang *et al.*, 2003; Robbins *et al.*, 2006).

Although its concentration is far lower than that of other ionic species in the cell, Ca²⁺ is a critical modulator of ion channel function, generally mediated by Ca²⁺-binding proteins such as calmodulin (CaM). However, the specific effects of intracellular Ca²⁺ on Kv7 channels are controversial. Most evidence indicates that Ca²⁺ relieves inactivation of Kv7.1 channels and further enhances non-inactivating Kv7.1/KCNE1 channels (Nitta *et al.*, 1994; Ghosh *et al.*, 2006). However, this effect may be tissue-dependent (Shen and Marcus, 1998; Boucherot *et al.*, 2001), and some studies in heterologous systems show little or no Ca²⁺ effect (Gamper *et al.*, 2005). M currents are enhanced by small increases in intracellular Ca²⁺, but at higher concentrations, the effect is generally inhibitory (Marrion *et al.*, 1991; Selyanko and Brown, 1996). Ca²⁺-dependent interaction between the N-terminal lobe of CaM and a C-terminal site on Kv7.2, Kv7.4, and Kv7.5 dramatically inhibits those channels (Gamper *et al.*, 2005). Ca²⁺/CaM may provide an additional mechanism for M current inhibition by GPCRs: whereas MI- and ATI-mediated inhibition relies primarily on depletion of PIP₂, other GPCRs including bradykinin and purinergic receptors colocalize with inositol trisphosphate (IP₃) receptors, which release Ca²⁺ from intracellular stores to further inhibit M channels (Delmas *et al.*, 2002; Bofill-Cardona *et al.*, 2000). Ca²⁺/CaM may also activate protein kinases to phosphorylate Kv7 channels (Higashida *et al.*, 2005). The modulatory role of intracellular Ca²⁺ is clearly complex and requires further study.

In addition to mediating complex interactions with Ca^{2+} , the Ca^{2+} -binding protein CaM plays a structural role in Kv7 channels. In both cardiac (Shamgar *et al.*, 2006; Schmitt *et al.*, 2007) and neuronal Kv7 subtypes (Wen and Levitan, 2002; Etxeberria *et al.*, 2007), disruption of CaM binding not only suppresses channel modulation but also traps channels in the ER. CaM is a ubiquitous intracellular signaling protein that mediates a wide range of interactions, including phosphorylation, generation of second messengers, and regulation of the cytoskeleton. The two EF hand domains on each CaM molecule can each coordinate two Ca^{2+} ions, and may each bind a target protein in a Ca^{2+} -dependent or constitutive fashion (Crivici and Ikura, 1995). Biochemical experiments indicate CaM binds Kv7 channels constitutively via both an IQ domain past the end of S6 and a I-5-I0 motif in a more distal portion of the C-terminus (Figure 3B); Ca^{2+} /CaM can bind to either motif, suggesting that Ca^{2+} binding elicits significant conformational changes in the channel as well as CaM (Wen and Levitan, 2002; Yus-Najera *et al.*, 2002). The distal CaM binding site overlaps a putative site for interactions with PIP_2 and AKAPs; thus, these molecules may play complementary roles in regulation (Figure 3B) (Zhang *et al.*, 2003). The complex roles of CaM in regulation and assembly of Kv7 channels is likely to be elucidated by future structural research.

Most Kv7 channels are modulated by phosphorylation, which in turn is regulated by a variety of kinases, phosphatases, and scaffolding proteins. The AKAP yotiao (AKAP450) directly modulates Kv7.1 (Kurokawa *et al.*, 2004) and mediates its phosphorylation by protein kinase A (PKA) and protein phosphatase I (PPI) in response to cyclic AMP (cAMP) (Marx *et al.*, 2002). Phosphorylation of an N-terminal Ser residue in Kv7.1 (Figure 3B) enhances channel open probability and shifts the voltage response to more negative voltages (Kurokawa *et al.*, 2003). Thus, under conditions of stress or

high exertion, β -adrenergic receptors stimulate adenylyl cyclase to produce cAMP, leading to phosphorylation upregulation of Kv7.1 and increased heartbeat (Terrenoire *et al.*, 2005). Chapter 2 of this thesis identifies a putative binding region for yotiao in the Kv7.1 C-terminus, on the basis of mutations that cause heart arrhythmias. Kv7.4 is similarly enhanced by PKA phosphorylation, which removes the channel's inactivation properties (Chambard *et al.*, 2005). Conversely, phosphorylation by Src kinase or protein kinase C (PKC) inhibits M channels consisting of Kv7.2, Kv7.3, and/or Kv7.5 subunits (Hoshi *et al.*, 2003; Li *et al.*, 2004b). PKC phosphorylation may provide yet another mechanism for muscarinic inhibition: receptor stimulation activates PLC, producing diacylglycerol (DAG); DAG activates PKC to phosphorylate the M channel, causing it to close (Figure 3B) (Higashida *et al.*, 2005). In addition, it has recently been suggested that selective PKC-dependent inhibition of Kv7.5 channels by endogenous Arg(8)-vasopressin increases action potential firing and is responsible for vasoconstriction in aortic smooth muscle cells (Brueggemann *et al.*, 2007). PKC docks to human AKAP79 (rat AKAP150), which—like PIP₂, CaM and yotiao—binds to the Kv7 C-terminus (Figure 3B) (Higashida *et al.*, 2005). A complex picture of Kv7 channel modulation is emerging in which multiple signaling elements are integrated on neighboring or overlapping sites of the channel C-terminus.

iv. Kv7 channels exhibit specific assembly properties mediated by C-terminal modular domains.

Kv7 channel function depends on specific assembly among pore-forming subunits as well as membrane ligands and intracellular proteins. Macroscopic currents recorded from homomeric Kv7 channels expressed in *Xenopus* oocytes show significant variability

between subtypes: Kv7.4 currents are several times larger than those of Kv7.1 or Kv7.2 (Kubisch *et al.*, 1999), which are similar to Kv7.5 (Schroeder *et al.*, 2000). Kv7.3 currents are very small, often indistinguishable from background noise (Schroeder *et al.*, 1998; Wang *et al.*, 1998); low current levels of Kv7.3 have been attributed to poor surface expression (Schwake *et al.*, 2000), absence of an N-glycosylation site (Schwake *et al.*, 2006), and inhibition by a Thr-Ala substitution at the end of the pore helix (Etxeberria *et al.*, 2004). As with other tetrameric K⁺ channels, Kv7 channels achieve further functional diversity by forming heteromers of different subtypes; however, interaction between subtypes is specific. Kv7.1 channels are highly selective and do not assemble with any other Kv7 subtypes (Schroeder *et al.*, 1998; Kubisch *et al.*, 1999; Lerche *et al.*, 2000). In contrast, Kv7.3 coassembles with and dramatically augments currents of Kv7.2 (Schroeder *et al.*, 1998; Wang *et al.*, 1998), Kv7.4 (Kubisch *et al.*, 1999), or Kv7.5 (Lerche *et al.*, 2000; Schroeder *et al.*, 2000)—any other subtype except Kv7.1. The capacity of Kv7.3 to form heteromers is physiologically relevant, as the classic M-current arises from apparent 2:2 heteromers of Kv7.3 with Kv7.2 or Kv7.5 (Hadley *et al.*, 2003). Although the significant current enhancement conferred by Kv7.3 has been exploited extensively as an assay for heteromeric assembly, its mechanism is unclear. The effect has been attributed to masking of an N-terminal inhibitory signal, partial compensation for a nonconductive Ala in the Kv7.3 pore loop, and increased surface expression (Schwake *et al.*, 2000; Etxeberria *et al.*, 2004).

The structural basis for tetrameric assembly in Kv7 channels is attributed to a novel C-terminal modular domain. None of the Kv7 subtypes contain domains homologous to the T1 assembly motif found in the N-termini of other Kv channels (Li *et al.*, 1992); in fact, Kv7 N-termini are relatively short and poorly conserved. Instead, a

100-amino-acid region of the Kv7 C-terminus, the *A-domain*, is responsible for channel assembly (Figure 3B). The significance of the A-domain was initially supported by a naturally occurring Kv7.1 mutation that deletes part of the C-terminus, causing severe cardiac disorder and deafness (Neyroud *et al.*, 1997). This disease mutant has diminished currents, but does not suppress wild-type channel currents, suggesting its assembly properties are disrupted (Wollnik *et al.*, 1997). A subset of the deleted region, corresponding to the A-domain, was later found to be required for assembly and functional expression of Kv7.1; this domain exerts a dominant negative effect, suppressing surface expression of full-length Kv7.1 channels (Schmitt *et al.*, 2000). Deletion of Kv7.1 from the A-domain to the end of the C-terminus traps channels in the ER (Kanki *et al.*, 2004). A similar deletion of the A-domain from Kv7.2 causes an autosomal dominant form of idiopathic epilepsy (Biervert *et al.*, 1998). This deletion inhibits currents by reducing surface expression (Schwake *et al.*, 2000). Kv7 A-domains are often ill-behaved in isolation (Schmitt *et al.*, 2000); however, the A-domain from Kv7.2 has been successfully extracted from inclusion bodies as a mixture of aggregated and oligomeric species consistent with tetramers (Wehling *et al.*, 2007). Thus, the A-domain has some features of a self-contained interaction domain, but may require additional factors for efficient folding.

In addition to substantiating the A-domain's role in channel tetramerization, studies of chimeric Kv7 channels indicate the motif carries determinants necessary for subtype-specific assembly (Maljevic *et al.*, 2003; Schwake *et al.*, 2003; Etxeberria *et al.*, 2004). As described above, while Kv7.1 channels do not assemble with other subtypes, Kv7.2/Kv7.3 heteromers have even higher surface expression and macroscopic currents compared to homomeric channels (Schroeder *et al.*, 1998; Wang *et al.*, 1998). However,

a chimera of Kv7.2 containing the C-terminus of Kv7.1 (Kv7.2_{1C}) gives very small currents that are not substantially enhanced by Kv7.3, indicating the construct cannot form Kv7.3 heteromers. The opposite chimera, Kv7.3 with the C-terminus of Kv7.1 (Kv7.3_{1C}), also gives small currents that are not enhanced by Kv7.2 (Maljevic *et al.*, 2003). Even a restricted chimera of Kv7.3 with just the A-domain of Kv7.1 (Kv7.3_{1A}) lacks current enhancement by Kv7.2; however, this construct exerts a dominant negative effect on wild-type Kv7.1, indicating the Kv7.1 A-domain is sufficient to drive assembly with Kv7.1 over Kv7.2 (Schwake *et al.*, 2003). Thus, the Kv7.1 A-domain confers selectivity for homotetrameric assembly.

Similarly, A-domains from Kv7.2 and Kv7.3 are involved in both subtype selection and current enhancement, particularly by modifying surface expression. Chimeras of Kv7.1 with the C-termini of Kv7.2 (Kv7.1_{2C}) or Kv7.3 (Kv7.1_{3C}) assemble with wild-type Kv7.3 and Kv7.2 channels, respectively, as shown by current enhancement; this effect requires intact A-domains (Maljevic *et al.*, 2003). A chimera of Kv7.1 with just the A-domain of Kv7.3 (Kv7.1_{3A}) also enhances Kv7.2 currents, at least partly by increasing Kv7.2 surface expression. Notably, Kv7.1_{3A} does not increase surface expression of Kv7.3, though it moderately enhances Kv7.3 currents (Schwake *et al.*, 2003). A chimera of Kv7.3 with the C-terminus of Kv7.2 (Kv7.3_{2C}) enhances surface expression of Kv7.3, although the Kv7.3_{2C}/Kv7.3 heteromer does not show augmented currents (Etxeberria *et al.*, 2004). Instead, Kv7.3_{2C} behaves like Kv7.3, giving small currents that are enhanced by Kv7.2. The opposite chimera, Kv7.2 with the C-terminus of Kv7.3 (Kv7.2_{3C}), functions like Kv7.2, giving large macroscopic currents that are enhanced by Kv7.3 (Maljevic *et al.*, 2003). Finally, a splice variant of Kv7.2 lacking most of the C-terminus suppresses Kv7.3 wild-type currents, suggesting the channels can

interact but without increasing surface expression or currents (Smith *et al.*, 2001). Thus, interactions between Kv7.2 and Kv7.3 A-domains are important in selecting binding partners and increasing surface expression, but additional mechanisms contribute to augmenting heteromeric Kv7.2/Kv7.3 currents.

v. *The Kv7 A-domain consists of distinct subdomains with different structural and functional properties.*

Several studies characterize the Kv7 A-domain as a series of distinct subdomains. The terminology, however, is inconsistent: various groups signify the N- and C-terminal portions of the A-domain as “helix C” and “helix D” (Yus-Najera *et al.*, 2002), “A-part” and “H-part” (Schwake *et al.*, 2003), “helix A” and “helix B” (Maljevic *et al.*, 2003), “coil 1” and “coil 2” (Kanki *et al.*, 2004), “TCC1” and “TCC2” (Schwake *et al.*, 2006), and variations thereof. To avoid confusing letter/number conventions, and to account for an additional variable region in the middle of the A-domain, the symbolic terms *Head*, *Linker* and *Tail* will be used here to identify the N-terminal, middle, and C-terminal subdomains of the A-domain (Figure 3B).

The A-domain Head is the most conserved subdomain, and is predicted to be primarily helical, possibly a coiled coil (Jenke *et al.*, 2003). The high conservation of this subdomain (63% – 90% pairwise identity) suggests it could form a consistent, well-folded assembly platform, but makes it an unlikely candidate for determining specificity. Indeed, mutations that delete or disrupt the helicity of the Head suppress surface expression and macroscopic currents of Kv7.2 and Kv7.3 channels (Schwake *et al.*, 2006), but still permit tetramerization of isolated A-domains (Wehling *et al.*, 2007). Notably, truncation of the Kv7.2 C-terminus past the end of the A-domain Head also suppresses

currents and prevents enhancement of Kv7.3 (Schwake *et al.*, 2006); hence, the Head is not sufficient for functional expression or interaction with other subtypes. In an *in vitro* translation system, the Kv7.1 C-terminus does not coimmunoprecipitate with the isolated Head subdomain (Schmitt *et al.*, 2000). Furthermore, disease-linked mutations in the Kv7.1 A-domain Head show no assembly or trafficking defects (Kanki *et al.*, 2004). A chimera of Kv7.1 with the C-terminus of Kv7.3 (Kv7.1_{3C}) gives large macroscopic currents, which are dramatically reduced by deletion of the Kv7.3 Head subdomain; however, this altered Kv7.1_{3C} chimera is still capable of assembling with Kv7.2 channels (Maljevic *et al.*, 2003). A more limited Kv7.1 chimera (Kv7.1_{3H}) containing only the Head from Kv7.3, the remainder of the A-domain being from Kv7.1, fails to enhance Kv7.2 currents or surface expression (Maljevic *et al.*, 2003; Schwake *et al.*, 2003; Schwake *et al.*, 2006). These results indicate that the A-domain Head confers some tetramerization properties, but is not the primary determinant of subtype specificity.

The Linker subdomain is highly variable in sequence and length (20% – 52% pairwise identity, 16 – 41 amino acids). It is shortest in Kv7.1, the most selective subtype, and longest in Kv7.3, the most “promiscuous” subtype. It is tempting to envision this region as a loop that could allow, in its longer forms, the conformational flexibility to overcome geometric differences and bind diverse partners. Nonetheless, there is little evidence for a major role of the A-domain Linker. An isolated peptide containing the Head and Linker of Kv7.1 is insufficient to pull down Kv7.1 C-termini in coprecipitation experiments (Schmitt *et al.*, 2000). Furthermore, the Kv7.1_{3C} chimera augments Kv7.2 currents even if the Linker subdomain is from Kv7.1 (Schwake *et al.*, 2006) or is deleted altogether (Maljevic *et al.*, 2003). The significance, if any, of the A-domain Linker remains unclear.

The A-domain Tail is the most likely candidate for encoding the specific assembly properties of Kv7 channels. Truncation of the Kv7.1 C-terminus before the A-domain Tail is sufficient to disrupt functional expression (Schmitt *et al.*, 2000) by trapping channels in the ER (Kanki *et al.*, 2004). In an isolated Kv7.1 A-domain, truncation before the Tail disrupts coimmunoprecipitation with the Kv7.1 C-terminus (Schmitt *et al.*, 2000). Similarly, disrupting the Tail of an isolated Kv7.2 A-domain inhibits tetramerization, reducing the peptide to a dimeric form with low helical content (Wehling *et al.*, 2007). However, A-domain Tail assembly may be of limited relevance to tetramerization of full-length Kv7.2, as disrupting or deleting the Kv7.2 Tail subdomain gives currents similar to wild-type (Schwake *et al.*, 2006). Instead, A-domain Tail assembly may play a critical role in specificity. A chimera of Kv7.1 with the Tail subdomain of Kv7.3 (Kv7.1_{3T}) augments currents, increases surface expression, and coimmunoprecipitates with Kv7.2 channels (Schwake *et al.*, 2006). Thus, the Kv7.3 A-domain Tail is sufficient to confer interaction with Kv7.2 onto Kv7.1. Kv7 Tail assembly may be particularly important in enhancing surface expression of heteromers. Disrupting or deleting the Kv7.2 A-domain Tail renders channels incapable of augmenting Kv7.3 currents. Conversely, an isolated peptide containing the A-domain Tail of Kv7.2 enhances Kv7.3 currents and surface expression (Schwake *et al.*, 2006). Thus, interaction between Kv7.2 and Kv7.3 Tail subdomains is sufficient for increased surface expression—even in the absence of Kv7.2 pore-forming domains.

The A-domain Tail is better conserved (31% – 61% pairwise identity) than the Linker, but less conserved than the Head. In terms of structure, the Tail is highly predicted to be a coiled-coil motif in all subtypes (Jenke *et al.*, 2003; Schwake *et al.*, 2006). Because the Kv7 channel is a tetramer, the Tail subdomain is expected to form a

symmetric four-stranded coiled coil. Indeed, in at least some subtypes, the pattern of coiled-coil interface residues is characteristic of a four-stranded complex, having a preponderance of Ile residues at “d”-positions and Leu residues at “a”-positions in the heptad repeat (Harbury *et al.*, 1998). The presence of some hydrophobic residues (Leu, Met, Val) at “e”-positions in the Kv7 A-domain Tail may also promote a four-stranded configuration (Liu *et al.*, 2006), while the remainder of predicted “e”- and “g”-position residues are poised to stabilize electrostatic interactions between subunits. Mutations that disrupt the coiled coil interfere with surface expression, while conservative mutations that only shift the register of the coils preserve expression and function (Kanki *et al.*, 2004). Recent evidence from our group as well as others indicates that A-domain Tails from most channel subtypes assemble independently as four-stranded coiled coils (Howard *et al.*, 2007; Wehling *et al.*, 2007). However, the coiled-coil structure of the Kv7 Tail subdomain may not be universal. The Kv7.3 Tail has a much lower coiled-coil propensity than other subtypes. Furthermore, a mutant Kv7.3 channel designed with a disrupted coiled coil is still able to enhance Kv7.2 currents, whereas disrupting the Kv7.2 coiled coil removes its interaction with Kv7.3 (Schwake *et al.*, 2006). Thus, specific assembly of heteromers may rely on a combination of intact and disrupted coiled coils. The structure of the A-domain Tail, in some cases as a four-stranded coiled coil, appears to be a crucial platform for specific assembly of pore-forming and accessory subunits. Our investigations in Chapters 2 and 3 of this thesis further the structural characterization of this subdomain and its implications for Kv7 channel assembly and specificity.

Several LQTS-linked mutations are located in the A-domain Tail. Because this region is important in channel assembly, a simple explanation would be that Tail

mutations might cause disease by disrupting tetramerization. However, none of the Kv7.1 Tail mutations linked to LQTS involve interface “a” or “d” residues; it may be that alterations at these positions are fatal. Three disease mutations—G₅₈₉D, a founder mutation in Finnish lineages (Piippo *et al.*, 2001); R₅₉₁H, which disrupts functional channel expression by trapping channels in the ER (Grunnet *et al.*, 2005); and L₆₁₉M (Tester *et al.*, 2005)—are found at “e”- and “g”-positions, and could disrupt important contacts in a four-stranded coiled coil. The other four identified mutations—T₅₈₇M, which abolishes currents and surface expression (Yamashita *et al.*, 2001); A₅₉₀T (Lupoglazoff *et al.*, 2004); R₅₉₄Q, which inhibits currents and trafficking from the ER, but is somewhat capable of assembling with wild-type channels (Huang *et al.*, 2001; Wilson *et al.*, 2005); and D₆₁₁Y, which mildly suppresses currents (Yamaguchi *et al.*, 2005)—are predicted to lie on the coiled-coil surface. This preponderance of disease mutations on the Tail subdomain surface suggests the mechanism for disorder in this region may be more complex.

At least two alternative models for channelopathies arising from Kv7.1 A-domain Tail mutations have been proposed. Pull-down experiments show that G₅₈₉D disrupts binding of the scaffolding protein yotiao (Figure 3B) (Marx *et al.*, 2002). Removing this scaffolding protein also destroys interaction with yotiao’s other binding partners, including PKA and PPI, which regulate channel phosphorylation due to β-adrenergic receptor stimulation. Arrhythmia would result from disruption of this regulatory pathway (Saucerman *et al.*, 2004). On the other hand, four LQTS mutations in the Tail region disrupt surface expression of Kv7.1 channels (Kanki *et al.*, 2004). This result suggests an accessory protein binds Kv7.1 to promote trafficking from the ER to the plasma membrane (Figure 3B), perhaps by promoting proper folding, blocking a

retention signal, or acting as a forward trafficking motif. The trafficking protein is unlikely to be yotiao, as a designed mutation (L₆₀₂A/I₆₀₉A) shown previously to disrupt yotiao binding (Marx *et al.*, 2002) does not diminish surface expression (Kanki *et al.*, 2004). The mechanism for disease arising from A-domain Tail mutations should be clarified by structural information about this subdomain, as we describe in Chapters 2 and 3 of this thesis.

Kv7 channels are promising targets for physiological and structural study. The Kv7 A-domain in particular may provide an alternative paradigm for ion channel tetramerization and subtype specificity. Our investigations below seek to amend the current lack of structural information about these channels, enhance our ability to treat channel-related disorders, and improve our understanding of membrane protein assembly and function.

C. References

- Abitbol, I., Peretz, A., Lerche, C., Busch, A. E., & Attali, B. (1999). Stilbenes and fenamates rescue the loss of I(KS) channel function induced by an LQT5 mutation and other IsK mutants. *The EMBO journal*, *18*(15), 4137-4148.
- Acharya, A., Ruvinov, S. B., Gal, J., Moll, J. R., & Vinson, C. (2002). A heterodimerizing leucine zipper coiled coil system for examining the specificity of a position interactions: amino acids I, V, L, N, A, and K. *Biochemistry*, *41*(48), 14122-14131.
- Aggarwal, S. K. & MacKinnon, R. (1996). Contribution of the S4 segment to gating charge in the Shaker K⁺ channel. *Neuron*, *16*(6), 1169-1177.
- Alabi, A. A., Bahamonde, M. I., Jung, H. J., Kim, J. I., & Swartz, K. J. (2007). Portability of paddle motif function and pharmacology in voltage sensors. *Nature*, *450*(7168), 370-375.
- Antonin, W., Fasshauer, D., Becker, S., Jahn, R., & Schneider, T. R. (2002). Crystal structure of the endosomal SNARE complex reveals common structural principles of all SNAREs. *Nature structural biology*, *9*(2), 107-111.
- Arndt, K. M., Pelletier, J. N., Müller, K. M., Alber, T., Michnick, S. W., & Plückthun, A. (2000). A heterodimeric coiled-coil peptide pair selected in vivo from a designed library-versus-library ensemble. *Journal of molecular biology*, *295*(3), 627-639.
- Arndt, K. M., Pelletier, J. N., Müller, K. M., Plückthun, A., & Alber, T. (2002). Comparison of in vivo selection and rational design of heterodimeric coiled coils.

- Structure (London, England : 1993)*, 10(9), 1235-1248.
- Ashcroft, F. M. (2006). From molecule to malady. *Nature*, 440(7083), 440-447.
- Baranauskas, G. (2007). Ionic channel function in action potential generation: current perspective. *Molecular neurobiology*, 35(2), 129-150.
- Barhanin, J., Lesage, F., Guillemare, E., Fink, M., Lazdunski, M., & Romey, G. (1996). K(V)LQT1 and Isk (minK) proteins associate to form the I(Ks) cardiac potassium current. *Nature*, 384(6604), 78-80.
- Baxevanis, A. D. & Vinson, C. R. (1993). Interactions of coiled coils in transcription factors: where is the specificity? *Current opinion in genetics & development*, 3(2), 278-285.
- Begenisich, T. & De Weer, P. (1977). Ionic interactions in the potassium channel of squid giant axons. *Nature*, 269(5630), 710-711.
- Bentzen, B. H., Schmitt, N., Calloe, K., Dalby Brown, W., Grunnet, M., & Olesen, S. P. (2006). The acrylamide (S)-1 differentially affects Kv7 (KCNQ) potassium channels. *Neuropharmacology*, 51(6), 1068-1077.
- Berger, B., Wilson, D. B., Wolf, E., Tonchev, T., Milla, M., & Kim, P. S. (1995). Predicting coiled coils by use of pairwise residue correlations. *Proceedings of the National Academy of Sciences of the United States of America*, 92(18), 8259-8263.
- Biervert, C., Schroeder, B. C., Kubisch, C., Berkovic, S. F., Propping, P., Jentsch, T. J. et al. (1998). A potassium channel mutation in neonatal human epilepsy. *Science (New York, NY)*, 279(5349), 403-406.
- Bofill-Cardona, E., Vartian, N., Nanoff, C., Freissmuth, M., & Boehm, S. (2000). Two different signaling mechanisms involved in the excitation of rat sympathetic neurons by uridine nucleotides. *Molecular pharmacology*, 57(6), 1165-1172.
- Börjesson, A., Karlsson, T., Adolfsson, R., Rönnlund, M., & Nilsson, L. (1999). Linopirdine (DUP 996): cholinergic treatment of older adults using successive and non-successive tests. *Neuropsychobiology*, 40(2), 78-85.
- Boucherot, A., Schreiber, R., & Kunzelmann, K. (2001). Regulation and properties of KCNQ1 (K(V)LQT1) and impact of the cystic fibrosis transmembrane conductance regulator. *The Journal of membrane biology*, 182(1), 39-47.
- Brioni, J. D., Curzon, P., Buckley, M. J., Arneric, S. P., & Decker, M. W. (1993). Linopirdine (DuP996) facilitates the retention of avoidance training and improves performance of septal-lesioned rats in the water maze. *Pharmacology, biochemistry, and behavior*, 44(1), 37-43.
- Brown, D. A. & Adams, P. R. (1980). Muscarinic suppression of a novel voltage-sensitive K⁺ current in a vertebrate neurone. *Nature*, 283(5748), 673-676.
- Brueggemann, L. I., Moran, C. J., Barakat, J. A., Yeh, J. Z., Cribbs, L. L., & Byron, K. L. (2007). Vasopressin stimulates action potential firing by protein kinase C-dependent inhibition of KCNQ5 in A7r5 rat aortic smooth muscle cells. *American journal of physiology Heart and circulatory physiology*, 292(3), H1352-63.
- Burkhard, P., Stetefeld, J., & Strelkov, S. V. (2001). Coiled coils: a highly versatile protein folding motif. *Trends in cell biology*, 11(2), 82-88.
- Busch, A. (1999). Cardiac Ion Channel Genes. *Cellular Physiology and Biochemistry*, 9, 177-178.
- Busson, B. & Doucet, J. (1999). Modeling alpha-helical coiled coils: analytic relations between parameters. *Journal of structural biology*, 127(1), 16-21.
- Caminos, E., Garcia-Pino, E., Martinez-Galan, J. R., & Juiz, J. M. (2007). The potassium

- channel KCNQ5/Kv7.5 is localized in synaptic endings of auditory brainstem nuclei of the rat. *The Journal of comparative neurology*, 505(4), 363-378.
- Carr, C. M. & Kim, P. S. (1993). A spring-loaded mechanism for the conformational change of influenza hemagglutinin. *Cell*, 73(4), 823-832.
- Chambard, J. M. & Ashmore, J. F. (2005). Regulation of the voltage-gated potassium channel KCNQ4 in the auditory pathway. *Pflügers Archiv : European journal of physiology*, 450(1), 34-44.
- Chatelain, F. C., Alagem, N., Xu, Q., Pancaroglu, R., Reuveny, E., & Minor, D. L. (2005). The pore helix dipole has a minor role in inward rectifier channel function. *Neuron*, 47(6), 833-843.
- Chen, H., Kim, L. A., Rajan, S., Xu, S., & Goldstein, S. A. (2003). Charybdotoxin binding in the I(Ks) pore demonstrates two MinK subunits in each channel complex. *Neuron*, 40(1), 15-23.
- Chen, X., Yamakage, M., Yamada, Y., Tohse, N., & Namiki, A. (2002). Inhibitory effects of volatile anesthetics on currents produced on heterologous expression of KvLQT1 and minK in *Xenopus* oocytes. *Vascular pharmacology*, 39(1-2), 33-38.
- Chung, H. J., Jan, Y. N., & Jan, L. Y. (2006). Polarized axonal surface expression of neuronal KCNQ channels is mediated by multiple signals in the KCNQ2 and KCNQ3 C-terminal domains. *Proceedings of the National Academy of Sciences of the United States of America*, 103(23), 8870-8875.
- Cooper, E. C. (2006). Exploiting the Other Inhibitory Ion: KCNQ Potassium Channels and Regulation of Excitability in Developing and Mature Brain. *Epilepsy currents / American Epilepsy Society*, 6(4), 133-135.
- Cooper, E. C. & Jan, L. Y. (2003). M-channels: neurological diseases, neuromodulation, and drug development. *Archives of neurology*, 60(4), 496-500.
- Cordero-Morales, J. F., Cuello, L. G., Zhao, Y., Jogini, V., Cortes, D. M., Roux, B. et al. (2006). Molecular determinants of gating at the potassium-channel selectivity filter. *Nature structural & molecular biology*, 13(4), 311-318.
- Cornea, R. L., Autry, J. M., Chen, Z., & Jones, L. R. (2000). Reexamination of the role of the leucine/isoleucine zipper residues of phospholamban in inhibition of the Ca²⁺ pump of cardiac sarcoplasmic reticulum. *The Journal of biological chemistry*, 275(52), 41487-41494.
- Costa, A. M. & Brown, B. S. (1997). Inhibition of M-current in cultured rat superior cervical ganglia by linopirdine: mechanism of action studies. *Neuropharmacology*, 36(11-12), 1747-1753.
- Crick, F. (1952). Is alpha-keratin a coiled coil? *Nature*, 170(4334), 882-883.
- Crick, F. (1953a). The Fourier Transform of a Coiled-Coil. *Acta Cryst*, 6, 685-689.
- Crick, F. (1953b). The Packing of α -Helices: Simple Coiled-Coils. *Acta Cryst*, 6, 689-697.
- Crivici, A. & Ikura, M. (1995). Molecular and structural basis of target recognition by calmodulin. *Annual review of biophysics and biomolecular structure*, 24, 85-116.
- Dedek, K. & Waldegger, S. (2001). Colocalization of KCNQ1/KCNE channel subunits in the mouse gastrointestinal tract. *Pflügers Archiv : European journal of physiology*, 442(6), 896-902.
- DeLano, W. L. & Brünger, A. T. (1994). Helix packing in proteins: prediction and energetic analysis of dimeric, trimeric, and tetrameric GCN4 coiled coil structures. *Proteins*, 20(2), 105-123.

- Delmas, P. & Brown, D. A. (2005). Pathways modulating neural KCNQ/M (Kv7) potassium channels. *Nature reviews. Neuroscience*, 6(11), 850-862.
- Delmas, P., Wanaverbecq, N., Abogadie, F. C., Mistry, M., & Brown, D. A. (2002). Signaling microdomains define the specificity of receptor-mediated InsP(3) pathways in neurons. *Neuron*, 34(2), 209-220.
- Delorenzi, M. & Speed, T. (2002). An HMM model for coiled-coil domains and a comparison with PSSM-based predictions. *Bioinformatics (Oxford, England)*, 18(4), 617-625.
- Deutsch, C. (2003). The birth of a channel. *Neuron*, 40(2), 265-276.
- Doi, T., Higashino, K., Kurihara, Y., Wada, Y., Miyazaki, T., Nakamura, H. et al. (1993). Charged collagen structure mediates the recognition of negatively charged macromolecules by macrophage scavenger receptors. *The Journal of biological chemistry*, 268(3), 2126-2133.
- Doi, T., Kurasawa, M., Higashino, K., Imanishi, T., Mori, T., Naito, M. et al. (1994). The histidine interruption of an alpha-helical coiled coil allosterically mediates a pH-dependent ligand dissociation from macrophage scavenger receptors. *The Journal of biological chemistry*, 269(41), 25598-25604.
- Doyle, D. A., Morais Cabral, J., Pfuetzner, R. A., Kuo, A., Gulbis, J. M., Cohen, S. L. et al. (1998). The structure of the potassium channel: molecular basis of K⁺ conduction and selectivity. *Science (New York, NY)*, 280(5360), 69-77.
- Dupuis, D. S., Schröder, R. L., Jespersen, T., Christensen, J. K., Christophersen, P., Jensen, B. S. et al. (2002). Activation of KCNQ5 channels stably expressed in HEK293 cells by BMS-204352. *European journal of pharmacology*, 437(3), 129-137.
- Earl, R. A., Zaczek, R., Teleha, C. A., Fisher, B. N., Maciag, C. M., Marynowski, M. E. et al. (1998). 2-Fluoro-4-pyridinylmethyl analogues of linopirdine as orally active acetylcholine release-enhancing agents with good efficacy and duration of action. *Journal of medicinal chemistry*, 41(23), 4615-4622.
- Engel, A. M., Cejka, Z., Lupas, A., Lottspeich, F., & Baumeister, W. (1992). Isolation and cloning of Omp alpha, a coiled-coil protein spanning the periplasmic space of the ancestral eubacterium *Thermotoga maritima*. *The EMBO journal*, 11(12), 4369-4378.
- Etxeberria, A., Aivar, P., Rodriguez-Alfaro, J. A., Alaimo, A., Villacé, P., Gómez-Posada, J. C. et al. (2007). Calmodulin regulates the trafficking of KCNQ2 potassium channels. *FASEB J.*
- Etxeberria, A., Santana-Castro, I., Regalado, M. P., Aivar, P., & Villarroel, A. (2004). Three mechanisms underlie KCNQ2/3 heteromeric potassium M-channel potentiation. *The Journal of neuroscience : the official journal of the Society for Neuroscience*, 24(41), 9146-9152.
- Freeman, L. C., Lippold, J. J., & Mitchell, K. E. (2000). Glycosylation influences gating and pH sensitivity of I(sK). *The Journal of membrane biology*, 177(1), 65-79.
- Gamper, N., Li, Y., & Shapiro, M. S. (2005). Structural requirements for differential sensitivity of KCNQ K⁺ channels to modulation by Ca²⁺/calmodulin. *Molecular biology of the cell*, 16(8), 3538-3551.
- Gamper, N. & Shapiro, M. S. (2007). Target-specific PIP(2) signalling: how might it work? *The Journal of physiology*, 582(Pt 3), 967-975.
- Gamper, N., Zaika, O., Li, Y., Martin, P., Hernandez, C. C., Perez, M. R. et al. (2006). Oxidative modification of M-type K⁺ channels as a mechanism of cytoprotective neuronal silencing. *The EMBO journal*, 25(20), 4996-5004.

- Gernert, K. M., Surlles, M. C., Labean, T. H., Richardson, J. S., & Richardson, D. C. (1995). The Alacoil: a very tight, antiparallel coiled-coil of helices. *Protein science : a publication of the Protein Society*, 4(11), 2252-2260.
- Ghosh, S., Nunziato, D. A., & Pitt, G. S. (2006). KCNQ1 assembly and function is blocked by long-QT syndrome mutations that disrupt interaction with calmodulin. *Circulation research*, 98(8), 1048-1054.
- Gonzalez, L., Brown, R. A., Richardson, D., & Alber, T. (1996a). Crystal structures of a single coiled-coil peptide in two oligomeric states reveal the basis for structural polymorphism. *Nature structural biology*, 3(12), 1002-1009.
- Gonzalez, L., Plecs, J. J., & Alber, T. (1996b). An engineered allosteric switch in leucine-zipper oligomerization. *Nature structural biology*, 3(6), 510-515.
- Gouaux, E. (1998). Single potassium ion seeks open channel for transmembrane travels: tales from the KcsA structure. *Structure (London, England : 1993)*, 6(10), 1221-1226.
- Grunnet, M., Behr, E. R., Calloe, K., Hofman-Bang, J., Till, J., Christiansen, M. et al. (2005). Functional assessment of compound mutations in the KCNQ1 and KCNH2 genes associated with long QT syndrome. *Heart rhythm : the official journal of the Heart Rhythm Society*, 2(11), 1238-1249.
- Gulbis, J. M., Zhou, M., Mann, S., & MacKinnon, R. (2000). Structure of the cytoplasmic beta subunit-T1 assembly of voltage-dependent K⁺ channels. *Science (New York, NY)*, 289(5476), 123-127.
- Gutman, G. A., Chandy, K. G., Adelman, J. P., Aiyar, J., Bayliss, D. A., Clapham, D. E. et al. (2003). International Union of Pharmacology. XLI. Compendium of voltage-gated ion channels: potassium channels. *Pharmacological reviews*, 55(4), 583-586.
- Hadley, J. K., Noda, M., Selyanko, A. A., Wood, I. C., Abogadie, F. C., & Brown, D. A. (2000). Differential tetraethylammonium sensitivity of KCNQ1-4 potassium channels. *British journal of pharmacology*, 129(3), 413-415.
- Hadley, J. K., Passmore, G. M., Tatulian, L., Al-Qatari, M., Ye, F., Wickenden, A. D. et al. (2003). Stoichiometry of expressed KCNQ2/KCNQ3 potassium channels and subunit composition of native ganglionic M channels deduced from block by tetraethylammonium. *The Journal of neuroscience : the official journal of the Society for Neuroscience*, 23(12), 5012-5019.
- Harbury, P. B., Kim, P. S., & Alber, T. (1994). Crystal structure of an isoleucine-zipper trimer. *Nature*, 371(6492), 80-83.
- Harbury, P. B., Plecs, J. J., Tidor, B., Alber, T., & Kim, P. S. (1998). High-resolution protein design with backbone freedom. *Science (New York, NY)*, 282(5393), 1462-1467.
- Harbury, P. B., Tidor, B., & Kim, P. S. (1995). Repacking protein cores with backbone freedom: structure prediction for coiled coils. *Proceedings of the National Academy of Sciences of the United States of America*, 92(18), 8408-8412.
- Harbury, P. B., Zhang, T., Kim, P. S., & Alber, T. (1993). A switch between two-, three-, and four-stranded coiled coils in GCN4 leucine zipper mutants. *Science (New York, NY)*, 262(5138), 1401-1407.
- Hawkins, R. J. & McLeish, T. C. (2006). Dynamic allostery of protein alpha helical coiled-coils. *Journal of the Royal Society, Interface / the Royal Society*, 3(6), 125-138.
- Heginbotham, L., Abramson, T., & MacKinnon, R. (1992). A functional connection between the pores of distantly related ion channels as revealed by mutant K⁺ channels. *Science (New York, NY)*, 258(5085), 1152-1155.

- Heginbotham, L., Odessey, E., & Miller, C. (1997). Tetrameric stoichiometry of a prokaryotic K⁺ channel. *Biochemistry*, 36(33), 10335-10342.
- Hendsch, Z. S. & Tidor, B. (1994). Do salt bridges stabilize proteins? A continuum electrostatic analysis. *Protein science : a publication of the Protein Society*, 3(2), 211-226.
- Higashida, H., Hoshi, N., Zhang, J. S., Yokoyama, S., Hashii, M., Jin, D. et al. (2005). Protein kinase C bound with A-kinase anchoring protein is involved in muscarinic receptor-activated modulation of M-type KCNQ potassium channels. *Neuroscience research*, 51(3), 231-234.
- Hille, B. & Schwarz, W. (1978). Potassium channels as multi-ion single-file pores. *The Journal of general physiology*, 72(4), 409-442.
- Hille, B. (2001). *Ion Channels of Excitable Membranes* (3rd ed.). Sunderland, MA: Sinauer Associates, Inc.
- Hodges, R. S., Saund, A. K., Chong, P. C., St-Pierre, S. A., & Reid, R. E. (1981). Synthetic model for two-stranded alpha-helical coiled-coils. Design, synthesis, and characterization of an 86-residue analog of tropomyosin. *The Journal of biological chemistry*, 256(3), 1214-1224.
- Hodgkin, A. L. & Keynes, R. D. (1955). The potassium permeability of a giant nerve fibre. *The Journal of physiology*, 128(1), 61-88.
- Horowitz, L. F., Hirdes, W., Suh, B. C., Hilgemann, D. W., Mackie, K., & Hille, B. (2005). Phospholipase C in living cells: activation, inhibition, Ca²⁺ requirement, and regulation of M current. *The Journal of general physiology*, 126(3), 243-262.
- Hoshi, N., Zhang, J. S., Omaki, M., Takeuchi, T., Yokoyama, S., Wanaverbecq, N. et al. (2003). AKAP150 signaling complex promotes suppression of the M-current by muscarinic agonists. *Nature neuroscience*, 6(6), 564-571.
- Hougaard, C., Klaerke, D. A., Hoffmann, E. K., Olesen, S. P., & Jorgensen, N. K. (2004). Modulation of KCNQ4 channel activity by changes in cell volume. *Biochimica et biophysica acta*, 1660(1-2), 1-6.
- Howard, R. J., Clark, K. A., Holton, J. M., & Minor, D. L. (2007). Structural insight into KCNQ (Kv7) channel assembly and channelopathy. *Neuron*, 53(5), 663-675.
- Huang, L., Bitner-Glindzicz, M., Tranebjaerg, L., & Tinker, A. (2001). A spectrum of functional effects for disease causing mutations in the Jervell and Lange-Nielsen syndrome. *Cardiovascular research*, 51(4), 670-680.
- Huang, Q., Sivaramakrishna, R. P., Ludwig, K., Korte, T., Böttcher, C., & Herrmann, A. (2003). Early steps of the conformational change of influenza virus hemagglutinin to a fusion active state: stability and energetics of the hemagglutinin. *Biochimica et biophysica acta*, 1614(1), 3-13.
- Isacoff, E. Y., Jan, Y. N., & Jan, L. Y. (1990). Evidence for the formation of heteromultimeric potassium channels in *Xenopus* oocytes. *Nature*, 345(6275), 530-534.
- Janin, J., Miller, S., & Chothia, C. (1988). Surface, subunit interfaces and interior of oligomeric proteins. *Journal of molecular biology*, 204(1), 155-164.
- Jenke, M., Sánchez, A., Monje, F., Stühmer, W., Weseloh, R. M., & Pardo, L. A. (2003). C-terminal domains implicated in the functional surface expression of potassium channels. *The EMBO journal*, 22(3), 395-403.
- Jenkinson, D. H. (2006). Potassium channels--multiplicity and challenges. *British journal of pharmacology*, 147 Suppl 1, S63-71.
- Jespersen, T., Grunnet, M., & Olesen, S. P. (2005). The KCNQ1 potassium channel: from

- gene to physiological function. *Physiology (Bethesda, Md)*, 20, 408-416.
- Jespersen, T., Membrez, M., Nicolas, C. S., Pitard, B., Staub, O., Olesen, S. P. et al. (2007). The KCNQ1 potassium channel is down-regulated by ubiquitylating enzymes of the Nedd4/Nedd4-like family. *Cardiovascular research*, 74(1), 64-74.
- Jespersen, T., Rasmussen, H. B., Grunnet, M., Jensen, H. S., Angelo, K., Dupuis, D. S. et al. (2004). Basolateral localisation of KCNQ1 potassium channels in MDCK cells: molecular identification of an N-terminal targeting motif. *Journal of cell science*, 117(Pt 19), 4517-4526.
- Jiang, Y., Lee, A., Chen, J., Cadene, M., Chait, B. T., & MacKinnon, R. (2002). Crystal structure and mechanism of a calcium-gated potassium channel. *Nature*, 417(6888), 515-522.
- Jiang, Y., Lee, A., Chen, J., Ruta, V., Cadene, M., Chait, B. T. et al. (2003). X-ray structure of a voltage-dependent K⁺ channel. *Nature*, 423(6935), 33-41.
- Junius, F. K., Mackay, J. P., Bubb, W. A., Jensen, S. A., Weiss, A. S., & King, G. F. (1995). Nuclear magnetic resonance characterization of the Jun leucine zipper domain: unusual properties of coiled-coil interfacial polar residues. *Biochemistry*, 34(18), 6164-6174.
- Kammerer, R. A., Schulthess, T., Landwehr, R., Lustig, A., Engel, J., Aebi, U. et al. (1998). An autonomous folding unit mediates the assembly of two-stranded coiled coils. *Proceedings of the National Academy of Sciences of the United States of America*, 95(23), 13419-13424.
- Kanki, H., Kupersmidt, S., Yang, T., Wells, S., & Roden, D. M. (2004). A structural requirement for processing the cardiac K⁺ channel KCNQ1. *The Journal of biological chemistry*, 279(32), 33976-33983.
- Kavinsky, C. J., Umeda, P. K., Sinha, A. M., Elzinga, M., Tong, S. W., Zak, R. et al. (1983). Cloned mRNA sequences for two types of embryonic myosin heavy chains from chick skeletal muscle. I. DNA and derived amino acid sequence of light meromyosin. *The Journal of biological chemistry*, 258(8), 5196-5205.
- Kharkovets, T., Hardelin, J. P., Safieddine, S., Schweizer, M., El-Amraoui, A., Petit, C. et al. (2000). KCNQ4, a K⁺ channel mutated in a form of dominant deafness, is expressed in the inner ear and the central auditory pathway. *Proceedings of the National Academy of Sciences of the United States of America*, 97(8), 4333-4338.
- Kreusch, A., Pfaffinger, P. J., Stevens, C. F., & Choe, S. (1998). Crystal structure of the tetramerization domain of the Shaker potassium channel. *Nature*, 392(6679), 945-948.
- Krylov, D., Barchi, J., & Vinson, C. (1998). Inter-helical interactions in the leucine zipper coiled coil dimer: pH and salt dependence of coupling energy between charged amino acids. *Journal of molecular biology*, 279(4), 959-972.
- Krylov, D., Mikhailenko, I., & Vinson, C. (1994). A thermodynamic scale for leucine zipper stability and dimerization specificity: e and g interhelical interactions. *The EMBO journal*, 13(12), 2849-2861.
- Kubisch, C., Schroeder, B. C., Friedrich, T., Lütjohann, B., El-Amraoui, A., Marlin, S. et al. (1999). KCNQ4, a novel potassium channel expressed in sensory outer hair cells, is mutated in dominant deafness. *Cell*, 96(3), 437-446.
- Kuo, A., Gulbis, J. M., Antcliff, J. F., Rahman, T., Lowe, E. D., Zimmer, J. et al. (2003). Crystal structure of the potassium channel KirBac1.1 in the closed state. *Science (New York, NY)*, 300(5627), 1922-1926.

- Kurokawa, J., Chen, L., & Kass, R. S. (2003). Requirement of subunit expression for cAMP-mediated regulation of a heart potassium channel. *Proceedings of the National Academy of Sciences of the United States of America*, *100*(4), 2122-2127.
- Kurokawa, J., Motoike, H. K., Rao, J., & Kass, R. S. (2004). Regulatory actions of the A-kinase anchoring protein Yotiao on a heart potassium channel downstream of PKA phosphorylation. *Proceedings of the National Academy of Sciences of the United States of America*, *101*(46), 16374-16378.
- Lauzon, A. M., Fagnant, P. M., Warshaw, D. M., & Trybus, K. M. (2001). Coiled-coil unwinding at the smooth muscle myosin head-rod junction is required for optimal mechanical performance. *Biophysical journal*, *80*(4), 1900-1904.
- Leonard, A. S., Yermolaieva, O., Hruska-Hageman, A., Askwith, C. C., Price, M. P., Wemmie, J. A. et al. (2003). cAMP-dependent protein kinase phosphorylation of the acid-sensing ion channel-1 regulates its binding to the protein interacting with C-kinase-1. *Proceedings of the National Academy of Sciences of the United States of America*, *100*(4), 2029-2034.
- Lerche, C., Bruhova, I., Lerche, H., Steinmeyer, K., Wei, A. D., Strutz-Seebohm, N. et al. (2007). Chromanol 293B binding in KCNQ1 (Kv7.1) channels involves electrostatic interactions with a potassium ion in the selectivity filter. *Molecular pharmacology*, *71*(6), 1503-1511.
- Lerche, C., Scherer, C. R., Seebohm, G., Derst, C., Wei, A. D., Busch, A. E. et al. (2000). Molecular cloning and functional expression of KCNQ5, a potassium channel subunit that may contribute to neuronal M-current diversity. *The Journal of biological chemistry*, *275*(29), 22395-22400.
- Li, M., Jan, Y. N., & Jan, L. Y. (1992). Specification of subunit assembly by the hydrophilic amino-terminal domain of the Shaker potassium channel. *Science (New York, NY)*, *257*(5074), 1225-1230.
- Li, M., Unwin, N., Stauffer, K. A., Jan, Y. N., & Jan, L. Y. (1994). Images of purified Shaker potassium channels. *Current biology : CB*, *4*(2), 110-115.
- Li, Y., Brown, J. H., Reshetnikova, L., Blazsek, A., Farkas, L., Nyitray, L. et al. (2003). Visualization of an unstable coiled coil from the scallop myosin rod. *Nature*, *424*(6946), 341-345.
- Li, Y., Gamper, N., Hilgemann, D. W., & Shapiro, M. S. (2005). Regulation of Kv7 (KCNQ) K⁺ channel open probability by phosphatidylinositol 4,5-bisphosphate. *The Journal of neuroscience : the official journal of the Society for Neuroscience*, *25*(43), 9825-9835.
- Li, Y., Gamper, N., & Shapiro, M. S. (2004a). Single-channel analysis of KCNQ K⁺ channels reveals the mechanism of augmentation by a cysteine-modifying reagent. *The Journal of neuroscience : the official journal of the Society for Neuroscience*, *24*(22), 5079-5090.
- Li, Y., Langlais, P., Gamper, N., Liu, F., & Shapiro, M. S. (2004b). Dual phosphorylations underlie modulation of unitary KCNQ K⁺ channels by Src tyrosine kinase. *The Journal of biological chemistry*, *279*(44), 45399-45407.
- Liang, W., Warrick, H. M., & Spudich, J. A. (1999). A structural model for phosphorylation control of Dictyostelium myosin II thick filament assembly. *The Journal of cell biology*, *147*(5), 1039-1048.
- Lieberman, E. A. & Skulachev, V. P. (1970). Conversion of biomembrane-produced energy into electric form. IV. General discussion. *Biochimica et biophysica acta*, *216*(1), 30-42.

- Liu, J., Cao, W., & Lu, M. (2002). Core side-chain packing and backbone conformation in Lpp-56 coiled-coil mutants. *Journal of molecular biology*, 318(3), 877-888.
- Liu, J., Zheng, Q., Deng, Y., Cheng, C. S., Kallenbach, N. R., & Lu, M. (2006). A seven-helix coiled coil. *Proceedings of the National Academy of Sciences of the United States of America*, 103(42), 15457-15462.
- Long, S. B., Campbell, E. B., & Mackinnon, R. (2005). Crystal structure of a mammalian voltage-dependent Shaker family K⁺ channel. *Science (New York, N.Y.)*, 309(5736), 897-903.
- Long, S. B., Tao, X., Campbell, E. B., & MacKinnon, R. (2007). Atomic structure of a voltage-dependent K⁺ channel in a lipid membrane-like environment. *Nature*, 450(7168), 376-382.
- Loussouarn, G., Park, K. H., Bellocq, C., Baró, I., Charpentier, F., & Escande, D. (2003). Phosphatidylinositol-4,5-bisphosphate, PIP₂, controls KCNQ1/KCNE1 voltage-gated potassium channels: a functional homology between voltage-gated and inward rectifier K⁺ channels. *The EMBO journal*, 22(20), 5412-5421.
- Lu, J., Robinson, J. M., Edwards, D., & Deutsch, C. (2001). T1-T1 interactions occur in ER membranes while nascent Kv peptides are still attached to ribosomes. *Biochemistry*, 40(37), 10934-10946.
- Lumb, K. J. & Kim, P. S. (1995). A buried polar interaction imparts structural uniqueness in a designed heterodimeric coiled coil. *Biochemistry*, 34(27), 8642-8648.
- Lundquist, A. L., Manderfield, L. J., Vanoye, C. G., Rogers, C. S., Donahue, B. S., Chang, P. A. et al. (2005). Expression of multiple KCNE genes in human heart may enable variable modulation of I(Ks). *Journal of molecular and cellular cardiology*, 38(2), 277-287.
- Lupas, A. (1996). Coiled coils: new structures and new functions. *Trends in biochemical sciences*, 21(10), 375-382.
- Lupoglazoff, J. M., Denjoy, I., Villain, E., Fressart, V., Simon, F., Bozio, A. et al. (2004). Long QT syndrome in neonates: conduction disorders associated with HERG mutations and sinus bradycardia with KCNQ1 mutations. *Journal of the American College of Cardiology*, 43(5), 826-830.
- MacKinnon, R. (1991). Determination of the subunit stoichiometry of a voltage-activated potassium channel. *Nature*, 350(6315), 232-235.
- MacKinnon, R., Aldrich, R. W., & Lee, A. W. (1993). Functional stoichiometry of Shaker potassium channel inactivation. *Science (New York, NY)*, 262(5134), 757-759.
- Maljevic, S., Lerche, C., Seeböhm, G., Alekov, A. K., Busch, A. E., & Lerche, H. (2003). C-terminal interaction of KCNQ2 and KCNQ3 K⁺ channels. *The Journal of physiology*, 548(Pt 2), 353-360.
- Marcus, D. C., Sunose, H., Liu, J., Shen, Z., & Scofield, M. A. (1997). P2U purinergic receptor inhibits apical IsK/KvLQT1 channel via protein kinase C in vestibular dark cells. *The American journal of physiology*, 273(6 Pt 1), C2022-9.
- Marrion, N. V. (1997). Control of M-current. *Annual review of physiology*, 59, 483-504.
- Marrion, N. V., Zucker, R. S., Marsh, S. J., & Adams, P. R. (1991). Modulation of M-current by intracellular Ca²⁺. *Neuron*, 6(4), 533-545.
- Marti, D. N. & Bosshard, H. R. (2003). Electrostatic interactions in leucine zippers: thermodynamic analysis of the contributions of Glu and His residues and the effect of mutating salt bridges. *Journal of molecular biology*, 330(3), 621-637.
- Marx, S. O., Kurokawa, J., Reiken, S., Motoike, H., D'Armiento, J., Marks, A. R. et al.

- (2002). Requirement of a macromolecular signaling complex for beta adrenergic receptor modulation of the KCNQ1-KCNE1 potassium channel. *Science (New York, N.Y.)*, 295(5554), 496-499.
- Matousek, W. M., Ciani, B., Fitch, C. A., Garcia-Moreno E, B., Kammerer, R. A., & Alexandrescu, A. T. (2007). Electrostatic Contributions to the Stability of the GCN4 Leucine Zipper Structure. *Journal of molecular biology*, 374(1), 206-219.
- Mazhari, R., Nuss, H. B., Armoundas, A. A., Winslow, R. L., & Marbán, E. (2002). Ectopic expression of KCNE3 accelerates cardiac repolarization and abbreviates the QT interval. *The Journal of clinical investigation*, 109(8), 1083-1090.
- Melman, Y. F., Um, S. Y., Krumerman, A., Kagan, A., & McDonald, T. V. (2004). KCNE1 binds to the KCNQ1 pore to regulate potassium channel activity. *Neuron*, 42(6), 927-937.
- Minor, D. L., Lin, Y. F., Mobley, B. C., Avelar, A., Jan, Y. N., Jan, L. Y. et al. (2000). The polar T1 interface is linked to conformational changes that open the voltage-gated potassium channel. *Cell*, 102(5), 657-670.
- Monera, O. D., Zhou, N. E., Lavigne, P., Kay, C. M., & Hodges, R. S. (1996). Formation of parallel and antiparallel coiled-coils controlled by the relative positions of alanine residues in the hydrophobic core. *The Journal of biological chemistry*, 271(8), 3995-4001.
- Munro, G. & Dalby-Brown, W. (2007). Kv7 (KCNQ) channel modulators and neuropathic pain. *Journal of medicinal chemistry*, 50(11), 2576-2582.
- Murata, Y., Iwasaki, H., Sasaki, M., Inaba, K., & Okamura, Y. (2005). Phosphoinositide phosphatase activity coupled to an intrinsic voltage sensor. *Nature*, 435(7046), 1239-1243.
- Nerbonne, J. M. & Kass, R. S. (2005). Molecular physiology of cardiac repolarization. *Physiological reviews*, 85(4), 1205-1253.
- Newman, J. R. & Keating, A. E. (2003). Comprehensive identification of human bZIP interactions with coiled-coil arrays. *Science (New York, NY)*, 300(5628), 2097-2101.
- Newman, J. R., Wolf, E., & Kim, P. S. (2000). A computationally directed screen identifying interacting coiled coils from *Saccharomyces cerevisiae*. *Proceedings of the National Academy of Sciences of the United States of America*, 97(24), 13203-13208.
- Neyroud, N., Tesson, F., Denjoy, I., Leibovici, M., Donger, C., Barhanin, J. et al. (1997). A novel mutation in the potassium channel gene KVLQT1 causes the Jervell and Lange-Nielsen cardioauditory syndrome. *Nature genetics*, 15(2), 186-189.
- Nishikawa, K. & Scheraga, H. A. (1976). Geometrical criteria for formation of coiled-coil structures of polypeptide chains. *Macromolecules*, 9(3), 395-407.
- Nitta, J., Furukawa, T., Marumo, F., Sawanobori, T., & Hiraoka, M. (1994). Subcellular mechanism for Ca²⁺-dependent enhancement of delayed rectifier K⁺ current in isolated membrane patches of guinea pig ventricular myocytes. *Circulation research*, 74(1), 96-104.
- O'Shea, E. K., Klemm, J. D., Kim, P. S., & Alber, T. (1991). X-ray structure of the GCN4 leucine zipper, a two-stranded, parallel coiled coil. *Science (New York, NY)*, 254(5031), 539-544.
- O'Shea, E. K., Lumb, K. J., & Kim, P. S. (1993). Peptide 'Velcro': design of a heterodimeric coiled coil. *Current biology : CB*, 3(10), 658-667.
- O'Shea, E. K., Rutkowski, R., & Kim, P. S. (1992). Mechanism of specificity in the Fos-Jun oncoprotein heterodimer. *Cell*, 68(4), 699-708.

- O'Shea, E. K., Rutkowski, R., Stafford, W. F., & Kim, P. S. (1989). Preferential heterodimer formation by isolated leucine zippers from fos and jun. *Science (New York, NY)*, 245(4918), 646-648.
- Oakley, M. G. & Kim, P. S. (1998). A buried polar interaction can direct the relative orientation of helices in a coiled coil. *Biochemistry*, 37(36), 12603-12610.
- Offer, G. & Sessions, R. (1995). Computer modelling of the alpha-helical coiled coil: packing of side-chains in the inner core. *Journal of molecular biology*, 249(5), 967-987.
- Pan, X. & Heitman, J. (2002). Protein kinase A operates a molecular switch that governs yeast pseudohyphal differentiation. *Molecular and cellular biology*, 22(12), 3981-3993.
- Papazian, D. M. (1999). Potassium channels: some assembly required. *Neuron*, 23(1), 7-10.
- Park, K. H., Piron, J., Dahimene, S., Mérot, J., Baró, I., Escande, D. et al. (2005). Impaired KCNQ1-KCNE1 and phosphatidylinositol-4,5-bisphosphate interaction underlies the long QT syndrome. *Circulation research*, 96(7), 730-739.
- Parsegian, A. (1969). Energy of an ion crossing a low dielectric membrane: solutions to four relevant electrostatic problems. *Nature*, 221(5183), 844-846.
- Passmore, G. M., Selyanko, A. A., Mistry, M., Al-Qatari, M., Marsh, S. J., Matthews, E. A. et al. (2003). KCNQ/M currents in sensory neurons: significance for pain therapy. *The Journal of neuroscience : the official journal of the Society for Neuroscience*, 23(18), 7227-7236.
- Pelletier, J. N., Arndt, K. M., Plückthun, A., & Michnick, S. W. (1999). An in vivo library-versus-library selection of optimized protein-protein interactions. *Nature biotechnology*, 17(7), 683-690.
- Peretz, A., Degani, N., Nachman, R., Uziyel, Y., Gibor, G., Shabat, D. et al. (2005). Meclofenamic acid and diclofenac, novel templates of KCNQ2/Q3 potassium channel openers, depress cortical neuron activity and exhibit anticonvulsant properties. *Molecular pharmacology*, 67(4), 1053-1066.
- Phillips, G. N., Flicker, P. F., Cohen, C., Manjula, B. N., & Fischetti, V. A. (1981). Streptococcal M protein: alpha-helical coiled-coil structure and arrangement on the cell surface. *Proceedings of the National Academy of Sciences of the United States of America*, 78(8), 4689-4693.
- Piippo, K., Swan, H., Pasternack, M., Chapman, H., Paavonen, K., Viitasalo, M. et al. (2001). A founder mutation of the potassium channel KCNQ1 in long QT syndrome: implications for estimation of disease prevalence and molecular diagnostics. *Journal of the American College of Cardiology*, 37(2), 562-568.
- Plosker, G. L. & Scott, L. J. (2006). Retigabine: in partial seizures. *CNS drugs*, 20(7), 601-8; discussion 609-10.
- Potekhin, S. A., Medvedkin, V. N., Kashparov, I. A., & SYu, V. (1994). Synthesis and properties of the peptide corresponding to the mutant form of the leucine zipper of the transcriptional activator GCN4 from yeast. *Protein engineering*, 7(9), 1097-1101.
- Poulsen, A. N. & Klaerke, D. A. (2007). The KCNE1 beta-subunit exerts a transient effect on the KCNQ1 K⁺ channel. *Biochemical and biophysical research communications*, 363(1), 133-139.
- Ravn, L. S., Hofman-Bang, J., Dixen, U., Larsen, S. O., Jensen, G., Haunsø, S. et al. (2005). Relation of 97T polymorphism in KCNE5 to risk of atrial fibrillation. *The American journal of cardiology*, 96(3), 405-407.
- Robbins, J. (2001). KCNQ potassium channels: physiology, pathophysiology, and

- pharmacology. *Pharmacology & therapeutics*, 90(1), 1-19.
- Robbins, J., Marsh, S. J., & Brown, D. A. (2006). Probing the regulation of M (Kv7) potassium channels in intact neurons with membrane-targeted peptides. *The Journal of neuroscience : the official journal of the Society for Neuroscience*, 26(30), 7950-7961.
- Roche, J. P., Westenbroek, R., Sorom, A. J., Hille, B., Mackie, K., & Shapiro, M. S. (2002). Antibodies and a cysteine-modifying reagent show correspondence of M current in neurons to KCNQ2 and KCNQ3 K⁺ channels. *British journal of pharmacology*, 137(8), 1173-1186.
- Rogawski, M. A. (2000). KCNQ2/KCNQ3 K⁺ channels and the molecular pathogenesis of epilepsy: implications for therapy. *Trends in neurosciences*, 23(9), 393-398.
- Rostock, A., Tober, C., Rundfeldt, C., Bartsch, R., Engel, J., Polymeropoulos, E. E. et al. (1996). D-23129: a new anticonvulsant with a broad spectrum activity in animal models of epileptic seizures. *Epilepsy research*, 23(3), 211-223.
- Sanguinetti, M. C., Curran, M. E., Zou, A., Shen, J., Spector, P. S., Atkinson, D. L. et al. (1996). Coassembly of K(V)LQT1 and minK (IsK) proteins to form cardiac I(Ks) potassium channel. *Nature*, 384(6604), 80-83.
- Sasaki, M., Takagi, M., & Okamura, Y. (2006). A voltage sensor-domain protein is a voltage-gated proton channel. *Science (New York, NY)*, 312(5773), 589-592.
- Saucerman, J. J., Healy, S. N., Belik, M. E., Puglisi, J. L., & McCulloch, A. D. (2004). Proarrhythmic consequences of a KCNQ1 AKAP-binding domain mutation: computational models of whole cells and heterogeneous tissue. *Circulation research*, 95(12), 1216-1224.
- Schmitt, N., Schwarz, M., Peretz, A., Abitbol, I., Attali, B., & Pongs, O. (2000). A recessive C-terminal Jervell and Lange-Nielsen mutation of the KCNQ1 channel impairs subunit assembly. *The EMBO journal*, 19(3), 332-340.
- Schnarr, N. A. & Kennan, A. J. (2002). Peptide tic-tac-toe: heterotrimeric coiled-coil specificity from steric matching of multiple hydrophobic side chains. *Journal of the American Chemical Society*, 124(33), 9779-9783.
- Schnell, J. R., Zhou, G. P., Zweckstetter, M., Rigby, A. C., & Chou, J. J. (2005). Rapid and accurate structure determination of coiled-coil domains using NMR dipolar couplings: application to cGMP-dependent protein kinase I α . *Protein science : a publication of the Protein Society*, 14(9), 2421-2428.
- Schoppa, N. E., McCormack, K., Tanouye, M. A., & Sigworth, F. J. (1992). The size of gating charge in wild-type and mutant Shaker potassium channels. *Science (New York, NY)*, 255(5052), 1712-1715.
- Schrempf, H., Schmidt, O., Kümmerlen, R., Hinnah, S., Müller, D., Betzler, M. et al. (1995). A prokaryotic potassium ion channel with two predicted transmembrane segments from *Streptomyces lividans*. *The EMBO journal*, 14(21), 5170-5178.
- Schroeder, B. C., Hechenberger, M., Weinreich, F., Kubisch, C., & Jentsch, T. J. (2000). KCNQ5, a novel potassium channel broadly expressed in brain, mediates M-type currents. *The Journal of biological chemistry*, 275(31), 24089-24095.
- Schroeder, B. C., Kubisch, C., Stein, V., & Jentsch, T. J. (1998). Moderate loss of function of cyclic-AMP-modulated KCNQ2/KCNQ3 K⁺ channels causes epilepsy. *Nature*, 396(6712), 687-690.
- Schulteis, C. T., Nagaya, N., & Papazian, D. M. (1996). Intersubunit interaction between amino- and carboxyl-terminal cysteine residues in tetrameric shaker K⁺ channels. *Biochemistry*, 35(37), 12133-12140.

- Schulteis, C. T., Nagaya, N., & Papazian, D. M. (1998). Subunit folding and assembly steps are interspersed during Shaker potassium channel biogenesis. *The Journal of biological chemistry*, 273(40), 26210-26217.
- Schulz, G. E. (1996). Porins: general to specific, native to engineered passive pores. *Current opinion in structural biology*, 6(4), 485-490.
- Schwake, M., Athanasiadu, D., Beimgraben, C., Blanz, J., Beck, C., Jentsch, T. J. et al. (2006). Structural determinants of M-type KCNQ (Kv7) K⁺ channel assembly. *The Journal of neuroscience : the official journal of the Society for Neuroscience*, 26(14), 3757-3766.
- Schwake, M., Jentsch, T. J., & Friedrich, T. (2003). A carboxy-terminal domain determines the subunit specificity of KCNQ K⁺ channel assembly. *EMBO reports*, 4(1), 76-81.
- Schwake, M., Pusch, M., Kharkovets, T., & Jentsch, T. J. (2000). Surface expression and single channel properties of KCNQ2/KCNQ3, M-type K⁺ channels involved in epilepsy. *The Journal of biological chemistry*, 275(18), 13343-13348.
- Schwartz, P. J., Priori, S. G., Spazzolini, C., Moss, A. J., Vincent, G. M., Napolitano, C. et al. (2001). Genotype-phenotype correlation in the long-QT syndrome: gene-specific triggers for life-threatening arrhythmias. *Circulation*, 103(1), 89-95.
- Seeböhm, G., Chen, J., Strutz, N., Culbertson, C., Lerche, C., & Sanguinetti, M. C. (2003a). Molecular determinants of KCNQ1 channel block by a benzodiazepine. *Molecular pharmacology*, 64(1), 70-77.
- Seeböhm, G., Pusch, M., Chen, J., & Sanguinetti, M. C. (2003b). Pharmacological activation of normal and arrhythmia-associated mutant KCNQ1 potassium channels. *Circulation research*, 93(10), 941-947.
- Selyanko, A. A. & Brown, D. A. (1996). Intracellular calcium directly inhibits potassium M channels in excised membrane patches from rat sympathetic neurons. *Neuron*, 16(1), 151-162.
- Selyanko, A. A., Hadley, J. K., Wood, I. C., Abogadie, F. C., Jentsch, T. J., & Brown, D. A. (2000). Inhibition of KCNQ1-4 potassium channels expressed in mammalian cells via M1 muscarinic acetylcholine receptors. *The Journal of physiology*, 522 Pt 3, 349-355.
- Seo, J. & Cohen, C. (1993). Pitch diversity in alpha-helical coiled coils. *Proteins*, 15(3), 223-234.
- Shen, N. V., Chen, X., Boyer, M. M., & Pfaffinger, P. J. (1993). Deletion analysis of K⁺ channel assembly. *Neuron*, 11(1), 67-76.
- Shen, Z. & Marcus, D. C. (1998). Divalent cations inhibit IsK/KvLQT1 channels in excised membrane patches of strial marginal cells. *Hearing research*, 123(1-2), 157-167.
- Shu, W., Liu, J., Ji, H., & Lu, M. (2000). Core structure of the outer membrane lipoprotein from Escherichia coli at 1.9 Å resolution. *Journal of molecular biology*, 299(4), 1101-1112.
- Smith, J. S., Iannotti, C. A., Dargis, P., Christian, E. P., & Aiyar, J. (2001). Differential expression of kcnq2 splice variants: implications to m current function during neuronal development. *The Journal of neuroscience : the official journal of the Society for Neuroscience*, 21(4), 1096-1103.
- Sodek, J., Hodges, R. S., Smillie, L. B., & Jurasek, L. (1972). Amino-acid sequence of rabbit skeletal tropomyosin and its coiled-coil structure. *Proceedings of the National Academy of Sciences of the United States of America*, 69(12), 3800-3804.

- Söllner, T., Bennett, M. K., Whiteheart, S. W., Scheller, R. H., & Rothman, J. E. (1993). A protein assembly-disassembly pathway in vitro that may correspond to sequential steps of synaptic vesicle docking, activation, and fusion. *Cell*, 75(3), 409-418.
- Spencer, R. H., Sokolov, Y., Li, H., Takenaka, B., Milici, A. J., Aiyar, J. et al. (1997). Purification, visualization, and biophysical characterization of Kv1.3 tetramers. *The Journal of biological chemistry*, 272(4), 2389-2395.
- Splawski, I., Tristani-Firouzi, M., Lehmann, M. H., Sanguinetti, M. C., & Keating, M. T. (1997). Mutations in the hminK gene cause long QT syndrome and suppress IKs function. *Nature genetics*, 17(3), 338-340.
- Steinmetz, M. O., Jelesarov, I., Matousek, W. M., Honnappa, S., Jahnke, W., Missimer, J. H. et al. (2007). Molecular basis of coiled-coil formation. *Proceedings of the National Academy of Sciences of the United States of America*, 104(17), 7062-7067.
- Strutz-Seebohm, N., Seebohm, G., Fedorenko, O., Baltaev, R., Engel, J., Knirsch, M. et al. (2006). Functional coassembly of KCNQ4 with KCNE-beta- subunits in *Xenopus* oocytes. *Cellular physiology and biochemistry : international journal of experimental cellular physiology, biochemistry, and pharmacology*, 18(1-3), 57-66.
- Sutton, R. B., Fasshauer, D., Jahn, R., & Brunger, A. T. (1998). Crystal structure of a SNARE complex involved in synaptic exocytosis at 2.4 Å resolution. *Nature*, 395(6700), 347-353.
- Suzuki, K., Doi, T., Imanishi, T., Kodama, T., & Tanaka, T. (1997). The conformation of the alpha-helical coiled coil domain of macrophage scavenger receptor is pH dependent. *Biochemistry*, 36(49), 15140-15146.
- Syme, C. A., Hamilton, K. L., Jones, H. M., Gerlach, A. C., Giltinan, L., Papworth, G. D. et al. (2003). Trafficking of the Ca²⁺-activated K⁺ channel, hK1, is dependent upon a C-terminal leucine zipper. *The Journal of biological chemistry*, 278(10), 8476-8486.
- Szilák, L., Moitra, J., Krylov, D., & Vinson, C. (1997a). Phosphorylation destabilizes alpha-helices. *Nature structural biology*, 4(2), 112-114.
- Szilák, L., Moitra, J., & Vinson, C. (1997b). Design of a leucine zipper coiled coil stabilized 1.4 kcal mol⁻¹ by phosphorylation of a serine in the e position. *Protein science : a publication of the Protein Society*, 6(6), 1273-1283.
- Tempel, B. L., Papazian, D. M., Schwarz, T. L., Jan, Y. N., & Jan, L. Y. (1987). Sequence of a probable potassium channel component encoded at Shaker locus of *Drosophila*. *Science (New York, NY)*, 237(4816), 770-775.
- Bendahhou, S., Marionneau, C., Haurogne, K., Larroque, M. M., Derand, R., Szuts, V. et al. (2005). In vitro molecular interactions and distribution of KCNE family with KCNQ1 in the human heart. *Cardiovascular research*, 67(3), 529-538.
- Terrenoire, C., Clancy, C. E., Cormier, J. W., Sampson, K. J., & Kass, R. S. (2005). Autonomic control of cardiac action potentials: role of potassium channel kinetics in response to sympathetic stimulation. *Circulation research*, 96(5), e25-34.
- Tester, D. J., Will, M. L., Haglund, C. M., & Ackerman, M. J. (2005). Compendium of cardiac channel mutations in 541 consecutive unrelated patients referred for long QT syndrome genetic testing. *Heart rhythm : the official journal of the Heart Rhythm Society*, 2(5), 507-517.
- Tian, C., Vanoye, C. G., Kang, C., Welch, R. C., Kim, H. J., George, A. L. et al. (2007). Preparation, functional characterization, and NMR studies of human KCNE1, a voltage-gated potassium channel accessory subunit associated with deafness and long QT syndrome. *Biochemistry*, 46(41), 11459-11472.

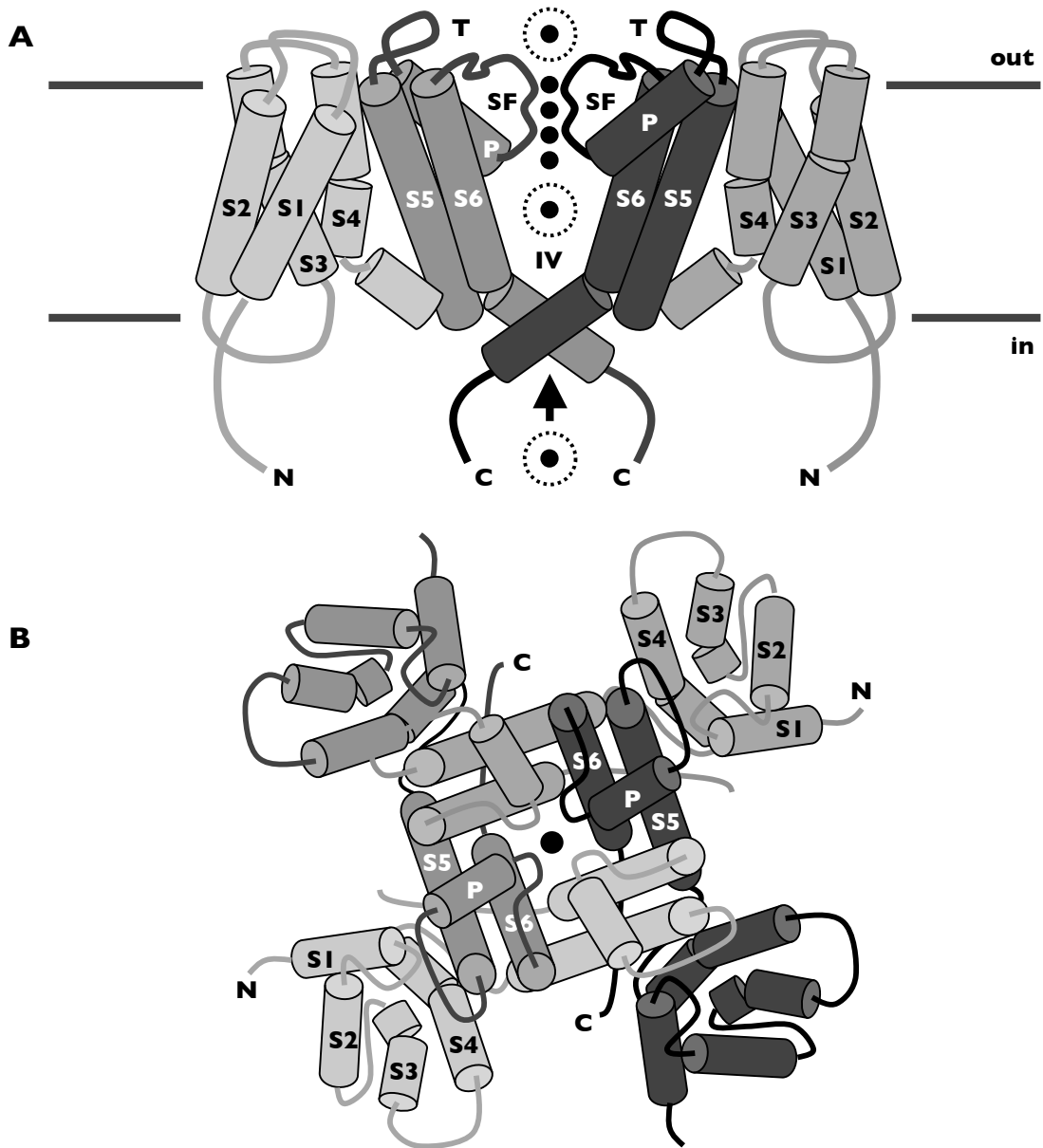
- Tinel, N., Diochot, S., Lauritzen, I., Barhanin, J., Lazdunski, M., & Borsotto, M. (2000). M-type KCNQ2-KCNQ3 potassium channels are modulated by the KCNE2 subunit. *FEBS letters*, 480(2-3), 137-141.
- Tripet, B., Wagschal, K., Lavigne, P., Mant, C. T., & Hodges, R. S. (2000). Effects of side-chain characteristics on stability and oligomerization state of a de novo-designed model coiled-coil: 20 amino acid substitutions in position "d". *Journal of molecular biology*, 300(2), 377-402.
- Tsuruda, P. R., Julius, D., & Minor, D. L. (2006). Coiled coils direct assembly of a cold-activated TRP channel. *Neuron*, 51(2), 201-212.
- Varro, A., Baláti, B., Iost, N., Takács, J., Virág, L., Lathrop, D. A. et al. (2000). The role of the delayed rectifier component IKs in dog ventricular muscle and Purkinje fibre repolarization. *The Journal of physiology*, 523 Pt 1, 67-81.
- Vinson, C. R., Hai, T., & Boyd, S. M. (1993). Dimerization specificity of the leucine zipper-containing bZIP motif on DNA binding: prediction and rational design. *Genes & development*, 7(6), 1047-1058.
- Walshaw, J. & Woolfson, D. N. (2001). Socket: a program for identifying and analysing coiled-coil motifs within protein structures. *Journal of molecular biology*, 307(5), 1427-1450.
- Wang, H. S., Pan, Z., Shi, W., Brown, B. S., Wymore, R. S., Cohen, I. S. et al. (1998). KCNQ2 and KCNQ3 potassium channel subunits: molecular correlates of the M-channel. *Science (New York, NY)*, 282(5395), 1890-1893.
- Wang, K. W., Tai, K. K., & Goldstein, S. A. (1996a). MinK residues line a potassium channel pore. *Neuron*, 16(3), 571-577.
- Wang, Q., Curran, M. E., Splawski, I., Burn, T. C., Millholland, J. M., VanRaay, T. J. et al. (1996b). Positional cloning of a novel potassium channel gene: KVLQT1 mutations cause cardiac arrhythmias. *Nature genetics*, 12(1), 17-23.
- Wangemann, P., Liu, J., & Marcus, D. C. (1995). Ion transport mechanisms responsible for K⁺ secretion and the transepithelial voltage across marginal cells of stria vascularis in vitro. *Hearing research*, 84(1-2), 19-29.
- Wehling, C., Beimgraben, C., Gelhaus, C., Friedrich, T., Saftig, P., Grötzinger, J. et al. (2007). Self-assembly of the isolated KCNQ2 subunit interaction domain. *FEBS letters*, 581(8), 1594-1598.
- Wen, H. & Levitan, I. B. (2002). Calmodulin is an auxiliary subunit of KCNQ2/3 potassium channels. *The Journal of neuroscience : the official journal of the Society for Neuroscience*, 22(18), 7991-8001.
- Wickenden, A. D., McNaughton-Smith, G., Roeloffs, R., London, B., Clark, S., Wilson, W. A. et al. (2005). ICA-27243: A novel, potent, and selective KCNQ2/Q3 potassium channel activator. *Soc. Neurosci. Abst. Prog.*, 153, 13.
- Wickenden, A. D., Yu, W., Zou, A., Jegla, T., & Wagoner, P. K. (2000). Retigabine, a novel anti-convulsant, enhances activation of KCNQ2/Q3 potassium channels. *Molecular pharmacology*, 58(3), 591-600.
- Wilson, A. J., Quinn, K. V., Graves, F. M., Bitner-Glindzicz, M., & Tinker, A. (2005). Abnormal KCNQ1 trafficking influences disease pathogenesis in hereditary long QT syndromes (LQTI). *Cardiovascular research*, 67(3), 476-486.
- Wolf, E., Kim, P. S., & Berger, B. (1997). MultiCoil: a program for predicting two- and three-stranded coiled coils. *Protein science : a publication of the Protein Society*, 6(6), 1179-1189.

- Wollnik, B., Schroeder, B. C., Kubisch, C., Esperer, H. D., Wieacker, P., & Jentsch, T. J. (1997). Pathophysiological mechanisms of dominant and recessive KVLQT1 K⁺ channel mutations found in inherited cardiac arrhythmias. *Human molecular genetics*, 6(11), 1943-1949.
- Wong, W. & Scott, J. D. (2004a). AKAP signalling complexes: focal points in space and time. *Nature reviews Molecular cell biology*, 5(12), 959-970.
- Wong, W. H., Hurley, K. M., & Eatock, R. A. (2004b). Differences between the negatively activating potassium conductances of Mammalian cochlear and vestibular hair cells. *Journal of the Association for Research in Otolaryngology : JARO*, 5(3), 270-284.
- Woolfson, D. N. & Alber, T. (1995). Predicting oligomerization states of coiled coils. *Protein science : a publication of the Protein Society*, 4(8), 1596-1607.
- Wuttke, T. V., Seebohm, G., Bail, S., Maljevic, S., & Lerche, H. (2005). The new anticonvulsant retigabine favors voltage-dependent opening of the Kv7.2 (KCNQ2) channel by binding to its activation gate. *Molecular pharmacology*, 67(4), 1009-1017.
- Xia, S., Lampe, P. A., Deshmukh, M., Yang, A., Brown, B. S., Rothman, S. M. et al. (2002). Multiple channel interactions explain the protection of sympathetic neurons from apoptosis induced by nerve growth factor deprivation. *The Journal of neuroscience : the official journal of the Society for Neuroscience*, 22(1), 114-122.
- Xiao, Q., Kenessey, A., & Ojamaa, K. (2002). Role of USF1 phosphorylation on cardiac alpha-myosin heavy chain promoter activity. *American journal of physiology Heart and circulatory physiology*, 283(1), H213-9.
- Xu, J., Yu, W., Jan, Y. N., Jan, L. Y., & Li, M. (1995). Assembly of voltage-gated potassium channels. Conserved hydrophilic motifs determine subfamily-specific interactions between the alpha-subunits. *The Journal of biological chemistry*, 270(42), 24761-24768.
- Yadav, M. K., Leman, L. J., Price, D. J., Brooks, C. L., Stout, C. D., & Ghadiri, M. R. (2006). Coiled coils at the edge of configurational heterogeneity. Structural analyses of parallel and antiparallel homotetrameric coiled coils reveal configurational sensitivity to a single solvent-exposed amino acid substitution. *Biochemistry*, 45(14), 4463-4473.
- Yadav, M. K., Redman, J. E., Leman, L. J., Alvarez-Gutiérrez, J. M., Zhang, Y., Stout, C. D. et al. (2005). Structure-based engineering of internal cavities in coiled-coil peptides. *Biochemistry*, 44(28), 9723-9732.
- Yamaguchi, M., Shimizu, M., Ino, H., Terai, H., Hayashi, K., Kaneda, T. et al. (2005). Compound heterozygosity for mutations Asp611I-->Tyr in KCNQ1 and Asp609-->Gly in KCNH2 associated with severe long QT syndrome. *Clinical science (London, England : 1979)*, 108(2), 143-150.
- Yamashita, F., Horie, M., Kubota, T., Yoshida, H., Yumoto, Y., Kobori, A. et al. (2001). Characterization and subcellular localization of KCNQ1 with a heterozygous mutation in the C terminus. *Journal of molecular and cellular cardiology*, 33(2), 197-207.
- Yan, Q., Sun, W., McNew, J. A., Vida, T. A., & Bean, A. J. (2004). Ca²⁺ and N-ethylmaleimide-sensitive factor differentially regulate disassembly of SNARE complexes on early endosomes. *The Journal of biological chemistry*, 279(18), 18270-18276.
- Yang, W. P., Levesque, P. C., Little, W. A., Conder, M. L., Ramakrishnan, P., Neubauer, M. G. et al. (1998). Functional expression of two KvLQT1-related potassium channels responsible for an inherited idiopathic epilepsy. *The Journal of biological chemistry*, 273(31), 19419-19423.

- Yu, W., Xu, J., & Li, M. (1996). NAB domain is essential for the subunit assembly of both alpha-alpha and alpha-beta complexes of shaker-like potassium channels. *Neuron*, 16(2), 441-453.
- Yus-Najera, E., Santana-Castro, I., & Villarroel, A. (2002). The identification and characterization of a noncontinuous calmodulin-binding site in noninactivating voltage-dependent KCNQ potassium channels. *The Journal of biological chemistry*, 277(32), 28545-28553.
- Zaczek, R., Chorvat, R. J., Saye, J. A., Pierdomenico, M. E., Maciag, C. M., Logue, A. R. et al. (1998). Two new potent neurotransmitter release enhancers, 10,10-bis(4-pyridinylmethyl)-9(10H)-anthracenone and 10,10-bis(2-fluoro-4-pyridinylmethyl)-9(10H)-anthracenone: comparison to linopirdine. *The Journal of pharmacology and experimental therapeutics*, 285(2), 724-730.
- Zagotta, W. N., Hoshi, T., Dittman, J., & Aldrich, R. W. (1994). Shaker potassium channel gating. II: Transitions in the activation pathway. *The Journal of general physiology*, 103(2), 279-319.
- Zaika, O., Lara, L. S., Gamper, N., Hilgemann, D. W., Jaffe, D. B., & Shapiro, M. S. (2006). Angiotensin II regulates neuronal excitability via phosphatidylinositol 4,5-bisphosphate-dependent modulation of Kv7 (M-type) K⁺ channels. *The Journal of physiology*, 575(Pt 1), 49-67.
- Zerangue, N., Jan, Y. N., & Jan, L. Y. (2000). An artificial tetramerization domain restores efficient assembly of functional Shaker channels lacking T1. *Proceedings of the National Academy of Sciences of the United States of America*, 97(7), 3591-3595.
- Zhang, H., Craciun, L. C., Mirshahi, T., Rohács, T., Lopes, C. M., Jin, T. et al. (2003). PIP(2) activates KCNQ channels, and its hydrolysis underlies receptor-mediated inhibition of M currents. *Neuron*, 37(6), 963-975.
- Zhong, H., Lai, J., & Yau, K. W. (2003). Selective heteromeric assembly of cyclic nucleotide-gated channels. *Proceedings of the National Academy of Sciences of the United States of America*, 100(9), 5509-5513.
- Zhou, Y., Morais-Cabral, J. H., Kaufman, A., & MacKinnon, R. (2001). Chemistry of ion coordination and hydration revealed by a K⁺ channel-Fab complex at 2.0 Å resolution. *Nature*, 414(6859), 43-48.
- Zhu, G., Okada, M., Murakami, T., Kamata, A., Kawata, Y., Wada, K. et al. (2000). Dysfunction of M-channel enhances propagation of neuronal excitability in rat hippocampus monitored by multielectrode dish and microdialysis systems. *Neuroscience letters*, 294(1), 53-57.

D. Figures

Figure 1. Architecture of a voltage-gated K^+ channel



A Transmembrane domains of a Kv channel viewed as a cross section of the lipid bilayer. For clarity, only the pore domains of subunits A and C (darker gray with white labels) and voltage-sensing domains of subunits B and D (lighter gray with black labels) are shown. Cylinders represent α -helices; black circles represent K^+ ions; dotted circles represent K^+ hydration shells. N, N-terminus; S1-S6, transmembrane helices 1-6; P, pore helix; T, turret domain; SF, selectivity filter; IV, inner vestibule; C, C-terminus.

B Transmembrane domains of a Kv channel, viewed from the extracellular side of the lipid bilayer. All of subunits A and C (dark gray, white labels) and B and D (light gray, black labels) are shown; however, only subunits shown in Figure 1A are labeled.

Figure 2. Geometric properties of coiled coils

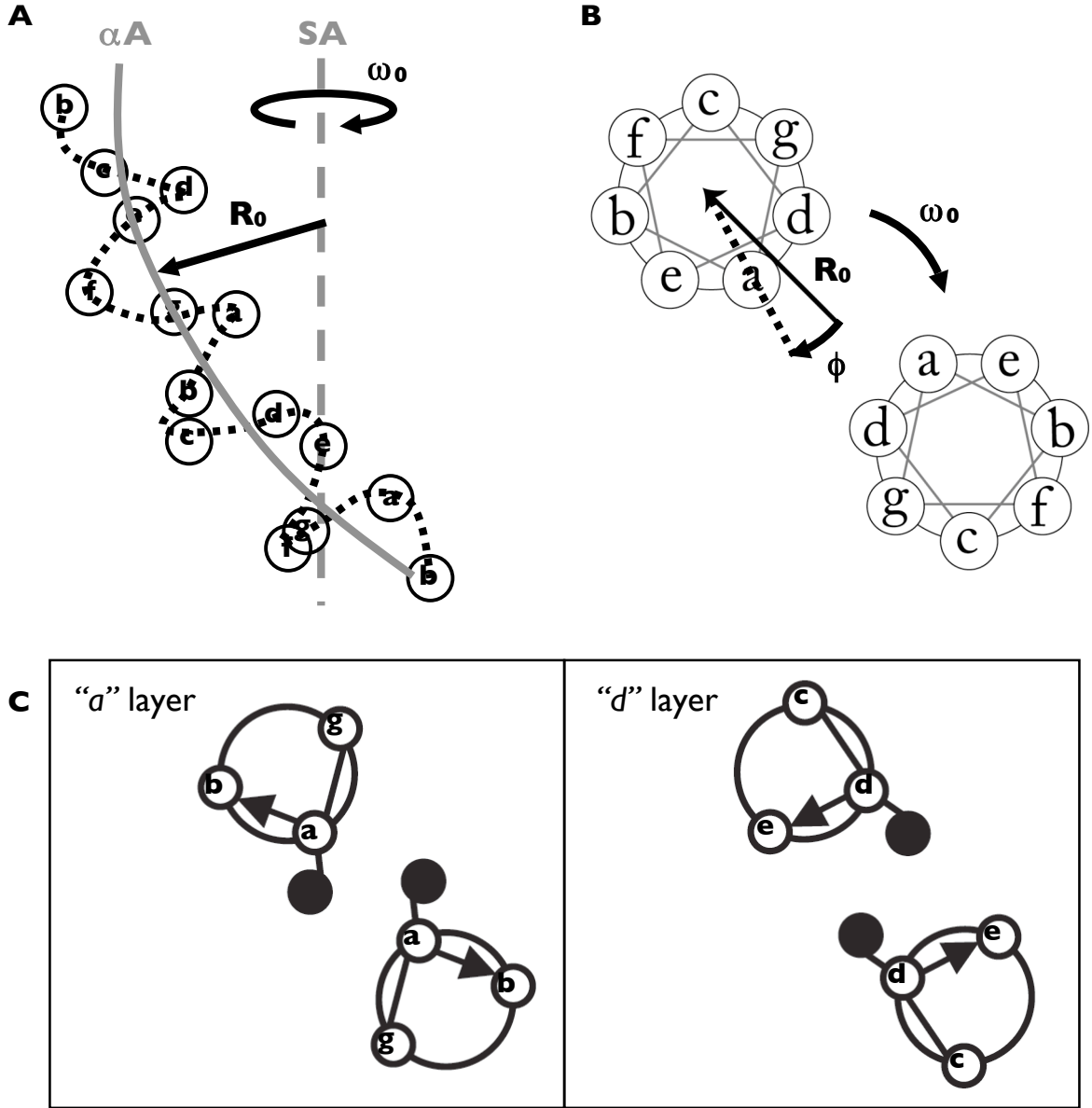
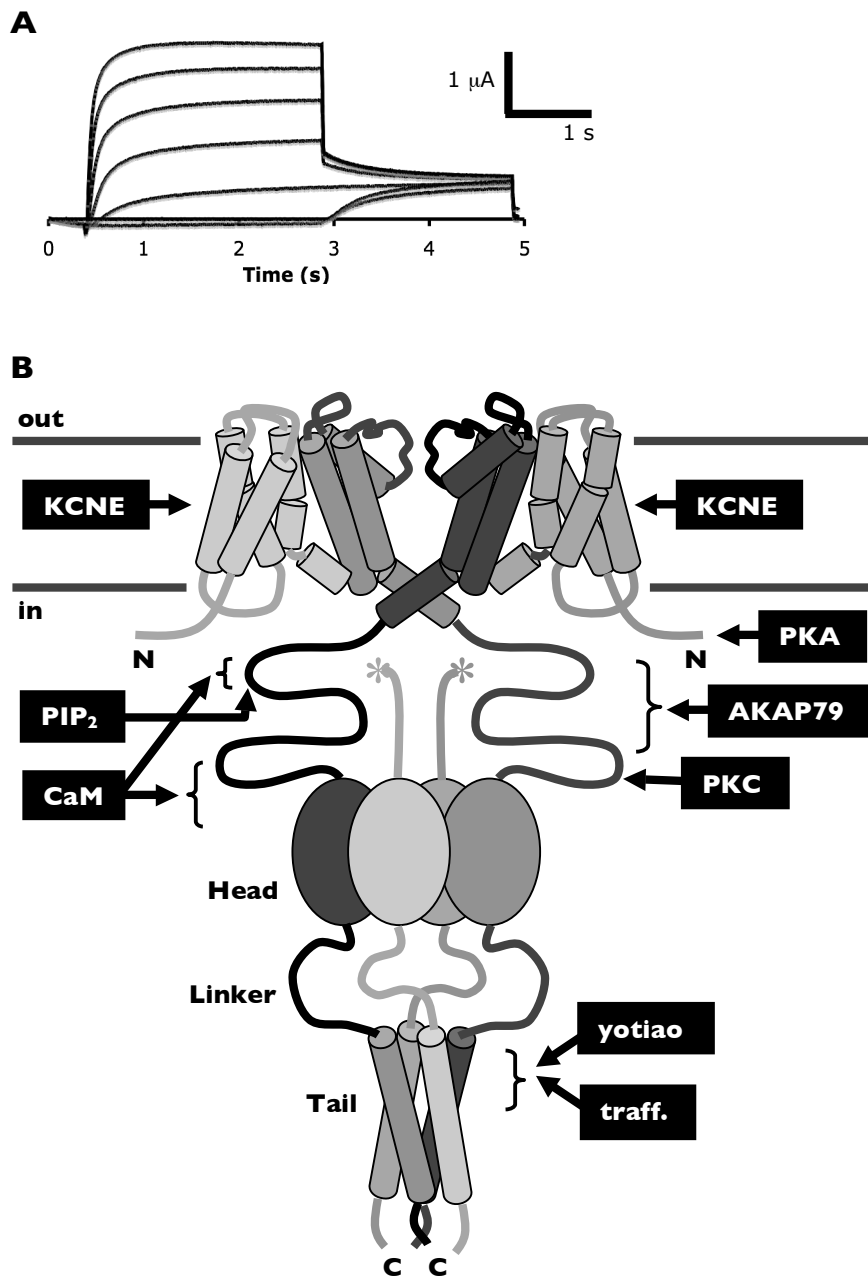


Figure 3. Architecture of Kv7 channels



A Example two-electrode voltage clamp recording from Kv7.2 channels expressed in oocytes. Cells pulsed for 2.5 s from a holding potential of -80 mV to voltages between -80 mV and +40 mV in steps of 15 mV, followed by a 2 s test pulse to -40 mV. For DNA construction, oocyte injection, and recording conditions, see Chapter 3.

B Model of the pore-forming subunits of a Kv7 channel complex. Putative binding sites for KCNE accessory subunits, PIP₂, CaM, AKAP79, yotiao, and an unidentified trafficking partner (traff.) are indicated. Sites for phosphorylation by PKA and PKC are labeled. Head, Linker, and Tail subdomains of the C-terminal A-domain are shown. Asterisks (*) represent pore domains of subunits B, D (light gray).

CHAPTER 2

**STRUCTURAL INSIGHT INTO KCNQ (Kv7) CHANNEL ASSEMBLY
AND CHANNELOPATHY**

Research completed in collaboration with

Kimberly A. Clark^{2,5}, James M. Holton^{3,6}, and Daniel L. Minor, Jr.^{2,3,4,5}

¹Chemistry and Chemical Biology Graduate Program, University of California, San Francisco, CA 94158-2330, USA

²Cardiovascular Research Institute, University of California, San Francisco, CA 94158-2330, USA

³Department of Biochemistry and Biophysics, University of California, San Francisco, CA 94158-2330, USA

⁴Department of Cellular and Molecular Pharmacology, University of California, San Francisco, CA 94158-2330, USA

⁵California Institute for Quantitative Biomedical Research, University of California, San Francisco, CA 94158-2330, USA

⁶Physical Biosciences Division, Lawrence Berkeley National Laboratory, Berkeley, CA 94720, USA

This chapter originally appeared in Neuron (2007), 53(5), 663-675.

A. Summary

Kv7.x (KCNQ) voltage-gated potassium channels form the cardiac and auditory IKs current and the neuronal M-current. The five Kv7 subtypes have distinct assembly preferences encoded by a C-terminal cytoplasmic assembly domain, the A-domain Tail. Here, we present the high-resolution structure of the Kv7.4 A-domain Tail together with biochemical experiments that show that the domain is a self-assembling, parallel, four-stranded coiled coil. Structural analysis and biochemical studies indicate conservation of the coiled coil in all Kv7 subtypes and that a limited set of interactions encode assembly specificity determinants. Kv7 mutations have prominent roles in arrhythmias, deafness, and epilepsy. The structure together with biochemical data indicate that A-domain Tail arrhythmia mutations cluster on the solvent-accessible surface of the subunit interface at a likely site of action for modulatory proteins. Together, the data provide a framework for understanding Kv7 assembly specificity and the molecular basis of a distinct set of Kv7 channelopathies.

B. Introduction

Members of the Kv7 (KCNQ) potassium channel family play important roles in the function of the heart, brain, auditory and vestibular organs, and epithelia (Jentsch, 2000; Jespersen *et al.*, 2005). These proteins belong to the voltage-gated ion channel superfamily (Hille, 2001) and constitute the pore-forming subunits of the IKs current that is present in cardiac myocytes, vestibular dark cells, and marginal cells of the stria vascularis (Barhanin *et al.*, 1996; Jentsch, 2000; Sanguinetti *et al.*, 1996; Wang *et al.*, 1996), and the classically studied neuronal M-current (Delmas and Brown, 2005; Wang

et al., 1998). Kv7 channels have a prominent role in human disease and harbor mutations that are linked to cardiac arrhythmias, deafness, and epilepsy (Jentsch, 2000). While there has been great effort in the functional characterization of Kv7 channels, little is known about their underlying structure. This is a particularly important problem because many disease mutations cause amino acid substitutions in the cytoplasmic regions of the protein where their direct functional consequences are not immediately obvious.

There are five mammalian Kv7 subtypes (Kv7.1–Kv7.5) (Gutman *et al.*, 2003). Functional studies indicate that each has distinct assembly preferences (Friedrich *et al.*, 2002; Kubisch *et al.*, 1999; Lerche *et al.*, 2000; Schroeder *et al.*, 2000). The subunit responsible for the IKs current, Kv7.1 (KCNQ1), does not coassemble with other Kv7 subunits. In contrast, Kv7.3 (KCNQ3) can form heterotetramers with all subunits except for Kv7.1 and is poorly expressed at the plasma membrane as a homotetramer (Schwake *et al.*, 2000). The other family members, Kv7.2 (KCNQ2), Kv7.4 (KCNQ4), and Kv7.5 (KCNQ5), can form functional homotetramers and functional heterotetramers with Kv7.3. Different combinations of Kv7 subunits display different biophysical properties that produce functional diversity (Hadley *et al.*, 2000; Kubisch *et al.*, 1999; Schwake *et al.*, 2000; Selyanko *et al.*, 2000; Wang *et al.*, 1998).

The molecular mechanisms that direct Kv7 subunit assembly selectivity are incompletely understood. Kv7 subunits contain a C-terminal region of 100 amino acids, called the A-domain, that appears to function as an assembly domain (Figure 1A) (Maljevic *et al.*, 2003; Schmitt *et al.*, 2000; Schwake *et al.*, 2003; Schwake *et al.*, 2000) and that carries all information for directing subtype-specific assembly properties (Friedrich *et al.*, 2002). Sequence alignment of the five Kv7 subtype A-domains indicates that the A-

domain has three subdomains (Figure 1B). Two of these, the Head (Jenke *et al.*, 2003) and the Tail (Jenke *et al.*, 2003 and Schwake *et al.*, 2006), have a high probability for forming coiled coils. The Head domain on its own appears incapable of supporting multimerization (Schmitt *et al.*, 2000). Surface expression seems to be closely tied to the integrity of the A-domain Tail (Kanki *et al.*, 2004). The A-domain Tail shows significant sequence variation among the subtypes. There is a clear role for this subdomain as the primary determinant of assembly specificity (Maljevic *et al.*, 2003; Schwake *et al.*, 2006; Schwake *et al.*, 2003), but how exactly this domain encodes specificity determinants remains unknown.

Understanding the nature of Kv7 A-domains has important consequences for elucidating the relationship between Kv7 channels and disease, as one class of disease mutations falls within the A-domain (Cooper and Jan, 2003; Jentsch, 2000). Some of these mutations prevent channel assembly and impair channel function by a simple truncation of the A-domain (Schmitt *et al.*, 2000; Schwake *et al.*, 2000). However, a number of A-domain Kv7.1 Long-QT (LQT) mutations in Romano Ward syndrome (RWS) and Jervell and Lange-Nielsen syndrome (JNLS) are missense mutations that reside in the A-domain Tail. One of the LQT mutants, G₅₈₉D, has been shown to disrupt β -adrenergic receptor modulation of Kv7.1 by interfering with the interaction of the channel with the scaffold protein yotiao. This interaction is necessary for anchoring protein kinase A and protein phosphatase I to the channel complex (Marx *et al.*, 2002). The exact mechanisms by which the other mutations, T₅₈₇M (Itoh *et al.*, 1998; Neyroud *et al.*, 1999), A₅₉₀T (Novotny *et al.*, 2006; Tester *et al.*, 2005), R₅₉₁H (Neyroud *et al.*, 1999), and R₅₉₄Q (Splawski *et al.*, 2000), act remain unclear. Elucidation of Kv7 A-domain

architecture should provide an important framework for understanding how such disease mutations act.

C. Results

i. Structure of the Kv7 Assembly Specificity Domain

The A-domain Tail carries the major determinants of channel assembly specificity (Maljevic *et al.*, 2003; Schwake *et al.*, 2006; Schwake *et al.*, 2003) and exhibits periodic heptad repeats, denoted (a-b-c-d-e-f-g)_n, (Figure 1B) in which the “a” and “d” positions are hydrophobic residues. This sequence motif is characteristic of coiled coils (Jenke *et al.*, 2003; Schwake *et al.*, 2006), common protein-protein interaction motifs (Lupas and Gruber, 2005; Woolfson, 2005). While it is relatively straightforward to discern likely coiled coils based on the presence of multiple heptad repeats, it is difficult to determine from the sequence alone which oligomeric state might be encoded, whether the sequence makes homomers or heteromers, what the heteromeric partners might be, and where the specificity determinants lie (Lupas and Gruber, 2005). Thus, we were interested in defining the structure of the Kv7 A-domain Tail to begin to understand the structural basis for Kv7 assembly specificity.

Sequence analysis suggests that the Kv7 Tail contains as many as four complete heptad repeats (Figure 1B). We expressed, purified, and crystallized a Kv7.4 A-domain Tail construct, residues 610–645, that was slightly longer than the identified heptads and that formed tetramers in solution (see below). The crystals grew in space group P4212 and diffracted synchrotron X-rays to 2.10 Å. Despite extensive effort, we were unable to determine phases by selenomethionine anomalous experiments, heavy metal derivatives, or by molecular replacement using parallel left-handed four-stranded

structures from SNARE complexes (Antonin *et al.*, 2002; Sutton *et al.*, 1998), Sendai virus (Tarbouriech *et al.*, 2000), and designed coiled coils (Harbury *et al.*, 1993).

Therefore, we decided to exploit the fact that coiled-coil backbone structure can be described by a simple parameterization (Crick, 1953; Harbury *et al.*, 1998; Harbury *et al.*, 1995) to build a library of de novo search models that could be used for molecular replacement.

We generated a library of 300 polyalanine search models in which the superhelix radius of the coiled-coil bundle, R_0 , the supercoil pitch (residues/superhelical turn), and the total number of residues were varied near their expected values for parallel left-handed four-stranded coiled coils (see Experimental Procedures). Each model was used as a molecular replacement search model in EPMR (Kissinger *et al.*, 2001). The best solution had two 28 residue peptides in the asymmetric unit, $R_0 = 5.0 \text{ \AA}$, and a pitch = 100 residues/superhelical turn. We were able to use this solution to build residues 612–642; however, we could not refine the structure to acceptable R/R_{free} values (Table 1). Because the electron density clearly showed the appropriate side chains within the coiled-coil core but had poor density for the C-terminal part of the bundle, we suspected that some degree of crystallographic disorder might be the source of the refinement difficulties. Therefore, we tested a series of truncation constructs to try to find one that would crystallize and yield data that were more amenable to structure solution and refinement.

Crystals of a C-terminal truncation, Kv7.4 residues 610–640, grew in space group I4 and diffracted X-rays to 2.07 \AA . We were able to solve the structure by molecular replacement using the program CNS (Brunger *et al.*, 1998) and the model from the P4212 crystals truncated to residue 638. Clear electron density was visible in

the initial maps for portions of the coil that were absent from the search model (Figure 1C). We were able to build all the atoms in the sequence except those of the three N-terminal residues and refine the structure to an acceptable level ($R/R_{\text{free}} = 19.6/22.4\%$) (Table 1).

The overall structure of the A-domain Tail assembly domain is that of a tightly twisted left-handed four-stranded coiled coil that is 24 Å wide and 40 Å long (Figures 1D and 1E). The last three C-terminal residues (Gly 638, Phe 639, and Tyr 640) splay outward to form a broad base (31 Å from C_{α} to C_{α} of opposite subunits) and participate in crystal contacts with neighboring molecules in the crystal lattice.

The Kv7.4 coiled-coil heptad repeat “a”- and “d”-positions interact by classical “knobs-into-holes” packing (Crick, 1953; Lupas and Gruber, 2005) to form alternating layers of the hydrophobic core of the coiled coil (Figures 2A and 2B). Two-, three-, and four-stranded coiled coils each have different characteristic “knobs-into-holes” packing geometries (Harbury *et al.*, 1993). In four-stranded coiled coils, the C_{α} - C_{β} vector of each “a”-position knob makes a perpendicular angle with the C_{α} - C_{α} vector of the “hole” formed by the “g” and “a” residues of the helix to the left (looking down the superhelical axis from the N terminus), whereas the C_{α} - C_{β} vector of each “d”-position knob runs parallel to the C_{α} - C_{α} vector of its “hole” formed by the “d”- and “e”-position residues of the helix to the right. The Kv7.4 A-domain Tail core packing uniformly corresponds to the canonical four-stranded coiled-coil geometry, having perpendicular “a” layers and parallel “d” layers (Figure 2B). Comparison of the superhelical parameters of the Kv7.4 A-domain Tail with previously determined four-stranded coiled-coil structures shows that the particular combination of supercoil radius, pitch, and radius of

curvature found in the A-domain Tail is unique and highlights the structural diversity that can be obtained from such a seemingly simple protein fold (Table 2).

The surface of the Kv7.4 A-domain Tail complex is predominantly polar and has two distinct networks of side chain salt bridges and hydrogen bonds, which we term “network 1” and “network 2,” that make interhelical contacts across helix interfaces (Figure 2C). In network 1, Glu₆₂₃, an “e” position in the heptad repeat, makes salt bridges to Arg₆₁₈, a “g” position from the neighboring helix, and Lys₆₂₄ from the “c” position of its own chain. Network 2 involves five side chains. The two central players are residues from neighboring helices: Glu₆₃₀, an “e” position, and Lys₆₃₂, a “g” position. Glu₆₃₀ makes hydrogen bonds to Gln₆₂₅ and Ser₆₂₈ and a salt bridge to Lys₆₃₂, three side chains from the adjacent helix. Lys₆₃₂ further participates in cross-subunit interactions by making a salt bridge to Asp₆₃₄ from the neighboring chain. The Gln₆₂₇ side chain is positioned between network 1 and network 2 and could form a bridge between the networks by making hydrogen bonds to Glu₆₂₃ and Gln₆₂₅. However, our structural data suggest that neither the geometry nor distances are optimal for this interaction, despite the proximity of Gln₆₂₇ to Glu₆₂₃ and Gln₆₂₅. Notably, this potential link between the networks is absent from Kv7.1 and Kv7.2 (Figure 1B). It is striking that the amino acids that form interactions in both network 1 and network 2 of the Kv7.4 A-domain Tail are changed in the Kv7 subtypes with specific assembly preferences, Kv7.1 and Kv7.3 (see Discussion).

ii. Kv7.4 is a Stable Tetramer in Solution

We used a number of biochemical and biophysical measures to probe the structure and assembly properties of the Kv7.4 A-domain Tail in aqueous solution. The

circular dichroism (CD) spectrum of Kv7.4 residues 610–645 shows minima at 208 and 222 nm that are characteristic of a protein with high helix content (Figure 3A).

Estimation of helical content fraction (Chen *et al.*, 1974) indicates that the peptide is 66.0% helical. This value is in good agreement with the structure where each helix contains 26 residues (Glu₆₁₂–Leu₆₃₇) that comprise 68.4% of the 38 residue peptide. The CD spectra of the complex at pH 3.0, 7.5, and 9.0 were superimposable and indicate that the Kv7.4 A-domain Tail retains its secondary structure over a wide range of pH conditions.

Both size exclusion chromatography and analytical ultracentrifugation corroborate the crystallographic observation that the Kv7.4 A-domain Tail is tetrameric. Size exclusion chromatography shows that the Kv7.4 A-domain Tail migrates as a single peak with an apparent molecular mass that is consistent with a tetramer (Figure 3B). Because size exclusion chromatography relies on the hydrodynamic radius, comparison of an elongated protein such as a coiled coil with globular protein standards could be misleading. Thus, we also used sedimentation equilibrium, a method that unlike gel filtration provides shape-independent mass information (Laue, 1995), to obtain a precise measurement of the oligomeric state. The equilibrium sedimentation data were well fit by a single-species model that corresponded to the molecular mass of a tetramer and had random residuals (Figure 3C). Together, these data establish unambiguously that the Kv7.4 A-domain Tail is a helical tetramer in solution that mirrors the crystal structure and the expected stoichiometry of Kv7 channels.

iii. Biochemical and Structural Comparisons of Kv7 A-Domain Tails

Sequence comparisons of Kv7 A-domain Tails show that the coiled-coil motif is conserved in all Kv7s (Figure 1B). To investigate self-assembly properties of the other Kv7 members, we expressed and purified fusion proteins of A-domain Tails from each subtype. Each fusion protein contained from N to C terminus: a hexahistidine tag, maltose binding protein, and a specific protease site (termed “HMT,” see Experimental Procedures) followed by the Kv7 coiled coil. The first two elements serve as orthogonal affinity purification tags. Gel filtration chromatography experiments show that purified Kv7.1, Kv7.2, Kv7.4, and Kv7.5 fusion proteins elute with apparent molecular weights corresponding to tetramers, and all behave similarly (Figure 4A). In contrast, the Kv7.3 A-domain Tail fusion protein elutes as a broad peak that suggests a mixture of monomers and dimers (Figure 4A). Thus, the A-domain Tails from the four subtypes (Kv7.1, Kv7.2, Kv7.4, and Kv7.5) in which the channels are known to form homotetramers retain the ability to oligomerize as independent domains while the A-domain Tail from the channel isoform that does not form robust homotetramers, Kv7.3 (Wang *et al.*, 1998), is impaired in its self-association ability.

Structure-based sequence comparisons indicate two sets of Kv7.3 amino acids that could impair assembly: there is a large aromatic residue, Phe₆₂₂, substituted at an “a” position and there are two amino acid substitutions, D₆₃₁ and G₆₃₃, that disrupt the interhelical salt bridge and hydrogen bond interactions of network 2 (Figure 4C). The recent structure determination of a tetrameric coiled coil bearing Phe at most “a” and “d” positions (Liu *et al.*, 2006) indicates that accommodation of Phe side chains in a coiled-coil hydrophobic core requires a superhelix radius that is significantly larger than that of the Kv7.4 A-domain Tail (Table 2). Thus, incorporation of four Phe residues into

the core of a homomeric Kv7.3 tetrameric coiled coil should incur a substantial steric and energetic penalty in the context of the coiled-coil core formed by the smaller alkyl side chains at the other “*a*”- and “*d*”-positions. To test whether the presence of Phe₆₂₂ was a major factor preventing tetramer formation by the Kv7.3 A-domain Tail, we mutated this position to a residue that was smaller, commonly found at four-stranded coiled-coil “*a*”-positions, and also found at the equivalent position of Kv7.2 (F₆₂₂L). Gel filtration experiments demonstrate that this single mutation was sufficient to convert the Kv7.3 A-domain Tail into a form that was predominantly tetrameric (Figure 4B). This result highlights the critical importance of the hydrophobic core in controlling Kv7 A-domain Tail assembly.

We also investigated the effects of restoring the network 2 interactions into the Kv7.3 coiled coil. Similar to the F₆₂₂L mutation, the double mutant D₆₃₁S/G₆₃₃E was sufficient to endow the Kv7.3 A-domain Tail with robust tetramerization properties (Figure 4B). Taken together, the biochemical and mutational analysis suggest that two factors prevent Kv7.3 A-domain Tail self-assembly: the incompatibility of making a stable tetramer bearing four Phe residues in the coiled-coil core and the lack of interstrand stabilizing interactions provided by network 2. These factors are likely to be important for determining the Kv7.3 preference for heteromer versus homomer formation. Experiments in *Xenopus* oocytes failed to show a functional enhancement of Kv7.3 channels bearing mutations that impart homotetramerization to the Kv7.3 Tail (data not shown). This observation is consistent with the poor expression of Kv7.3 homomeric chimeras bearing A-domains or A-domain portions from other Kv7 channels (Maljevic *et al.*, 2003; Schwake *et al.*, 2003) and suggests that other yet to be defined factors besides

the assembly defects in the A-domain Tail play a role in impairing Kv7.3 homotetramer surface expression.

iv. Structural Insight into Cardiac Arrhythmia Mutations

The Kv7.1 A-domain Tail bears five mutations that are associated with cardiac Long QT syndromes (LQT) known as Romano Ward syndrome (RWS) and Jervell and Lange-Nielsen syndrome (JLNS): T₅₈₇M (Chen *et al.*, 2003; Itoh *et al.*, 1998; Neyroud *et al.*, 1999), G₅₈₉D (Piippo *et al.*, 2001), A₅₉₀T (Novotny *et al.*, 2006; Tester *et al.*, 2005), R₅₉₁H (Neyroud *et al.*, 1999), and R₅₉₄Q (Splawski *et al.*, 2000). The exact mechanisms by which these mutations cause arrhythmia remain unclear. Prior work has shown that G₅₈₉D is able to abolish sympathetic regulation of cardiac I_{Ks} currents by disrupting the assembly of a macromolecular complex of Kv7.1 and the scaffolding protein yotiao (Marx *et al.*, 2002). Three of the mutants, T₅₈₇M (Yamashita *et al.*, 2001), R₅₉₁H (Grunnet *et al.*, 2005), and R₅₉₄Q (Huang *et al.*, 2001), appear to be incapable of making functional homomeric channels. T₅₈₇M (Yamashita *et al.*, 2001) and R₅₉₁H (Grunnet *et al.*, 2005) cannot coassemble with wild-type Kv7.1 subunits. Four mutations, T₅₈₇M (Kanki *et al.*, 2004; Yamashita *et al.*, 2001), G₅₈₉D (Kanki *et al.*, 2004), R₅₉₁H (Grunnet *et al.*, 2005; Kanki *et al.*, 2004), and R₅₉₄Q (Kanki *et al.*, 2004), compromise the ability of the channel to reach the plasma membrane. R₅₉₄Q appears to coassemble with wild-type and has a weak dominant-negative effect (Huang *et al.*, 2001). No functional characterization of A₅₉₀T has yet been reported.

To examine the impact of LQTS mutations on assembly of the Kv7.1 A-domain Tail, we made and tested the effects of each of them in the background of Kv7.1 HMT-fusion protein. Gel filtration experiments show that none of the LQT mutations disrupt

Kv7.1 A-domain Tail assembly (Figure 5A). While it is possible that there are subtle effects on tetramerization affinity caused by the mutations, the observation that there are no substantial changes in assembly properties suggests that some other mechanism must underlie their arrhythmogenic effects.

Comparison of the positions of the Kv7.1 mutations with their equivalent positions on the Kv7.4 A-domain Tail structure reveals a striking pattern. The sites cluster around a common surface pocket at the interhelix cleft that defines a three-dimensional mutational “hotspot” (Figure 5B). Notably, we observe that this pocket is the site of protein-protein contacts within the Kv7.4 A-domain Tail crystal lattice (Figure 5C). The observation that none of the A-domain Tail disease mutants disrupt the self-assembly of this part of the channel and that a mutation in the center of the cluster, G₅₈₉D, disrupts the binding of a necessary regulatory complex (Kanki *et al.*, 2004; Marx *et al.*, 2002) suggests that all members of this family of LQTS mutations may act by a similar mechanism.

D. Discussion

The minimal functional unit of any voltage-gated potassium channel is a homotetramer or heterotetramer of pore-forming subunits. Because different combinations of pore-forming subunits can have profound effects on functional properties, it is critical for all members of this channel class to encode assembly determinants and assembly specificity preferences to direct association with the appropriate partners (Deutsch, 2002; Deutsch, 2003; Hille, 2001; Papazian, 1999). Despite the fundamental nature of this problem, the mechanisms that drive channel assembly and assembly specificity remain imperfectly understood.

Voltage-gated ion channel family members are most similar within the membrane domain but exhibit considerable diversity within their extramembranous domains (Hille, 2001). While contacts between membrane-spanning regions may provide some stability, the more diverse cytoplasmic domains appear to play a major role in driving assembly and assembly specificity. The best understood case involves the Shaker-type KV family (Kv1-Kv4 subunits), where an independently folded, N-terminal intracellular module, called the “T1 domain,” drives tetramerization and assembly specificity (Bixby *et al.*, 1999; Li *et al.*, 1992; Shen and Pfaffinger, 1995). T1 domains are unique to Shaker-type Kv channels (Hille, 2001) and pose an important question: do other voltage-gated potassium channels use modular intracellular domains to drive assembly and assembly specificity?

A number of Kv7 A-domain functional properties mirror those of T1 and suggest that the A-domain is another example of an independent channel intracellular assembly module: the isolated A-domain forms stable multimeric complexes (Schmitt *et al.*, 2000); Kv7 channels bearing A-domain deletions, including those that are a consequence of certain disease mutations, fail to assemble into functional channels (Schmitt *et al.*, 2000; Schwake *et al.*, 2000); and coexpression of Kv7.1 A-domain sequences act as dominant-negatives on Kv7.1 channel assembly (Schmitt *et al.*, 2000). The A-domain and T1 domain amino acid sequences are unrelated and have different locations relative to the pore-forming transmembrane domain (C-terminal versus N-terminal, respectively). These differences suggest that voltage-gated channel superfamily members have exploited diverse types of protein-protein interaction domains to direct channel assembly.

i. Kv7 A-Domain Tails and Assembly Specificity

Our structural data demonstrate that the A-domain Tail is a self-assembling, four-stranded, parallel coiled coil (Figures 1D and 1E) that is conserved among Kv7 subtypes (Figures 1B and 4) and establish a framework for understanding Kv7 assembly. Sequence variations among the Kv7 subtypes at both the hydrophobic core of the coil and the polar network at the subunit interfaces appear as candidates for sites of specificity. Kv7.2, Kv7.4, and Kv7.5 can form functional channels as either homomers or as heteromers with Kv7.3 (Schwake *et al.*, 2003). Comparison of the core and electrostatic contacts that make protein-protein contacts shows that Kv7.4 and Kv7.5 are identical (Figure 4C). Kv7.4 and Kv7.2 differ by only two conservative variations, V₆₁₉L and I₆₂₉M, that are at “a”- and “d”-positions, respectively (for simplicity, all comparisons use Kv7.4 amino acid numbers). In contrast, Kv7.1, the channel that does not coassemble with any of the other subtypes (Schwake *et al.*, 2003), has changes at both the core positions (M₆₁₅I, V₆₁₉L, I₆₂₉L, and L₆₃₆I) and in network 1 (K₆₂₄D) and network 2 (E₃₆₀D and K₆₃₂A) relative to Kv7.4. The K₆₂₄D Kv7.1 change in network 1 alters the network surrounding Glu₆₂₃. The Kv7.1 network 2 would be completely rearranged as one of the central players in the ionic and hydrogen bond network is shortened by a methylene group, E₆₃₀D, and the other is eliminated, K₆₃₂A. It is striking that the remaining positions of the Kv7.1 network 2 are changed in a way that could still form a hydrogen bond and ionic network of side chain interactions around E₆₃₀D. These observations suggest the hypothesis that the differences in network 2 play a role in preventing Kv7.1 A-domain Tails from associating with other Kv7 subtypes.

Kv7.3 does not express robustly as a homomeric channel (Schwake *et al.*, 2000) but does show robust channel activity when coassembled with Kv7.2 (Schroeder *et al.*,

1998; Wang *et al.*, 1998), Kv7.4 (Kubisch *et al.*, 1999), and Kv7.5 (Schroeder *et al.*, 2000). Our work indicates that the Kv7.3 Tails are divergent at a number of critical positions (Figure 4C). There are changes at two coiled-coil core positions: V₆₁₉F, an “a”-position, and I₆₂₉M, a “d”-position. The changes in the interhelical interface networks include a reversal in the relative positions of the basic residues that surround Glu₆₂₃ in network 1, R₆₁₈K and K₆₂₄R, and a relocation of the carboxylate of one of the central side chains in network 2, E₆₃₀G, to a position at a similar altitude on the adjacent subunit by the S₆₂₈D change (Figure 2C). These alterations in the core and the interface networks appear to be critical for the unique assembly properties of the Kv7.3 Tail.

Our biochemical experiments suggest a rationale for the poor self-assembly and promiscuous heteromer formation properties of Kv7.3. The Kv7.3 A-domain Tail is prevented from making stable tetramers by both the incompatibility of placing four Phe residues within the core of the tetramer at the “a”-position of the coiled coil and by the disruption of the interhelical hydrogen bond and salt bridge interactions made by network 2. Although the combination of both factors is important for impairing homotetramerization, neither factor alone is incompatible with homotetramer formation (i.e., Kv7.3 Tails bearing the core Phe can make tetramers provided network 2 is intact, and tetramers lacking network 2 interactions can form provided the steric problems in the core caused by the “a”-position Phe are relieved). Thus, it appears that the Kv7.3 A-domain Tails are poised to form tetramers provided that the destabilizing factors can be overcome.

This property of being poised for assembly is particularly interesting when considered in the context of the promiscuous assembly behavior of Kv7.3 with Kv7.2, Kv7.4, and Kv7.5. Each non-Kv7.3 subunit would bring smaller hydrophobic residues at

the Kv7.3 F₆₂₂ “d” level of the coiled-coil core (Figure 4C) that would relieve some of the steric penalty for including the F₆₂₂ from each Kv7.3 subunit and promote heteromer formation. Network 1 and network 2 residues are identical in Kv7.2, Kv7.4, and Kv7.5 (Figure 4C). Consideration of the amino acid combinations that would be present in both networks in the context of a heterotetramers suggests that these interfaces should remain compatible across the Kv7.2/Kv7.3, Kv7.4/Kv7.3, and Kv7.5/Kv7.3 A-domain Tail interface and could contribute to the stability of a heteromeric complex. The precise arrangements of interactions at such interfaces are not evident from the current structure and will require further study.

ii. Structural Consequences for Kv7.1 Arrhythmia Mutations and Implications for Coiled Coils as Sites of Ion Channel Regulatory Complex Assembly

In addition to providing insight into the likely sources of assembly specificity, the Kv7.4 coiled-coil structure suggests a new hypothesis as to how certain Kv7.1 LQTS mutants act. One of the LQTS mutations, G₅₈₉D, is known to interfere with the recruitment of a macromolecular complex that responds to β -adrenergic receptor stimulation and includes the scaffolding protein yotiao, protein kinase A, and protein phosphatase I (Marx *et al.*, 2002). Both G₅₈₉D and simultaneous mutation of two “d”-positions to Ala (L₆₀₂A/I₆₀₉A) in the A-domain Tail prevent yotiao binding. Based on these mutations, Marx *et al.* suggested that that the A-domain heptad repeats interact directly with similar repeats in yotiao through a leucine-zipper-like mechanism (Marx *et al.*, 2002). Our structural and biochemical data show that the position of G₅₈₉D is on the coiled-coil surface and that the G₅₈₉D mutation does not affect tetramerization. Together, these data suggest a different scenario for how G₅₈₉D and other LQTS

mutations within the A-domain Tail act (Figure 6). We propose that yotiao interacts with the exterior surface of the helical bundle and that disease mutations such as G₅₈₉D interfere with yotiao binding to the intact A-domain Tail coiled-coil. In support of this idea, it is striking that all of the known A-domain Tail disease mutations map to a single hotspot on the coiled-coil surface. This clustering of mutations to a single area on the surface of the assembled domain suggests that this site may be the binding site for yotiao and that all four Long-QT syndrome mutations cause disease by a similar mechanism to G₅₈₉D. It is notable that this hotspot is composed of residues from adjacent subunits and is only present when the domain is intact and assembled as a coiled coil. Because the integrity of the A-domain Tail appears to be critical for proper channel trafficking (Kanki *et al.*, 2004) and T₅₈₇M (Kanki *et al.*, 2004; Yamashita *et al.*, 2001), G₅₈₉D (Kanki *et al.*, 2004), R₅₉₁H (Grunnet *et al.*, 2005; Kanki *et al.*, 2004), and R₅₉₄Q (Kanki *et al.*, 2004) compromise the ability of the channel to reach the plasma membrane, binding of accessory proteins in this region may be a mechanism of quality control for correctly assembled subunits.

Recent work indicates that a variety of voltage-gated ion channel superfamily members employ C-terminal cytoplasmic coiled-coil domains as a modular means for directing subunit assembly (Jenke *et al.*, 2003). Coiled coils are one of the most widespread and versatile protein-protein interaction domains and are found in diverse types of proteins (Lupas and Gruber, 2005; Woolfson, 2005). The characteristic coiled-coil heptad repeat (“*a-b-c-d-e-f-g*”) _n in which “*a*” and “*d*” are usually hydrophobic side chains makes coiled-coil identification from protein sequences straightforward; however, the oligomeric state, homomeric versus heteromeric preferences, and parallel or antiparallel orientation specified by a particular sequence remain difficult to discern from

sequence information alone (Lupas and Gruber, 2005). To date, there is experimental evidence for coiled-coil assembly domains in varied types of voltage-gated ion channel superfamily members, including Kv7 channels (Schwake *et al.*, 2006) (and this work), eag channels (Jenke *et al.*, 2003), cyclic nucleotide gated channels (Zhong *et al.*, 2003; Zhong *et al.*, 2002), intermediate conductance channels (Syme *et al.*, 2003), and TRPM channels (Tsuruda *et al.*, 2006). Thus, the coiled-coil motif appears to represent a general strategy for directing channel assembly in this diverse superfamily of channels.

Interactions between coiled-coil sequences and regulatory proteins are an emerging theme in channel regulation and disease (Kass *et al.*, 2003; Marx *et al.*, 2002). The presence of coiled-coil assembly domains in a wide variety of voltage-gated ion channels and the insights provided from the structural analysis presented here suggest that beyond channel assembly these domains may be important sites of nucleation for protein complexes that regulate channel activity (Figure 6). Furthermore, disruption of protein-protein interaction regulatory networks that are assembled on such intracellular channel domains is likely to be an important mechanism of dysregulation and channelopathies such as Long QT syndrome.

E. Experimental Procedures

i. Protein Cloning, Expression, and Purification

DNA fragments of Kv7.1 (residues 583–623), Kv7.2 (residues 614–654), Kv7.3 (residues 613–653), Kv7.4 (residues 610–645), Kv7.4 (residues 610–640), and Kv7.5 (residues 597–633) were amplified by PCR and ligated into the NarI/HindIII or NarI/XhoI sites of a pET27 (Novagen) derived vector (pSV272) denoted “HMT” (Van Petegem *et al.*, 2004) that contains, in sequence, a hexahistidine tag, maltose binding

protein, and a cleavage site for the Tobacco Etch Mosaic Virus (TEV) protease. Point mutations were made using mutated oligonucleotide extension (Pfu Turbo Polymerase, Strategene) from plasmid templates harboring the HMT fusion of interest, digested with DpnI (New England Biolabs), and transformed into DH5 α cells. All constructs were verified by complete DNA sequencing of the HMT fusion.

HMT fusion proteins were expressed in *Escherichia coli* (BL21(DE3)pLysS) grown in 2YT media at 37°C and induced at OD_{600nm} = 0.4–0.8 with 0.4 mM IPTG for 4 hr. Cells were harvested by centrifugation at 5000 x g for 20 min at 4°C, and cell pellets were frozen at –20°C. Thawed cell pellets were lysed by sonication in lysis buffer (100 mM Tris pH 7.6, 200 mM KCl, 10% sucrose, 25 mM β -octylglucoside, 20 μ g/ml lysozyme, 25 μ g/ml DNaseI, 5 mM MgCl₂, 1 mM PMSF). Insoluble material was precipitated by centrifugation for 20 min at 12,000 x g at 4°C. The resulting soluble fraction, which contained the HMT fusion protein, was applied to a 45 ml Poros20MC (Perseptive Biosystems) nickel-charged column, washed in wash buffer (10 mM PO₄²⁻, pH 7.3, 250 mM KCl, 1 mM PMSF), and eluted on a linear gradient to 300 mM imidazole in the same buffer on an ÄKTA-FPLC system (Pharmacia). Imidazole was removed using a Centriprep YM-10 concentrator (Millipore). Fusion proteins were then applied to a 60 ml Amylose (New England Biolabs) column, washed in wash buffer, and eluted in maltose buffer (10 mM PO₄²⁻, pH 7.3, 250 mM KCl, 10 mM maltose). To prepare purified Kv7.4 A-domain Tails, the HMT-fusion protein was cleaved with TEV protease (Kapust *et al.*, 2001). Coiled-coil peptides were collected in the flow-through from another Poros20MC nickel column and concentrated in a Centriprep YM-4. Protein concentration was determined by absorbance (Edelhoch, 1967).

ii. Crystallization and Data Collection

Crystals of two Kv7.4 coiled-coil constructs, one comprising residues 610–645 and the other 610–640, were obtained at 16°C by sitting-drop vapor-diffusion. For the longer construct, 1 µl peptide (4 mg/ml in 10 mM PO₄²⁻, pH 7.3, 250 mM KCl) was mixed with 1 µl of a reservoir solution containing 0.1 M citric acid pH 3.0, 23% (w/v) PEG 1000 and 10% (v/v) n-propanol. For the shorter construct, 1 µl peptide (0.1 mg/ml in 10 mM PO₄²⁻, pH 7.3, 250 mM KCl) was mixed with 1 µl 0.1 M Bis-Tris, pH 5.5, 0.2 M NH₄ acetate and 45% (v/v) MPD. For data collection, crystals of the longer construct were transferred to a solution containing 0.1 M citric acid, pH 3.0, 23% PEG 1000 and 15% n-propanol and flash-cooled in liquid nitrogen. Crystals of the shorter construct were frozen directly out of the drop in liquid nitrogen. Data were collected at ≤100 K at Advanced Lightsource Beamline 8.3.1 (Lawrence Berkeley National Laboratory, Berkeley, CA) equipped with a Quantum 210 CCD detector (Area Detector Systems). All data were processed using HKL2000 (HKL Research) (Otwinowski and Minor, 1997).

iii. Structure Determination

A library of 300 polyalanine parallel four-stranded left-handed coiled-coil models was generated based on the coiled-coil geometric parameterization (Crick, 1953) and the helix generator code (Harbury *et al.*, 1998) (helix generator code is available at <http://bl831.als.lbl.gov/jamesh/scripts/supertwist.awk>). Models varied by number of residues per monomer (28–40), superhelical radius R₀ (4.0–8.0 Å), and residues per superhelical turn (90–190). Each model in the library was used for molecular

replacement with EPMR (Kissinger *et al.*, 2001) in a dataset collected from crystals of Kv7.4 (residues 610–645). The de novo model giving the best correlation coefficient (0.641; second best = 0.635) and R factor (77.6%; second best = 76.2%) was used for a second round of molecular replacement with PHASER (Storoni *et al.*, 2004). This initial refinement led to a model with a superhelical radius of 7 Å for each molecule in the asymmetric unit. Refinement and iterative model building were performed using ARP/wARP (Perrakis *et al.*, 1999) and CNS (Brunger *et al.*, 1998). The structure could not be refined fully. The best model was used as a molecular replacement model in data collected from crystals of Kv7.4 (residues 610–640) using CNS (Brunger *et al.*, 1998). The resulting solution was built manually and refined using CNS (Brunger *et al.*, 1998) and the CCP4 program suite (Collaborative Computational Project, Number 4, 1994). Structure quality was monitored with PROCHECK. Structure and cavity volumes were calculated in SwissPDB (Schwede *et al.*, 2003). Coiled-coil parameters were calculated using the FITCC script (M. Sales and T. Alber, personal communication: <http://ucxray.berkeley.edu/mark/fitcc.html>). Table I summarizes the data collection, refinement, and model quality. Figures were prepared with PyMOL (DeLano, 2002).

iv. CD Spectroscopy

Twenty-five μM purified Kv7.4 coiled-coil peptide in a buffer of 250 mM NaCl and 2 mM each Na acetate, borate, citrate, and phosphate, pH as indicated in Figure 3A was analyzed with an Aviv Model 215 spectropolarimeter (Aviv Biomedical) equipped with a peltier device. Wavelength scans from 315 nm to 190 nm were taken at 2°C in a cuvette of 1 mm path length. Molar ellipticity per residue of the buffer-subtracted CD

spectrum was calculated as a function of concentration, path length, and number of residues per monomer:

$$[\theta]_{\text{MRD}} = \theta \cdot M / (c \cdot l \cdot N_R)$$

where $[\theta]_{\text{MRD}}$ is the molar ellipticity per residue in $\text{deg} \cdot \text{cm}^2 (\text{dmol} \cdot \text{res})^{-1}$, θ is the experimental ellipticity in millidegrees, M is the molecular mass of the peptide, c is the protein concentration in μM , l is the cuvette path length in cm, and N_R is the number of residues in the peptide. The percent helicity was estimated by:

$$\% \text{ helicity} = [\theta]_{222} / [\theta]_{222}^{\infty} (1 - i \cdot \kappa / N_R) \cdot 100$$

where $[\theta]_{222}$ is the experimental molar ellipticity per residue at 222 nm, $[\theta]_{222}^{\infty}$ is the molar ellipticity for a helix of infinite length at 222 nm (i.e. $-39,500 \text{ deg} \cdot \text{cm}^2 (\text{dmol} \cdot \text{res})^{-1}$), i is the number of helices, and κ is a wavelength-specific constant with a value of 2.57 at 222 nm (Chen *et al.*, 1974).

v. Size Exclusion Chromatography

For the isolated Kv7.4 coiled coil, 100 μl peptide (500 μM peptide in 250 mM KCl, 10 mM PO_4^{2-} , pH 7.3) was passed through a Superdex75 HR 10/30 column (Amersham Biosciences) in HEPES buffer (250 mM KCl, 1 mM EDTA, 10 mM maltose, 20 mM HEPES, pH 7.3) on an ÄKTA-FPLC system (Pharmacia) at 4°C. For HMT fusion proteins, 100 μl at 2 $\mu\text{g}/\text{ml}$ was loaded on a Superdex200 column (Amersham Biosciences) equilibrated with high-salt buffer (400 mM KCl, 1 mM EDTA, 10 mM PO_4^{2-} , pH 7.3). On both columns, eluates were monitored at 280 nm over a flow rate of 0.3 ml min⁻¹. Each column was calibrated using at least four standard protein molecular mass markers. Elution volumes from at least three runs were averaged.

vi. Equilibrium Sedimentation

Sedimentation equilibrium experiments were performed at 4°C in a Beckman Optima XL-A analytical ultracentrifuge (Beckman Coulter). Kv7.4 coiled-coil peptide (700 μM in 10 mM PO₄²⁻, pH 7.3, 250 mM KCl) was loaded in a six-chamber analytical ultracentrifuge cuvette, using buffer in the adjacent chamber as a blank. The molecular mass was calculated from a single-species exponential fit (Excel) to the distribution of concentration over the radius of the chamber:

$$M = (2RT / ((1-v\rho)\omega^2)) \cdot (d(\ln(c)) / d(r^2))$$

where M is the molecular weight in g/mol, R is the gas constant (8.314 J(mol•K)⁻¹), T is the temperature in K, v is the partial specific volume of the protein in ml/g, ρ is the density of the solvent in g/mL, ω is the angular velocity of centrifugation in rad/s, and r is the distance in cm from the center of the rotor to a given position in the cell (Laue, 1995). Partial specific volume was calculated from the sum of the volumes of individual residues in the protein. Solvent density was calculated from the components of the buffer. Residuals were calculated as the difference between the measured absorbance value and the predicted value extrapolated from the calculated molecular mass.

F. Acknowledgments

The authors would like to thank T. Jentsch for the Kv7 clones, F. Van Petegem for help with data collection and processing, J.M. Berger and A. Moroni for comments on the manuscript, and members of the Minor laboratory for support at all stages of this work. This work was supported by awards to D.L.M. from the Alfred P Sloan

Foundation, March of Dimes Basil O'Connor Scholar Program, Sandler Family Supporting Foundation, McKnight Foundation for Neuroscience, and the NIH. R.J.H. is supported by predoctoral fellowships from the NSF and AHA Western States Affiliate. D.L.M. is a Alfred P. Sloan Research Fellow, Basil O'Connor Scholar, and a McKnight Foundation Scholar. The coordinates and structure factors have been deposited with PDB structure code 2OVC.

G. References

- Antonin, W., Fasshauer, D., Becker, S., Jahn, R., & Schneider, T. R. (2002). Crystal structure of the endosomal SNARE complex reveals common structural principles of all SNAREs. *Nature structural biology*, *9*(2), 107-111.
- Barhanin, J., Lesage, F., Guillemare, E., Fink, M., Lazdunski, M., & Romey, G. (1996). K(V)LQT1 and IsK (minK) proteins associate to form the I(Ks) cardiac potassium current. *Nature*, *384*(6604), 78-80.
- Bixby, K. A., Nanao, M. H., Shen, N. V., Kreusch, A., Bellamy, H., Pfaffinger, P. J. et al. (1999). Zn²⁺-binding and molecular determinants of tetramerization in voltage-gated K⁺ channels. *Nature structural biology*, *6*(1), 38-43.
- Brünger, A. T., Adams, P. D., Clore, G. M., DeLano, W. L., Gros, P., Grosse-Kunstleve, R. W. et al. (1998). Crystallography & NMR system: A new software suite for macromolecular structure determination. *Acta crystallographica Section D, Biological crystallography*, *54*(Pt 5), 905-921.
- Chen, S., Zhang, L., Bryant, R. M., Vincent, G. M., Flippin, M., Lee, J. C. et al. (2003). KCNQ1 mutations in patients with a family history of lethal cardiac arrhythmias and sudden death. *Clinical genetics*, *63*(4), 273-282.
- Chen, Y. H., Yang, J. T., & Chau, K. H. (1974). Determination of the helix and beta form of proteins in aqueous solution by circular dichroism. *Biochemistry*, *13*(16), 3350-3359.
- Collaborative Computational Project, N. (1994). The CCP4 suite: programs for protein crystallography. *Acta crystallographica Section D, Biological crystallography*, *50*(Pt 5), 760-763.
- Cooper, E. C. & Jan, L. Y. (2003). M-channels: neurological diseases, neuromodulation, and drug development. *Archives of neurology*, *60*(4), 496-500.
- Crick, F. (1953). The Packing of α -Helices: Simple Coiled-Coils. *Acta Cryst*, *6*, 689-697.
- DeLano, W. L. (2002). The PyMOL Molecular Graphics System. San Carlos, CA: DeLano Scientific.
- Delmas, P. & Brown, D. A. (2005). Pathways modulating neural KCNQ/M (Kv7) potassium channels. *Nature reviews. Neuroscience*, *6*(11), 850-862.
- Deutsch, C. (2002). Potassium channel ontogeny. *Annual review of physiology*, *64*, 19-46.

- Deutsch, C. (2003). The birth of a channel. *Neuron*, 40(2), 265-276.
- Edelhoch, H. (1967). Spectroscopic determination of tryptophan and tyrosine in proteins. *Biochemistry*, 6(7), 1948-1954.
- Friedrich, T., Schwake, M., Bamberg, E., & Jentsch, T. J. (2002). A KCNQ1 construct containing a C-terminal heteromerization domain from KCNQ3 functionally interacts with KCNQ2 and KCNQ3. *Biophysical Journal*, 82(1), 577a.
- Grunnet, M., Behr, E. R., Calloe, K., Hofman-Bang, J., Till, J., Christiansen, M. et al. (2005). Functional assessment of compound mutations in the KCNQ1 and KCNH2 genes associated with long QT syndrome. *Heart rhythm : the official journal of the Heart Rhythm Society*, 2(11), 1238-1249.
- Gutman, G. A., Chandy, K. G., Adelman, J. P., Aiyar, J., Bayliss, D. A., Clapham, D. E. et al. (2003). International Union of Pharmacology. XLI. Compendium of voltage-gated ion channels: potassium channels. *Pharmacological reviews*, 55(4), 583-586.
- Hadley, J. K., Noda, M., Selyanko, A. A., Wood, I. C., Abogadie, F. C., & Brown, D. A. (2000). Differential tetraethylammonium sensitivity of KCNQ1-4 potassium channels. *British journal of pharmacology*, 129(3), 413-415.
- Harbury, P. B., Plecs, J. J., Tidor, B., Alber, T., & Kim, P. S. (1998). High-resolution protein design with backbone freedom. *Science*, 282(5393), 1462-1467.
- Harbury, P. B., Tidor, B., & Kim, P. S. (1995). Repacking protein cores with backbone freedom: structure prediction for coiled coils. *Proceedings of the National Academy of Sciences of the United States of America*, 92(18), 8408-8412.
- Harbury, P. B., Zhang, T., Kim, P. S., & Alber, T. (1993). A switch between two-, three-, and four-stranded coiled coils in GCN4 leucine zipper mutants. *Science*, 262(5138), 1401-1407.
- Hille, B. (2001). *Ion Channels of Excitable Membranes* (3rd ed.). Sunderland, MA: Sinauer Associates, Inc.
- Huang, L., Bitner-Glindzicz, M., Tranebjaerg, L., & Tinker, A. (2001). A spectrum of functional effects for disease causing mutations in the Jervell and Lange-Nielsen syndrome. *Cardiovascular research*, 51(4), 670-680.
- Itoh, T., Tanaka, T., Nagai, R., Kikuchi, K., Ogawa, S., Okada, S. et al. (1998). Genomic organization and mutational analysis of KVLQT1, a gene responsible for familial long QT syndrome. *Human genetics*, 103(3), 290-294.
- Jenke, M., Sánchez, A., Monje, F., Stühmer, W., Weseloh, R. M., & Pardo, L. A. (2003). C-terminal domains implicated in the functional surface expression of potassium channels. *The EMBO journal*, 22(3), 395-403.
- Jentsch, T. J. (2000). Neuronal KCNQ potassium channels: physiology and role in disease. *Nature reviews. Neuroscience*, 1(1), 21-30.
- Jespersen, T., Grunnet, M., & Olesen, S. P. (2005). The KCNQ1 potassium channel: from gene to physiological function. *Physiology*, 20, 408-416.
- Kanki, H., Kupersmidt, S., Yang, T., Wells, S., & Roden, D. M. (2004). A structural requirement for processing the cardiac K⁺ channel KCNQ1. *The Journal of biological chemistry*, 279(32), 33976-33983.
- Kapust, R. B., Tözsér, J., Fox, J. D., Anderson, D. E., Cherry, S., Copeland, T. D. et al. (2001). Tobacco etch virus protease: mechanism of autolysis and rational design of stable mutants with wild-type catalytic proficiency. *Protein engineering*, 14(12), 993-1000.

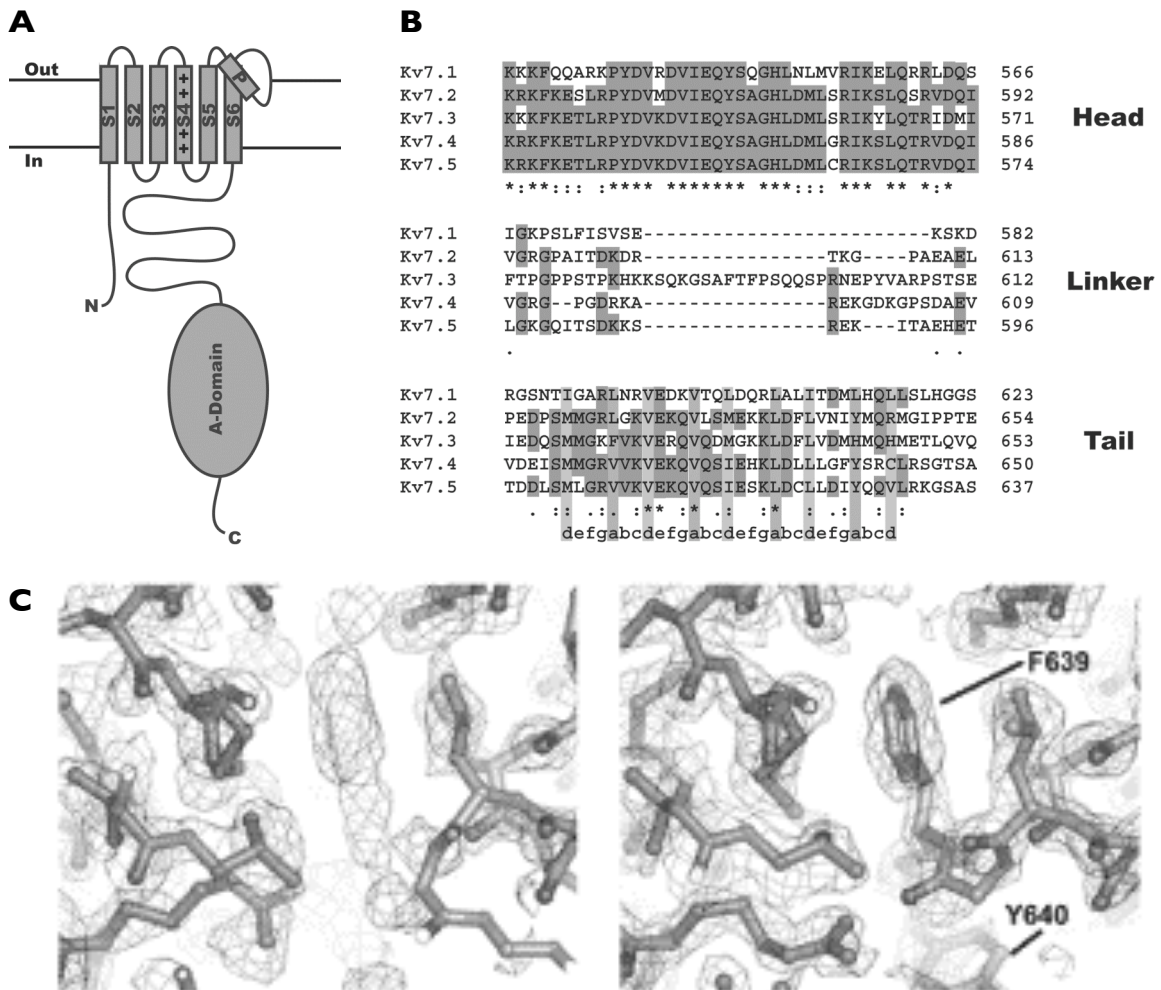
- Kass, R. S., Kurokawa, J., Marx, S. O., & Marks, A. R. (2003). Leucine/isoleucine zipper coordination of ion channel macromolecular signaling complexes in the heart. Roles in inherited arrhythmias. *Trends in cardiovascular medicine*, 13(2), 52-56.
- Kissinger, C. R., Gehlhaar, D. K., Smith, B. A., & Bouzida, D. (2001). Molecular replacement by evolutionary search. *Acta crystallographica Section D, Biological crystallography*, 57(Pt 10), 1474-1479.
- Kubisch, C., Schroeder, B. C., Friedrich, T., Lütjohann, B., El-Amraoui, A., Marlin, S. et al. (1999). KCNQ4, a novel potassium channel expressed in sensory outer hair cells, is mutated in dominant deafness. *Cell*, 96(3), 437-446.
- Laue, T. M. (1995). Sedimentation equilibrium as thermodynamic tool. *Methods in enzymology*, 259, 427-452.
- Lerche, C., Scherer, C. R., Seeböhm, G., Derst, C., Wei, A. D., Busch, A. E. et al. (2000). Molecular cloning and functional expression of KCNQ5, a potassium channel subunit that may contribute to neuronal M-current diversity. *The Journal of biological chemistry*, 275(29), 22395-22400.
- Li, M., Jan, Y. N., & Jan, L. Y. (1992). Specification of subunit assembly by the hydrophilic amino-terminal domain of the Shaker potassium channel. *Science*, 257(5074), 1225-1230.
- Liu, J., Zheng, Q., Deng, Y., Kallenbach, N. R., & Lu, M. (2006). Conformational transition between four and five-stranded phenylalanine zippers determined by a local packing interaction. *Journal of molecular biology*, 361(1), 168-179.
- Lupas, A. N. & Gruber, M. (2005). The structure of alpha-helical coiled coils. *Advances in protein chemistry*, 70, 37-78.
- Maljevic, S., Lerche, C., Seeböhm, G., Alekov, A. K., Busch, A. E., & Lerche, H. (2003). C-terminal interaction of KCNQ2 and KCNQ3 K⁺ channels. *The Journal of physiology*, 548(Pt 2), 353-360.
- Marx, S. O., Kurokawa, J., Reiken, S., Motoike, H., D'Armiento, J., Marks, A. R. et al. (2002). Requirement of a macromolecular signaling complex for beta adrenergic receptor modulation of the KCNQ1-KCNE1 potassium channel. *Science*, 295(5554), 496-499.
- Neyroud, N., Richard, P., Vignier, N., Donger, C., Denjoy, I., Demay, L. et al. (1999). Genomic organization of the KCNQ1 K⁺ channel gene and identification of C-terminal mutations in the long-QT syndrome. *Circulation research*, 84(3), 290-297.
- Novotny, T., Kadlecova, J., Papousek, I., Chroust, K., Bittnerova, A., Florianova, A. et al. (2006). Mutational analysis of LQT genes in individuals with drug induced QT interval prolongation. *Vnitr Lek*, 52(2), 116.
- Otwinowski, Z. & Minor, W. (1997). Processing of X-ray diffraction data collected in oscillation mode. *Methods Enzymol*, 276, 307.
- Papazian, D. M. (1999). Potassium channels: some assembly required. *Neuron*, 23(1), 7-10.
- Perrakis, A., Morris, R., & Lamzin, V. S. (1999). Automated protein model building combined with iterative structure refinement. *Nature structural biology*, 6(5), 458-463.
- Piippo, K., Swan, H., Pasternack, M., Chapman, H., Paavonen, K., Viitasalo, M. et al. (2001). A founder mutation of the potassium channel KCNQ1 in long QT syndrome: implications for estimation of disease prevalence and molecular diagnostics. *Journal of the American College of Cardiology*, 37(2), 562-568.

- Sanguinetti, M. C., Curran, M. E., Zou, A., Shen, J., Spector, P. S., Atkinson, D. L. et al. (1996). Coassembly of K(V)LQT1 and minK (IsK) proteins to form cardiac I(Ks) potassium channel. *Nature*, 384(6604), 80-83.
- Schmitt, N., Schwarz, M., Peretz, A., Abitbol, I., Attali, B., & Pongs, O. (2000). A recessive C-terminal Jervell and Lange-Nielsen mutation of the KCNQ1 channel impairs subunit assembly. *The EMBO journal*, 19(3), 332-340.
- Schroeder, B. C., Hechenberger, M., Weinreich, F., Kubisch, C., & Jentsch, T. J. (2000). KCNQ5, a novel potassium channel broadly expressed in brain, mediates M-type currents. *The Journal of biological chemistry*, 275(31), 24089-24095.
- Schroeder, B. C., Kubisch, C., Stein, V., & Jentsch, T. J. (1998). Moderate loss of function of cyclic-AMP-modulated KCNQ2/KCNQ3 K⁺ channels causes epilepsy. *Nature*, 396(6712), 687-690.
- Schwake, M., Athanasiadu, D., Beimgraben, C., Blanz, J., Beck, C., Jentsch, T. J. et al. (2006). Structural determinants of M-type KCNQ (Kv7) K⁺ channel assembly. *The Journal of neuroscience : the official journal of the Society for Neuroscience*, 26(14), 3757-3766.
- Schwake, M., Jentsch, T. J., & Friedrich, T. (2003). A carboxy-terminal domain determines the subunit specificity of KCNQ K⁺ channel assembly. *EMBO reports*, 4(1), 76-81.
- Schwake, M., Pusch, M., Kharkovets, T., & Jentsch, T. J. (2000). Surface expression and single channel properties of KCNQ2/KCNQ3, M-type K⁺ channels involved in epilepsy. *The Journal of biological chemistry*, 275(18), 13343-13348.
- Schwede, T., Kopp, J., Guex, N., & Peitsch, M. C. (2003). SWISS-MODEL: An automated protein homology-modeling server. *Nucleic acids research*, 31(13), 3381-3385.
- Selyanko, A. A., Hadley, J. K., Wood, I. C., Abogadie, F. C., Jentsch, T. J., & Brown, D. A. (2000). Inhibition of KCNQ1-4 potassium channels expressed in mammalian cells via M1 muscarinic acetylcholine receptors. *The Journal of physiology*, 522 Pt 3, 349-355.
- Shen, N. V. & Pfaffinger, P. J. (1995). Molecular recognition and assembly sequences involved in the subfamily-specific assembly of voltage-gated K⁺ channel subunit proteins. *Neuron*, 14(3), 625-633.
- Splawski, I., Shen, J., Timothy, K. W., Lehmann, M. H., Priori, S., Robinson, J. L. et al. (2000). Spectrum of mutations in long-QT syndrome genes. KVLQT1, HERG, SCN5A, KCNE1, and KCNE2. *Circulation*, 102(10), 1178-1185.
- Storoni, L. C., McCoy, A. J., & Read, R. J. (2004). Likelihood-enhanced fast rotation functions. *Acta crystallographica Section D, Biological crystallography*, 60(Pt 3), 432-438.
- Sutton, R. B., Fasshauer, D., Jahn, R., & Brunger, A. T. (1998). Crystal structure of a SNARE complex involved in synaptic exocytosis at 2.4 Å resolution. *Nature*, 395(6700), 347-353.
- Syme, C. A., Hamilton, K. L., Jones, H. M., Gerlach, A. C., Giltinan, L., Papworth, G. D. et al. (2003). Trafficking of the Ca²⁺-activated K⁺ channel, hK1, is dependent upon a C-terminal leucine zipper. *The Journal of biological chemistry*, 278(10), 8476-8486.
- Tarbouriech, N., Curran, J., Ruigrok, R. W., & Burmeister, W. P. (2000). Tetrameric coiled coil domain of Sendai virus phosphoprotein. *Nature structural biology*, 7(9), 777-781.
- Tester, D. J., Will, M. L., Haglund, C. M., & Ackerman, M. J. (2005). Compendium of cardiac channel mutations in 541 consecutive unrelated patients referred for long

- QT syndrome genetic testing. *Heart rhythm : the official journal of the Heart Rhythm Society*, 2(5), 507-517.
- Tsuruda, P. R., Julius, D., & Minor, D. L. (2006). Coiled coils direct assembly of a cold-activated TRP channel. *Neuron*, 51(2), 201-212.
- Van Petegem, F., Clark, K. A., Chatelain, F. C., & Minor, D. L. (2004). Structure of a complex between a voltage-gated calcium channel beta-subunit and an alpha-subunit domain. *Nature*, 429(6992), 671-675.
- Wang, H. S., Pan, Z., Shi, W., Brown, B. S., Wymore, R. S., Cohen, I. S. et al. (1998). KCNQ2 and KCNQ3 potassium channel subunits: molecular correlates of the M-channel. *Science*, 282(5395), 1890-1893.
- Wang, Q., Curran, M. E., Splawski, I., Burn, T. C., Millholland, J. M., VanRaay, T. J. et al. (1996). Positional cloning of a novel potassium channel gene: KVLQT1 mutations cause cardiac arrhythmias. *Nature genetics*, 12(1), 17-23.
- Woolfson, D. N. (2005). The design of coiled-coil structures and assemblies. *Advances in protein chemistry*, 70, 79-112.
- Yamashita, F., Horie, M., Kubota, T., Yoshida, H., Yumoto, Y., Kobori, A. et al. (2001). Characterization and subcellular localization of KCNQ1 with a heterozygous mutation in the C terminus. *Journal of molecular and cellular cardiology*, 33(2), 197-207.
- Zhong, H., Lai, J., & Yau, K. W. (2003). Selective heteromeric assembly of cyclic nucleotide-gated channels. *Proceedings of the National Academy of Sciences of the United States of America*, 100(9), 5509-5513.
- Zhong, H., Molday, L. L., Molday, R. S., & Yau, K. W. (2002). The heteromeric cyclic nucleotide-gated channel adopts a 3A:1B stoichiometry. *Nature*, 420(6912), 193-198.

H. FIGURES

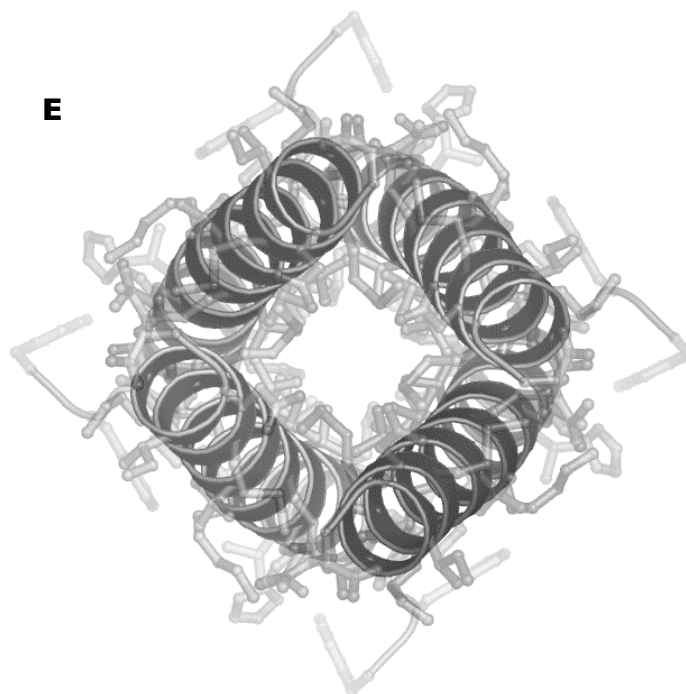
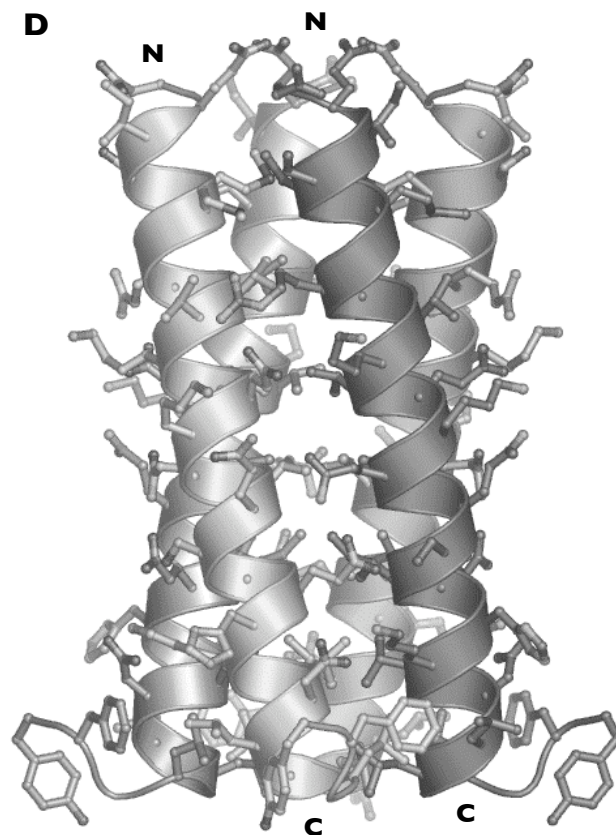
Figure 1. Structure of the Kv7 Coiled-Coil Assembly Domain



A Topology cartoon for one Kv7 subunit. The S1-S6 transmembrane segments and pore-forming “P region” are labeled. The voltage-sensor helix, S4, is indicated by the plus symbols. The A-domain is shown as an oval.

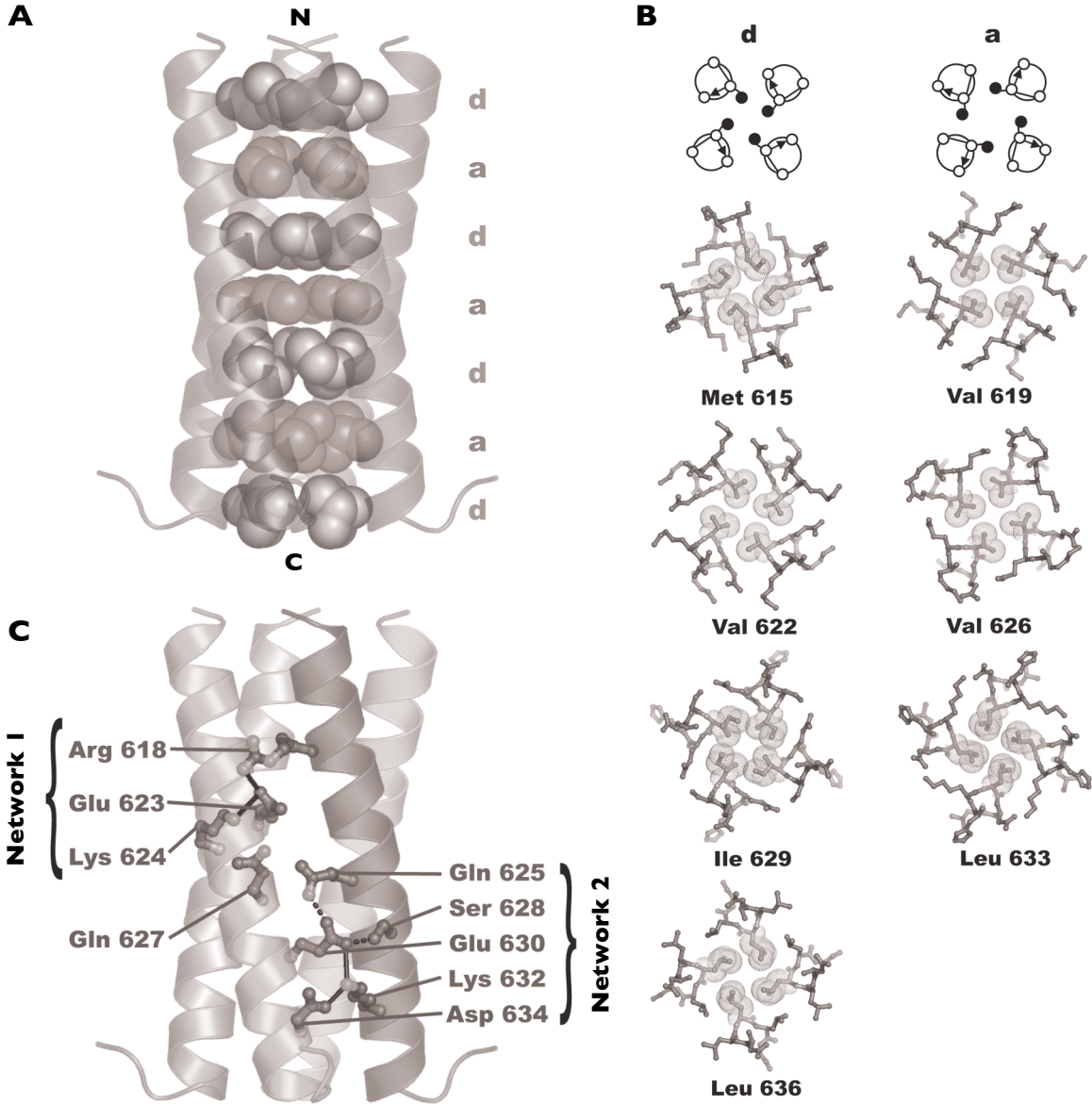
B Sequence alignment of A-domains from all five Kv7 family members, indicating the positions of the Head, Linker, and Tail regions. Dark highlighting and symbols below alignments indicate sequence conservation (asterisk, identical residues; colon, conservative substitution; period, weakly conservative substitution). In the Tail region, the positions of the coiled-coil heptad repeat (“a-b-c-d-e-f-g”) are indicated below the alignment. Coiled-coil residues occupying hydrophobic “a” and “d” positions are denoted by light highlighting.

C (Left) Kv7.4 A-domain Tail coiled-coil model used for molecular replacement and calculated $2F_o - F_c$ map after initial rigid body refinement. F_{639} , for which there is clear electron density, was absent from the model. (Right) Final refined structure and composite-omit $2F_o - F_c$ map built by random omission of 5% of model. Both maps are contoured at 1.2σ . The positions of F_{639} and Y_{640} from one subunit are indicated.



D Ribbon diagram of the Kv7.4 A-domain Tail coiled coil with side chains shown in ball-and-stick representation. The N- and C-terminal ends of the front subunits are indicated. The positions of F₆₃₉ and Y₆₄₀ of the front right subunit are also labeled.
E Ribbon diagram looking down the helical axis from the N terminus.

Figure 2. Hydrophobic and Electrostatic Contacts in the Kv7.4 Coiled-Coil Domain

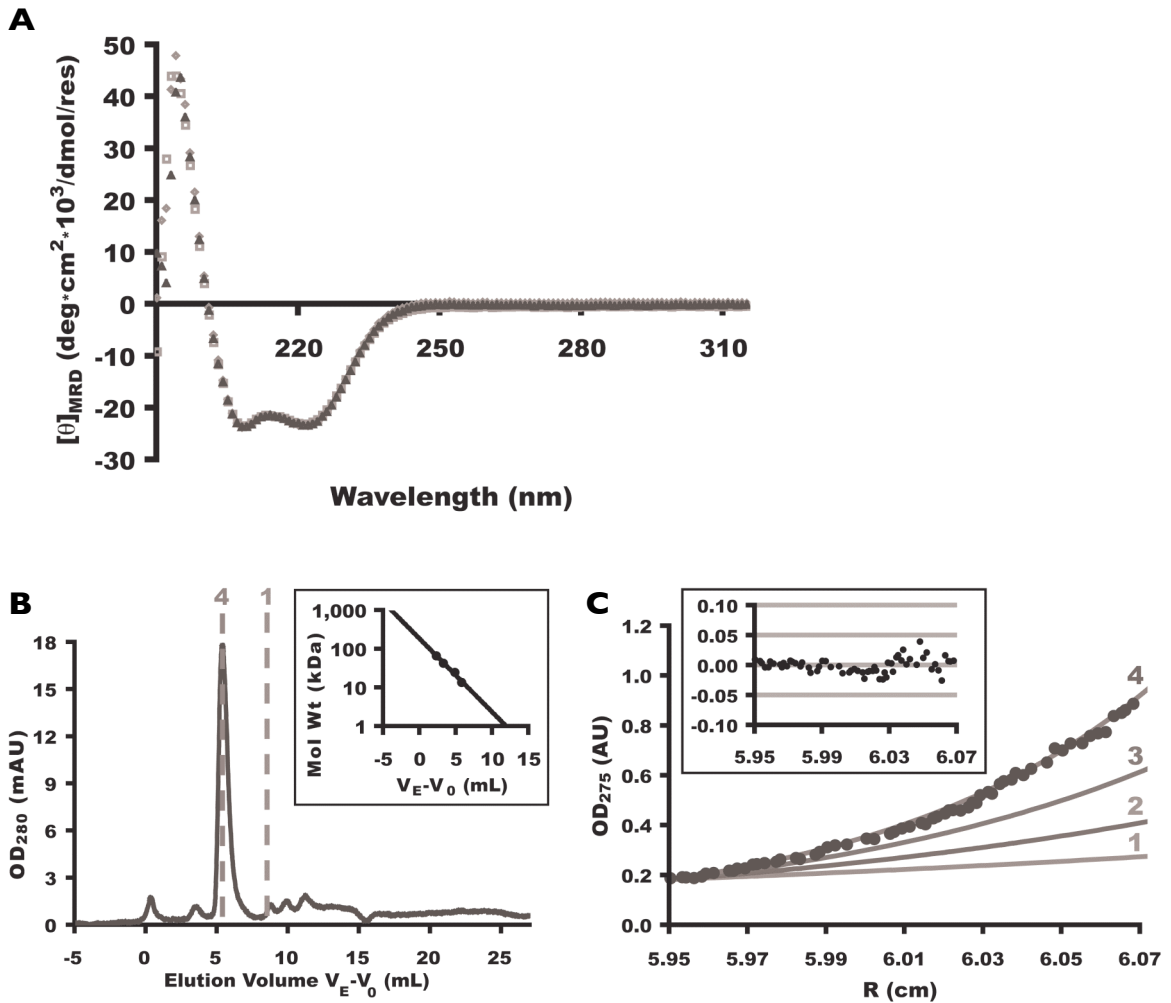


A Hydrophobic layers of the coiled-coil core. Van der Waals spheres depicting the side chains of the “a” and “d” layers on a ribbon backbone are shown. The N- and C-terminal ends of the coiled coil are indicated.

B Geometry of individual coiled-coil “a” and “d” layers. Top pictograms represent “a” (right) and “d” layers (left). Arrows show the direction from the N to C terminus, open circles represent the C_α atoms, and black circles the C_β atoms. Ball-and-stick representations show each layer of the core. Van der Waals spheres indicate core residues.

C Intra- and intermolecular electrostatic interactions. Ribbon diagram of tetramer shows network 1 and network 2 interactions between the side chains (shown as sticks) of the front subunits. Salt bridges (black lines) and hydrogen bonds (dotted lines) are indicated.

Figure 3. Solution Properties of the Kv7.4 A-Domain Tail

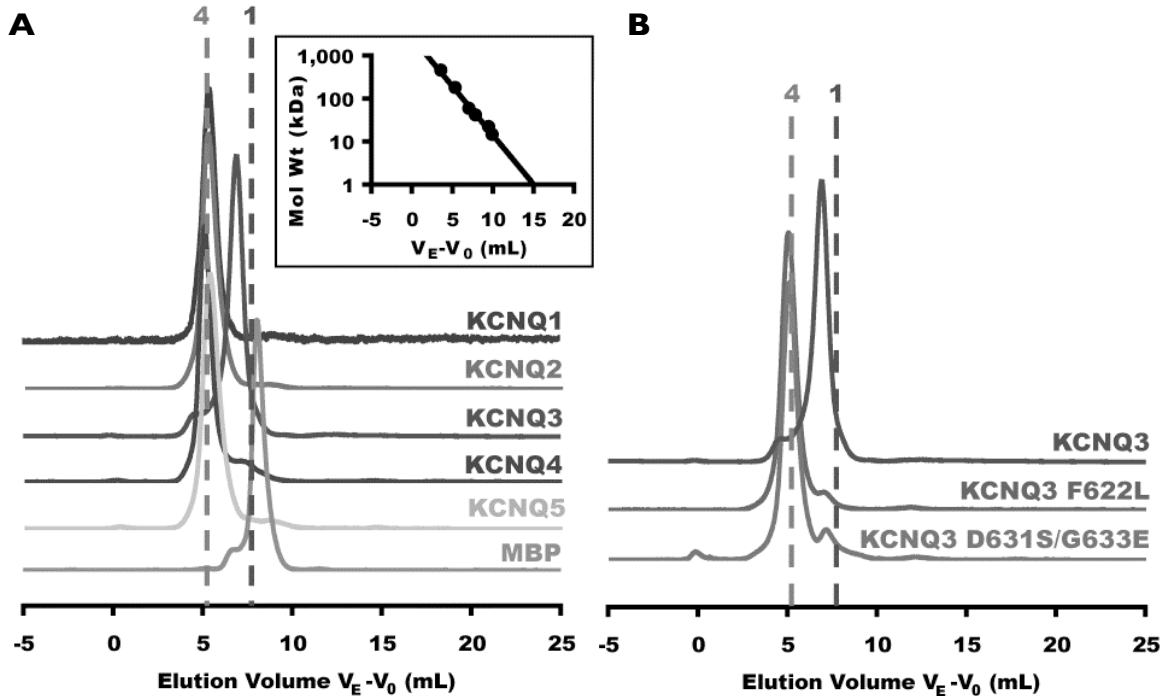


A Circular dichroism (CD) spectrum of the Kv7.4 A-domain Tail is insensitive to pH over a wide range. Overlaid CD spectra of 25 μM Kv7.4 A-domain Tail residues 610–645 at pH 3.0 (diamonds), 7.5 (triangles), and 9.0 (squares).

B Superdex75 (Amersham Biosciences) size exclusion chromatography of 500 μM Kv7.4 residues 610–642 monitored at 280 nm. Horizontal axis shows elution volume V_E corrected for void elution volume by subtracting that of blue dextran (V_0). Vertical dotted lines indicate predicted elutions of tetrameric (4) and monomeric (1) peptides. (Inset) Standard curve used to calculate molecular weight of eluted peptides on the Superdex75 column. Molecular weights are 17.1 kD, observed; 3.98 kD, expected monomer; and 15.9 kD, expected tetramer.

C Sedimentation equilibrium of Kv7.4 residues 610–645. Equilibrium distribution of peptide (circles) measured by its absorbance at 275 nm is plotted as a function of radial distance at 33,800 rpm at 4°C. Initial protein concentration was 600 μM . Raw data shown relative to predicted curves for tetrameric (4), trimeric (3), dimeric (2), and monomeric (1) species. (Inset) Random distribution of residuals as a function of radial distance.

Figure 4. Comparing Interactions in Alternative Kv7 Subtypes



A Stoichiometry of coiled-coil assembly domains in all five Kv7 subtypes shown by Superdex200 (Amersham Biosciences) size exclusion chromatography. Normalized absorbance is plotted against elution volume V_E corrected for void elution volume V_0 as in Figure 3B. All samples were loaded at a concentration of 50 μ M. Vertically displaced chromatograms show traces for, from top to bottom, Kv7.1, Kv7.2, Kv7.3, Kv7.4, Kv7.5, and MBP. Vertical dotted lines indicate the predicted elution volumes of tetrameric (4) and monomeric (1) fusion proteins. (Inset) Standard curve used to calculate molecular weight of eluted proteins on the Superdex200 column. Molecular weights for each are as follows (observed \pm SD, expected monomer, expected tetramer); Kv7.1 (180 \pm 2 kD, 49.4 kD, 198 kD); Kv7.2 (203 \pm 6 kD, 49.3 kD, 197 kD); Kv7.3 (90.3 \pm 2 kD, 49.9 kD, 200 kD); Kv7.4 (207 \pm 6 kD, 48.8 kD, 195 kD); Kv7.5 (191 \pm 6 kD, 48.9 kD, 196 kD).

B Stoichiometry of mutant coiled-coil assembly domains as determined by size exclusion. Kv7.3 A-domain Tail mutants F₆₂₂L and D₆₃₁S/G₆₃₃E restore tetramerization. Molecular weights for each are as follows (observed, expected monomer, expected tetramer); Kv7.3 (90.3 kD, 49.9 kD, 200 kD); Kv7.3 F₆₂₂L (212 kD, 49.9 kD, 200 kD); Kv7.3 D₆₃₁S/G₆₃₃E (208 kD, 49.9 kD, 200 kD). All samples were loaded onto the column at a concentration of 50 μ M.

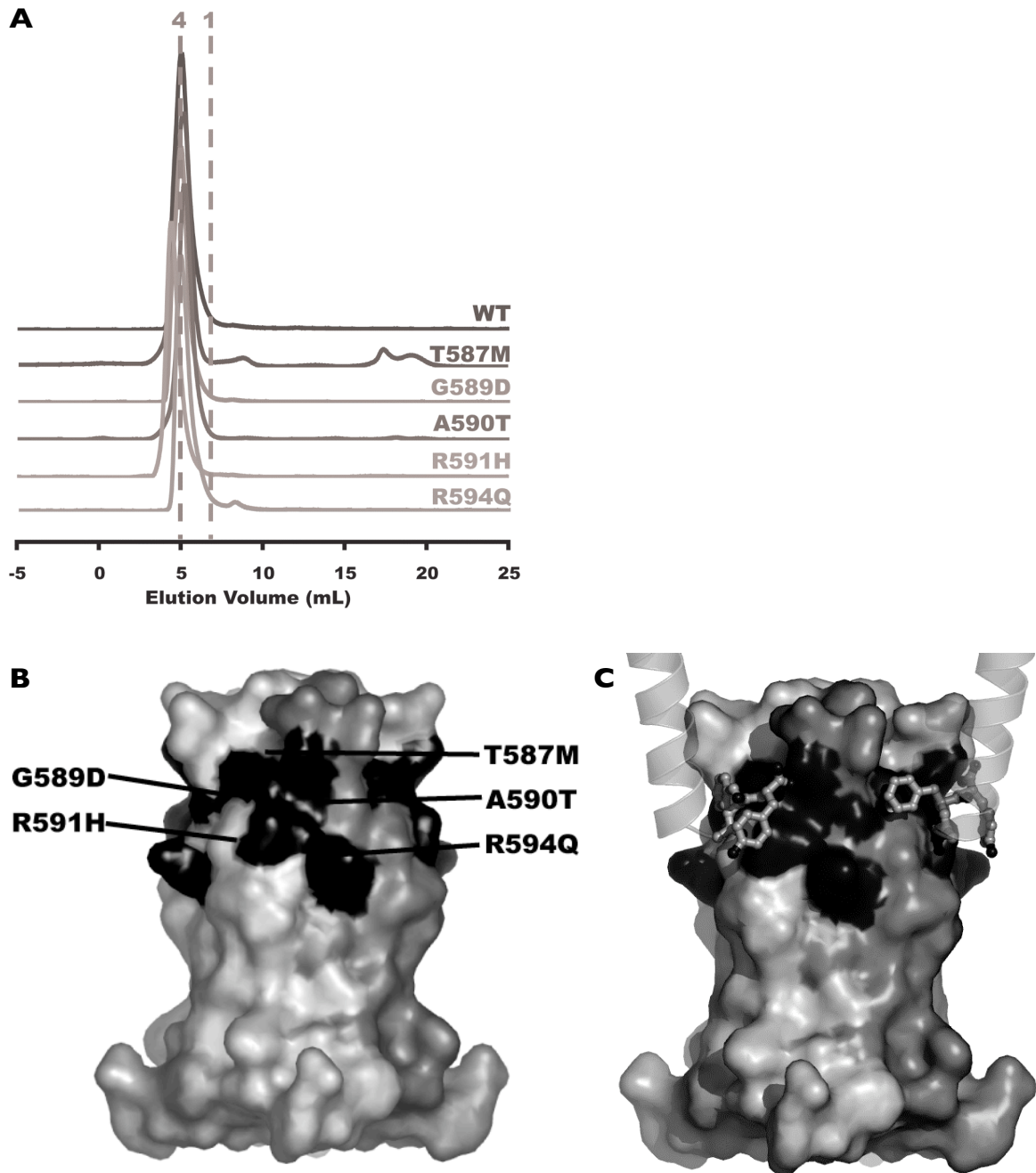
C

	Core Contacts							Electrostatic Contacts					
	d	a	d	a	d	a	d	g-e	f-e	g-e	e-c	g-e	g-b
	Met 615	Val 619	Val 622	Val 626	Ile 629	Leu 633	Leu 636	Arg 618 Glu 623	Lys 624 Glu 623	Gln 625 Glu 630	Ser 628 Glu 630	Lys 632 Glu 630	Lys 632 Asp 634
Kv7.1	I	L	V	V	L	L	I	R--E	D--E	K--D	Q--D	R--D	R--A
Kv7.2	M	L	V	V	M	L	L	R--E	K--E	Q--E	S--E	K--E	K--D
Kv7.3	M	F	V	V	M	L	L	K--E	R--E	Q--G	D--G	K--G	K--D
Kv7.4	M	V	V	V	I	L	L	R--E	K--E	Q--E	S--E	K--E	K--D
Kv7.5	M	V	V	V	I	L	L	R--E	K--E	Q--E	S--E	K--E	K--D

Network 1
Network 2

C Comparative interaction mapping in all subtypes. Column labels identify residue types involved in hydrophobic “a” and “d” layer contacts (medium gray) and electrostatic interactions (dark gray) observed in the Kv7.4 coiled-coil structure. Light gray boxes indicate nonconserved residues that are still capable of interacting as predicted; white boxes indicate unfavorable contacts. Electrostatic interactions involved in networks 1 and 2 are indicated below the alignment.

Figure 5. Mapping of Long-QT Syndrome Mutations

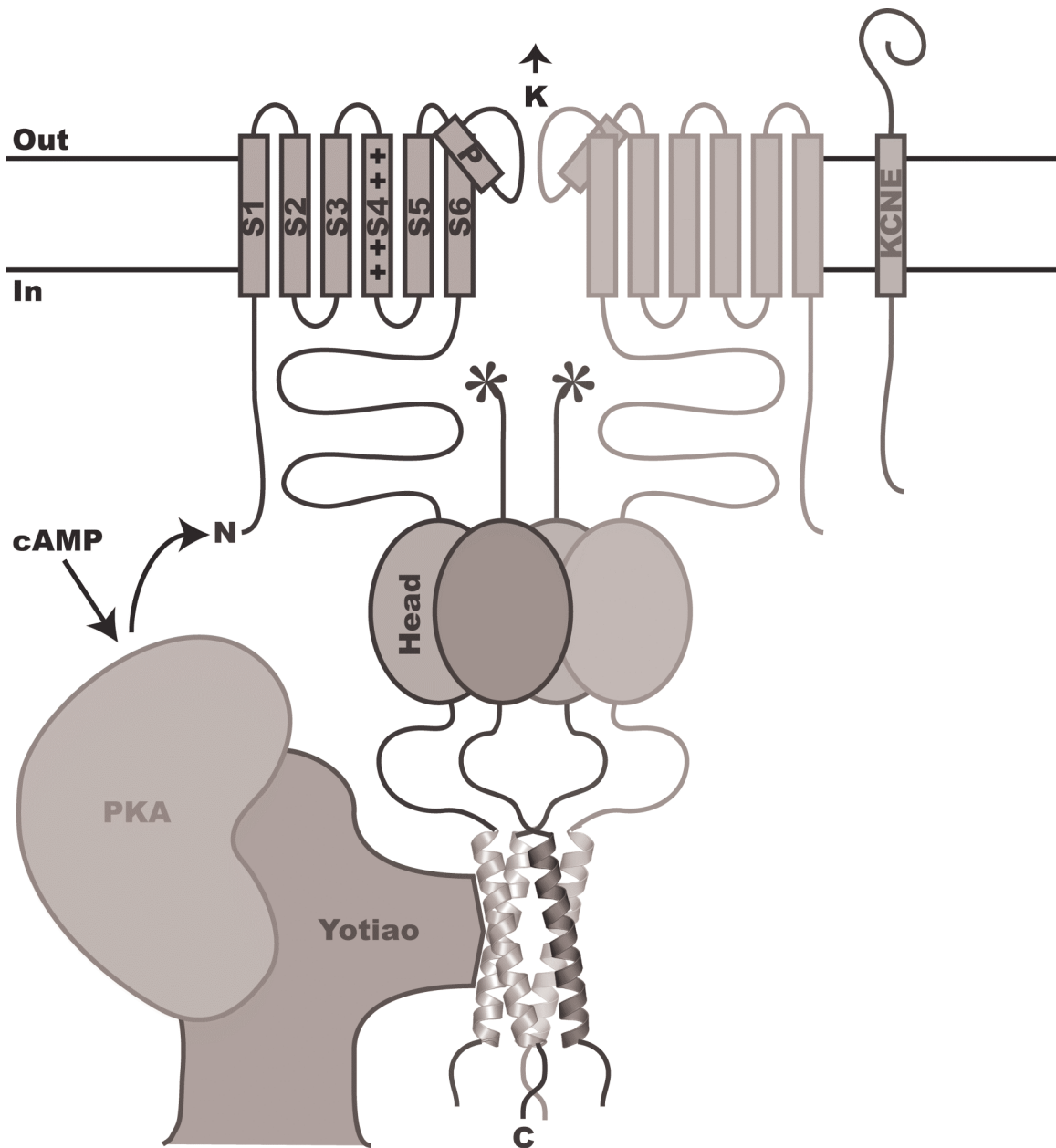


A Stoichiometry of Kv7.1 disease mutants. Normalized size exclusion chromatograms for Kv7.1 MBP-fusions: from top to bottom, wild-type, T₅₈₇M, G₅₈₉D, A₅₉₀T, R₅₉₁H, and R₅₉₄Q.

B Surface representation of Kv7.4 coiled-coil domain with helices colored separately. LQTS mutation sites have been mapped onto equivalent positions (black) in Kv7.4.

C Crystal lattice contacts between Kv7.4 tetramers. One complete Kv7.4 Tail is shown with subunits from neighboring molecules in light gray. Positions of the corresponding Kv7.1 LQT mutations are shown.

Figure 6. Model of a Kv7 Channel Regulatory Complex



Cartoon of a Kv7 channel regulatory complex. Two complete Kv7 pore-forming subunits are shown. S1-S6 transmembrane segments and the pore helix (P) are indicated for the green subunit. “+”s indicate the S4 voltage sensor segment. All four subunits of the Kv7 A-domain are shown. The Head domain is shown as an oval. The Tail domain helices are shown. The Linker domain connects the Head and Tail. An interaction between a portion of the scaffolding protein yotiao and the channel is shown bringing protein kinase A (PKA) near the channel. The stoichiometry of the yotiao/channel complex is not known.

Table 1. Data Collection and Refinement Statistics

Data Collection	Kv7.4 (610–645)	Kv7.4 (610–640)
Space group	P 4 ₂ ,2	I 4
Cell dimensions		
<i>a</i> , <i>b</i> , <i>c</i> (Å)	30.53, 30.53, 139.94	33.18, 33.18, 55.28
α , β , γ (°)	90, 90, 90	90, 90, 90
Resolution (Å)	50–2.10 (2.18–2.10)	50–2.07 (2.14–2.07)
R_{sym}	11.3 (52.7)	5.3 (9.6)
<i>I</i> / σ <i>I</i>	18.7 (2.5)	28.4 (12.6)
Completeness (%)	96.7 (89.5)	99.6 (100.0)
Redundancy	12.5 (7.2)	7.3 (6.1)
Refinement		
Resolution (Å)	2.10	2.07
No. of reflections	53,620	13,350
$R_{\text{work}}/R_{\text{free}}$	32.1 / 36.1	19.6 / 22.4
Total protein atoms		249
Water molecules		18
Average B factors: protein (Å ²)		21.1
Average B factors: water (Å ²)		36.5
RMSD in bond lengths (Å)		0.014
RMSD in bond angles (°)		1.59

Values in parentheses are for the highest-resolution shell.

$$R_{\text{sym}} = \frac{\sum_{\text{hkl}} \sum_i (|I_i(\text{hkl}) - \langle I(\text{hkl}) \rangle| / I_i(\text{hkl}))}{\sum_{\text{hkl}} \sum_i I_i(\text{hkl})}$$

$$R_{\text{work}} = \frac{\sum_{\text{hkl}} ||F_{\text{obs}}(\text{hkl})| - |F_{\text{calc}}(\text{hkl})||}{\sum_{\text{hkl}} |F_{\text{obs}}(\text{hkl})|}$$

$R_{\text{free}} = R_{\text{work}}$ calculated using 5% of the reflection data chosen randomly and omitted from the start of refinement.

Table 2. Coiled-Coil Parameters^a

Superhelical parameters	Kv7.4 (613-637)	GCN4-pLI (1-31) ^b	SeVP (67-111) ^c	nSNARE (32-83) ^d	eSNARE (12-63) ^e	Phe-14M (13-54) ^f
Supercoil radius (Å)	7.30±0.15	7.54±0.08	7.77±0.51	6.99±0.24	7.09±0.25	8.24±0.22
Residues / superhelix turn	105±8	133±8	183±54	107±13	120±14	123±13
Supercoil pitch (Å)	152±12	197±13	273±81	152±19	175±22	178±21
Radius of curvature (Å)	87.4±11.9	139±12	267±155	91±20	118±27	106±21
Helix-crossing angle (°)	33.8±2.1	27.1±1.5	21.6±4.9	32.6±2.8	28.8±2.8	32.8±3.1
α-helical parameters						
Residues / turn	3.61±0.03	3.59±0.02	3.61±0.07	3.62±0.03	3.61±0.03	3.61±0.03
Rise / residue (Å)	1.52±0.02	1.52±0.02	1.52±0.05	1.48±0.02	1.50±0.02	1.50±0.01
α-helical radius	2.28±0.04	2.24±0.03	2.27±0.05	2.25±0.03	2.26±0.03	2.29±0.03
Helix-crossing angle (°)	23.7±1.5	19.0±1.1	15.2±3.4	22.9±1.9	20.3±2.0	23.0±2.1
Interhelix distance (Å)	10.3±0.2	10.7±0.1	11.0±0.7	9.9±0.3	10.0±0.4	11.7±0.3

^aHelical and superhelical parameters obtained by fitting the C_α backbone to the supercoil parameterization suggested by Crick (Crick, 1953a).

^bDesigned parallel four-stranded coiled coil based on the GCN4 dimeric leucine zipper peptide (Harbury *et al.*, 1993).

^cSendai virus phosphoprotein oligomerization domain (Tarbouriech *et al.*, 2000).

^dNeuronal SNARE core complex; numbering as synaptobrevin 2 (Sutton *et al.*, 1998).

^eEndosomal SNARE core complex; numbering as endobrevin (Antonin *et al.*, 2002).

^fDesigned parallel four-stranded “Phe-zipper” coiled coil based on the Major Outer Membrane Lipoprotein (Liu *et al.*, 2006).

CHAPTER 3

CRITICAL AMINO ACID INTERACTIONS IN Kv7 COILED-COIL ASSEMBLY

A. Results

i. A-domain Tails from different subtypes have varying propensities to form coiled-coil oligomers

In order to explore the coiled-coil properties of all subtypes of Kv7 A-domain Tails, we calculated the coiled-coil propensity of every residue in each subtype over 21-residue windows by the COILS algorithm (Lupas *et al.*, 1991) (Figure 1A). The Tail subdomain in every subtype has at least a 50% probability of forming a coiled-coil; in some subtypes, the probability is nearly 90%. The A-domain Head also shows a likelihood of forming a coiled coil, especially in Kv7.1, but its coiled-coil propensity is dramatically lower than that of the Tail subdomain in all other subtypes. The Kv7.3 Tail is least likely to assemble as a coiled coil, with a probability less than 60%.

We were interested in exploring the oligomerization properties of the Kv7.3 A-domain Tail in particular, as its coiled-coil propensity is lower than that of other subtypes. Previous measurements show that oligomerization correlates with the coiled-coil propensities in Figure 1A: the Kv7.3 A-domain Tail populates a primarily monomeric state, while other subtypes are oligomeric (Howard *et al.*, 2007). We measured the molecular weight of the Kv7.3 A-domain Tail in the context of an HMT fusion protein, in which the Tail subdomain is fused to maltose binding protein (MBP) and a hexahistidine tag for efficient expression and purification. His-tagged MBP was

previously shown not to oligomerize nor abolish oligomerization of fusion partners (Howard *et al.*, 2007).

Surprisingly, we found that the Kv7.3 A-domain Tail HMT fusion protein behaves as an oligomer when injected onto a size exclusion column immediately after dilution from a highly concentrated stock. Under these conditions, the fusion protein runs between the predicted molecular weight of trimeric and tetrameric species even at a low (1 μM) injected concentration (Figure 1B, top trace). We allowed this diluted protein to incubate at room temperature for 1, 2, or 3 days before injection onto the same size exclusion column. The results demonstrate a slow equilibrium between oligomerization states (Figure 1B). After 1 day, a discrete peak appears slightly before the predicted elution volume of a monomer. After 3 days, the protein predominantly populates this smaller state, with only a minor peak at the oligomer elution volume. Further equilibration does not significantly change the relative peak sizes (data not shown). Therefore, we performed all subsequent experiments on the Kv7.3 A-domain Tail fusion protein following at least 3 days incubation at room temperature.

In order to estimate the affinity of Kv7.3 A-domain Tail oligomerization, we subjected various concentrations of Kv7.3 A-domain Tail HMT fusion proteins to size exclusion chromatography. The initial stock after purification (444 μM) runs at the elution volume of an oligomer, between the predicted volumes of trimeric and tetrameric species (Figure 1C, top trace). We observe negligible contribution from low-molecular-weight species at this concentration. At 125 μM , the Kv7.3 Tail fusion protein elutes as a broad peak spanning the predicted volumes of tetramers to monomers (Figure 1C, second trace from the top). Left- and right-hand shoulders in

the ranges of tetramers and monomers, respectively, indicate discrete populations of both these states, with the remainder of the protein in a rapid equilibrium between species. At 50 μM and 5 μM , the protein elutes primarily slightly before the elution volume of a monomer; this low-molecular weight peak is narrowest at the lowest concentration (Figure 1C, bottom traces). Denaturing gel electrophoresis shows the Kv7.3 A-domain Tail fusion protein is not substantially degraded after equilibration at diluted concentrations (Figure 1C, Inset). Therefore, equilibration, not degradation, is responsible for the slow appearance of the stable, primarily monomeric state of the Kv7.3 A-domain Tail fusion protein at concentrations $\leq 50 \mu\text{M}$.

ii. Mutations at predicted interfaces modify oligomerization of Kv7 coiled coils.

In order to explore the specific amino acid interactions important for oligomerization in various Kv7 subtypes, we engineered mutations in Kv7.1 and Kv7.3 A-domain Tail subdomains. These mutations occur at positions that, in the high-resolution structure of Kv7.4 (Howard *et al.*, 2007), bridge hydrophobic or electrostatic interactions. We initially generated these mutations in the context of A-domain Tail HMT fusion proteins.

By size exclusion chromatography, the wild-type Kv7.1 A-domain HMT fusion protein at 50 μM runs as an oligomer (Figure 2A, top trace). Oligomerization is almost completely disrupted in a mutant of Kv7.1 in which two hydrophobic residues (Leu₆₀₂ and Leu₆₀₆) predicted to occupy the coiled-coil interface are mutated to Lys: the resulting size exclusion peak is close to the predicted elution volume of a monomer (Figure 2A, bottom trace). Mutating the same two residues to Ala partially disrupts

oligomerization, giving rise to both high- and low-molecular weight species (Figure 2A, middle trace). Because the Ala mutant has an intermediate phenotype, we investigated the concentration dependence of its oligomerization. At 10-fold higher concentration (500 μM) the Kv7.1 L₆₀₂A/L₆₀₆A mutant is predominantly oligomeric, with an additional population of higher-order oligomer apparent in the left-hand shoulder of the peak (Figure 2B, top trace). At \sim 10-fold lower concentration (6 μM), the mutant is predominantly monomeric (Figure 2B, bottom trace). Thus, oligomerization of the Kv7.1 double-Ala mutant is concentration-dependent in the 6 – 500 μM range: oligomerization is disrupted relative to wild-type Kv7.1, but favorable relative to the double-Lys mutant.

To obtain more accurate measurements of oligomerization in the Kv7.1 wild-type and double-Ala mutant A-domain Tail fusion proteins, we measured their apparent molecular weights by sedimentation equilibrium at multiple concentrations. The radial distribution of absorbance of the wild-type Kv7.1 Tail subdomain fusion protein at 2 μM fits the predicted profile of a single trimeric species (Figure 3A). The distribution of apparent molecular weights of the wild-type Kv7.1 Tail fits the predicted distribution for a moderate monomer-trimer equilibrium ($K_D \approx 50$ nM) (Figure 3B). The apparent molecular weight of this construct at 2 μM also fits a weak monomer-tetramer equilibrium, but the higher-concentration measurements do not fit this model. Alternative models involving additional intermediate configurations, such as monomer-dimer-tetramer or monomer-dimer-trimer-tetramer equilibria, are also possible, and could be fit with additional data. Furthermore, apparent molecular weights decrease slightly at higher concentrations, indicating partial nonideality of the protein in solution

(Laue, 1995); inclusion of additional data may allow explicit incorporation of nonideality in assembly modeling. Thus, the association strength of the Kv7.1 A-domain Tail fusion protein complex remains uncertain, but it is likely to be a high-order (trimer or tetramer) species at concentrations of 2 μM and higher.

The radial distribution of absorbance of the Kv7.1 A-domain Tail fusion protein with double Ala mutations ($L_{602}A/L_{606}A$) at 2 μM fits the predicted profile of a single monomeric species (Figure 3C). However, the apparent molecular weight of this mutant construct increases at higher concentrations, indicating self-association (Laue, 1995). The distribution of apparent molecular weights fits a weak monomer-tetramer equilibrium ($K_D \approx 40 \text{ mM}$) (Figure 3D). The apparent molecular weights of the mutant construct at 2 μM and 10 μM also fit a monomer-trimer equilibrium ($K_D \approx 2 \text{ mM}$), but the measurements at 40 μM do not fit this model. Thus, double Ala mutations at the predicted coiled-coil interface of the Kv7.1 A-domain Tail destabilize assembly dramatically, weakening the dissociation constant of oligomeric species and reducing the complex primarily to a monomeric state at concentrations of 10 μM and below.

We also investigated the ability of Kv7.1 wild-type and mutant A-domain Tails to bind the Tails of various Kv7 subtypes. To this end, we constructed expression vectors with Kv7 A-domain Tails fused to the BI domain of protein G (GBI) (Gronenborn *et al.*, 1991), which is a useful tag for promoting solubility and allowing affinity purification on IgG-labeled beads (Huth *et al.*, 1997). Constructs of A-domain Tails from all Kv7 subtypes were prepared; however, the Kv7.3 A-domain Tail GBI fusion did not express well, and is not shown. We coexpressed GBI fusion proteins with Kv7.1 A-domain Tail HMT fusion proteins, which can be purified by metal- or maltose-affinity

chromatography (van Petegem *et al.*, 2004). We purified the resulting cell lysates by Co^{2+} -affinity. The appearance of the GBI fusion protein in the imidazole elution step represents binding between HMT and GBI tagged proteins. As expected, the wild-type Kv7.1 A-domain Tail HMT fusion protein pulls down the GBI fusion protein from Kv7.1, but not Kv7.2, Kv7.4, or Kv7.5 (Figure 4A). The Kv7.1 Tail fusion containing double Ala mutations ($\text{L}_{602}\text{A}/\text{L}_{606}\text{A}$) is similar to wild-type, pulling down the Tail of wild-type Kv7.1 but not Kv7.2, Kv7.4, or Kv7.5 (Figure 4B). Conversely, the Kv7.1 Tail fusion with double Lys mutations ($\text{L}_{602}\text{K}/\text{L}_{606}\text{K}$) appears to be disrupted, as it does not pull down the Tails of any subtype (Figure 4C). Thus, while double Ala mutations have little or no effect on binding, double Lys mutations abolish binding of Kv7.1 A-domain Tails.

The Kv7.3 A-domain Tail contains three residues that are predicted to disrupt hydrophobic or electrostatic interactions based on the Kv7.4 A-domain Tail structure (Howard *et al.*, 2007). Phe_{622} occupies an interface “d”-position that, in other subtypes, is either Val or Leu; it is unlikely that the bulky Phe side chain would be tolerated at this position without structural rearrangement (Liu *et al.*, 2006). Kv7.3 Asp_{631} is a “c”-position residue that aligns with Kv7.4 Ser_{628} , which forms an intermolecular hydrogen bond with the Kv7.4 “e” residue Glu_{630} ; substitution of Asp for Ser would remove this interaction. Kv7.3 Gly_{633} aligns with Kv7.4 Glu_{630} , which is involved in two additional intermolecular electrostatic interactions besides Ser_{628} ; substitution of Gly for Glu would abolish all three of these contacts. Therefore, we mutated Kv7.3 Phe_{622} , Asp_{631} , and Gly_{633} to their equivalent amino acids from Kv7.2, generating the mutations F_{622}L , D_{631}S , and G_{633}E ; all three of these mutations are predicted to stabilize the oligomeric state of Kv7.3. We also generated a putative destabilizing mutation in Kv7.1 by mutating Kv7.1 Leu_{592} , which is equivalent to Kv7.3 Phe_{622} , to Phe (L_{592}F).

Oligomerization of the Kv7.1 A-domain HMT fusion protein is not abolished by the L₅₉₂F mutation at 50 μ M, though a small additional peak appears at the elution volume of a monomer (Figure 2C, top two traces). Conversely, mutating the equivalent position in Kv7.3 from Phe to Leu (F₆₂₂L), or changing the electrostatic interaction sites Asp₆₃₁ and Gly₆₃₃ to their equivalent amino acids from Kv7.2, restores tetramerization almost entirely (Figure 2C, third and fourth traces). A triple mutant (F₆₂₂L/D₆₃₁S/G₆₃₃E) with all three interaction sites changed to their equivalent residues in Kv7.2 shows almost no remaining population of monomer (Figure 2C, fifth trace). Thus, although disrupting a single hydrophobic interaction is not sufficient to abolish oligomerization of the Kv7.1 Tail subdomain, augmentation of one or more hydrophobic or electrostatic interactions can contribute substantially to oligomerization of Kv7.3.

iii. Long QT syndrome mutations do not abolish oligomerization of Kv7.1 A-domain Tails.

Several missense mutations linked to LQTS occur in the Kv7.1 A-domain Tail. Because this subdomain was previously shown to affect channel assembly, it was suggested that A-domain Tail mutations might cause disease by interfering with tetramerization (Piippo *et al.*, 2001). However, other groups have suggested alternative phenotypes for these mutations including interference with trafficking (Kanki *et al.*, 2004) and binding of scaffolding proteins (Marx *et al.*, 2002). Furthermore, we previously showed by size exclusion chromatography that the T₅₈₇M (Itoh *et al.*, 1998), G₅₈₉D (Piippo *et al.*, 2001), A₅₉₀T (Lupoglazoff *et al.*, 2004), R₅₉₁H (Neyroud *et al.*, 1999), and R₅₉₄Q (Splawski *et al.*, 2000) mutations do not dramatically disrupt oligomerization of Kv7.1 A-domain Tails (Howard *et al.*, 2007).

In light of the concentration dependence of oligomerization in wild-type Kv7.3 and the Kv7.1 double-Ala interface mutant, we proposed that Kv7.1 A-domain Tail LQTS mutations might also disrupt assembly weakly, such that their effect would only be seen at concentrations lower than 50 μ M. In order to test this hypothesis, we measured the elution volumes of wild-type and LQTS mutant Kv7.1 A-domain Tail HMT fusion proteins by size exclusion chromatography at 10- and 100-fold lower concentrations than previously tested. We were also interested in testing an additional Kv7.1 interface mutant in which two consecutive “d”-position residues, Leu₆₀₂ and Ile₆₀₉, are mutated to Ala. This mutant was initially shown to disrupt coiled-coil formation on the basis of diminished binding of the scaffolding protein yotiao (Marx *et al.*, 2002). However, another group found this mutant to have little effect on coiled-coil probability or surface trafficking (Kanki *et al.*, 2004). To explain these results, we proposed the Leu₆₀₂/Ile₆₀₉ mutation could modify the coiled-coil structure just enough to alter the Tail subdomain surface, without abolishing its assembly and trafficking properties.

The Kv7.1 wild-type Tail subdomain fusion protein elutes between the predicted elution volumes of trimeric and tetrameric species at 50 μ M, 5 μ M, and 500 nM (Figure 5A). The LQTS mutants G₅₈₉D, A₅₉₀T, and R₅₉₄Q have little or no effect on oligomerization, giving very similar elution profiles (Figure 5B, 5C, 5E). The R₅₉₁H mutation does not disrupt oligomerization; in fact, at all concentrations tested, it elutes earlier than the predicted volume of tetrameric species, substantially earlier than wild-type Kv7.1 and other LQTS mutants (Figure 5D). The L₆₀₂A/I₆₀₉A mutant is the only mutant with a concentration-dependent phenotype. At 50 μ M, the oligomeric state of

this mutant (Figure 5F, top trace) is more favored than in the previously tested $L_{602}A/L_{606}A$ mutant (Figure 2B). However, at 5 μ M a peak near the elution volume of a monomer begins to predominate (Figure 5F, top trace), and at 500 nM this low-molecular weight peak is almost exclusively represented (Figure 5F, bottom trace).

We used sedimentation equilibrium to obtain a more precise measurement of molecular mass of the Kv7.1 LQTS and $L_{602}A/I_{609}A$ mutants. The equilibrium distributions of absorbance of Kv7.1 A-domain Tail HMT fusion proteins with $G_{589}D$, $A_{590}T$, and $R_{594}Q$ mutations are similar at 5 μ M to that of the wild-type protein, and close to the predicted distribution of a trimeric species (Figure 6A, 6B, 6C, 6E). The distribution of the $R_{591}H$ construct fits a higher-order complex, close to a single tetrameric species (Figure 6D). The $L_{602}A/I_{609}A$ construct fits the predicted distribution of a monomer (Figure 6F). Thus, sedimentation equilibrium indicates that size exclusion chromatography overestimates the molecular weight of Kv7 A-domain Tail fusion proteins, but that the relative sizes measured by both methods are consistent: the $R_{591}H$ mutant is largest, wild-type Kv7.1 and remaining LQTS mutants are lower-order oligomers, and the $L_{602}A/I_{609}A$ mutant is effectively a monomer at 5 μ M.

iv. Mutations that promote oligomerization also increase currents of chimeric channels containing Kv7.3 coiled coils.

The ability of interface mutations to restore tetramerization to the Kv7.3 A-domain Tail suggests these mutations should have a significant impact on full-length channel function. Kv7.3 channels produce small currents in heterologous expression systems; in some cases, they are indistinguishable from background (Schroeder *et al.*,

1998; Wang *et al.*, 1998). Reduced surface expression, possibly due to assembly defects, plays a role in reducing Kv7.3 currents (Schwake *et al.*, 2000). Therefore, we hypothesized that restoring oligomerization to the Kv7.3 A-domain Tail might also promote surface expression and currents of full-length Kv7.3 channels.

Full-length Kv7.2 channels expressed in oocytes give moderate currents as measured by two-electrode voltage clamp at +40 mV (Figure 7A). Currents recorded from Kv7.3 are much smaller, close to background levels (Figure 7B). Mutating Phe₆₂₂, Asp₆₃₁, and Gly₆₃₃ to their equivalent residues from Kv7.2 (F₆₂₂L/D₆₃₁S/G₆₃₃E) does not enhance Kv7.3 currents (Figure 7C). However, it is possible that there is a change in current levels, but that currents are too small for the change to be detectable above variations due to noise. The small size of Kv7.3 wild-type and mutant currents is not due to faulty protein synthesis, as coinjection with Kv7.2 leads to large enhancement of currents (Figure 7D, 7E). In the context of coinjection, the F₆₂₂L/D₆₃₁S/G₆₃₃E mutations again do not enhance currents (Figure 7E). This result could indicate that the mutations do not promote oligomerization; however, it could also arise from saturation of currents in the vicinity of 10 μ A, or from compensation by coassembly with Kv7.2 subunits. The latter hypothesis could partially explain the enhanced currents observed in heteromeric Kv7.2/Kv7.3 channels.

To measure the effect of Kv7.3 mutations more definitively, we constructed a chimeric channel in which the N-terminal, transmembrane, proximal C-terminal and distal C-terminal domains are from Kv7.2, while the A-domain Tail is from Kv7.3. This chimera (Kv7.2_{3T}, Figure 7F) gives much larger currents than Kv7.3 but smaller currents than Kv7.2, indicating the Kv7.3 A-domain Tail disrupts channel function. Introduction

of the $F_{622}L/D_{631}S/G_{633}E$ mutations into this channel increases currents about 2-fold (Figure 7G), approximately to the level of wild-type Kv7.2. Thus, in the chimeric channel, increased currents correlate with enhanced assembly properties of the isolated Tail subdomain.

We measured currents in Kv7.3 and Kv7.2_{3T} channels containing mutations at predicted hydrophobic ($F_{622}L$) and electrostatic ($D_{631}S/G_{633}E$) interactions separately and together (Figure 7H). Kv7.3 currents are low, about one-fourth the level of Kv7.2, with no significant increase in single-, double-, or triple-mutants. Kv7.2_{3T} currents are about 60% of Kv7.2 currents, a statistically significant difference ($p < 0.05$); the single $F_{622}L$ or triple $F_{622}L/D_{631}S/G_{633}E$ mutations significantly increase Kv7.2_{3T} currents ($p < 0.05$), approximately to the level of Kv7.2. The double mutant Kv7.2_{3T} $D_{631}S/G_{633}E$, in which three putative electrostatic contacts are abolished, gives larger average currents than Kv7.2_{3T}, but the difference has not been shown to be statistically significant.

B. Discussion

The high-resolution structure of the Kv7.4 A-domain Tail (Howard *et al.*, 2007) leaves several questions unanswered, particularly with regard to subtypes other than Kv7.4. First, we wished to corroborate the oligomeric coiled-coil structures of A-domain Tails in all Kv7 subtypes, particularly Kv7.3, which we showed does not oligomerize with the same affinity as other subtypes (Howard *et al.*, 2007). Second, specific amino acid interactions stabilizing native Kv7 A-domain Tail structures have yet to be identified. Characterizing these critical contacts could inform our understanding of specificity determination in Kv7 channels, establish a paradigm for coiled-coil assembly

in a wide range of ion channels (Jenke *et al.*, 2003), and elucidate the mechanisms by which some Kv7 mutations cause disease.

To better understand the structural properties of Kv7 A-domain Tails, we have probed specific amino acid positions in predicted Kv7 coiled coils, primarily by size exclusion chromatography of HMT fusion proteins. Although size exclusion is a widespread and informative technique for estimating a protein's molecular weight, it can be influenced by a number of other factors, including a protein's shape (Le Maire *et al.*, 1989) and interaction with column beads (Potschka, 1987). Kv7 A-domain Tails that we previously identified as "oligomeric" elute between the predicted volumes of trimeric and tetrameric species (Howard *et al.*, 2007). This finding could indicate a mixture of three- and four-stranded species, or could arise from inaccurate estimation of molecular weight. We also note that "disrupted" Kv7 Tail subdomains, which are most likely to be monomeric, elute somewhat earlier than the predicted volumes of monomers (Figure 1B, 1C, 2, 5F), suggesting a systematic overestimation of molecular weight by this method. We have corroborated this trend by sedimentation equilibrium, a technique based on the physical properties of the protein, solvent, and centrifugal system; in ideal solutions, values obtained by this method are independent of protein shape (Laue, 1995). In all cases, we calculate a lower oligomerization state by sedimentation equilibrium than by size exclusion, further indicating that size exclusion overestimates molecular weight of Kv7 Tail HMT fusion proteins (Figure 3, 6). To account for this effect, we describe proteins below as "monomeric" if they elute slightly before the predicted volume of monomers, and as "tetrameric" only if they elute earlier than the predicted volume of tetramers; we describe proteins of

intermediate elution volumes as “oligomeric.” However, it should be noted throughout the discussion that these terms are approximations.

Our calculations indicate that A-domain Tails in all Kv7 subtypes are likely to form coiled coils (Figure 1A). The conservation of this structural motif is supported by size exclusion chromatography, which shows that HMT fusion A-domain Tails from Kv7.1, Kv7.2, and Kv7.5 are oligomeric; notably, they all elute at a similar volume to Kv7.4, which is known to be a four-stranded coiled coil (Howard *et al.*, 2007). Recently, Wehling *et al.* further demonstrated that disrupting the coiled-coil propensity of the Kv7.2 A-domain Tail interferes with its tetramerization, indicating that the Kv7.2 Tail is also a four-stranded coiled coil (Wehling *et al.*, 2007). However, the Kv7.3 Tail subdomain has a low coiled-coil propensity relative to other subtypes (Figure 1A, third trace). This finding correlates with the oligomerization properties of the Kv7.3 A-domain Tail, which assembles at high concentrations but exists as a lower-order species at low concentrations (Figure 1C). Notably, we found that the oligomeric form of Kv7.3 is tightly associated, such that ≥ 3 days equilibration at room temperature is required to dissociate it fully at low concentrations (Figure 1B). It is unclear whether the Kv7.3 A-domain Tail forms a coiled coil in the context of the full-length protein; even if it does, its properties may be substantially different from those of other subtypes.

A likely target for disrupting coiled-coil assembly is the hydrophobic interface. These contacts comprise “a”- and “d”-positions in the characteristic heptad repeat (“a-b-c-d-e-f-g”) of coiled coils, and pack like “knobs-into-holes” to form the buried interface between participating helices (Crick, 1953). In some cases, a relatively conservative point mutation—for example, substitution of Ala for a larger, more hydrophobic

residue—at an “a”- or “d”-position is tolerated (Shu *et al.*, 2000), but in other cases it is significantly destabilizing (Liu *et al.*, 2002). Some studies have suggested that multiple Ala substitutions disrupt Kv7 coiled-coil formation (Marx *et al.*, 2002), while others find them to be functionally conservative (Kanki *et al.*, 2004). In our hands, double-Ala interface mutations in the Kv7.1 A-domain Tail disfavor oligomerization in a concentration-dependent manner (Figure 2B, 3, 5F, 6F). However, coexpressed L₆₀₂A/L₆₀₆A and wild-type Kv7.1 Tail subdomains retain strong inter-subunit binding (Figure 4B). Thus, Ala mutations at hydrophobic interface residues in Kv7.1 do not abolish assembly of Tail subdomains, but may alter their affinity and structural properties.

Mutations other than Ala at hydrophobic coiled-coil interfaces can have more dramatic effects on Kv7 assembly. Substitution of Phe can increase coiled-coil stoichiometry (Liu *et al.*, 2006); a polar or charged residue can reduce coiled-coil stoichiometry (Woolfson and Alber, 1995); and Pro tends to disrupt assembly altogether (Conway and Parry, 1988). We previously demonstrated that the presence of a single Phe residue at the predicted hydrophobic interface of Kv7.3 is sufficient to disrupt assembly compared to other subtypes (Howard *et al.*, 2007), although assembly of Kv7.1 is more tolerant of an interface Phe (Figure 2C). More dramatically, mutation of hydrophobic interface residues to Asp or Pro suppresses trafficking of Kv7.1 (Kanki *et al.*, 2004) and tetramerization and current augmentation of Kv7.2 (Wehling *et al.*, 2007; Schwake *et al.*, 2006). Accordingly, in our hands, mutating interface Leu residues in Kv7.1 to Lys reduces oligomerization to a greater degree than mutating the same positions to Ala (Figure 2A). The double-Lys mutation also disrupts binding of wild-type A-domain Tails (Figure 4C). The dramatic effect of charged residue substitutions on

oligomerization substantiates the coiled-coil structure of this domain and the importance of interface hydrophobic interactions in stabilizing assembly.

Peripheral (“b, c, e, f, g”) positions in coiled coils are usually polar, but the importance of specific polar interactions in coiled-coil stability is controversial (Mason and Arndt, 2004). We showed previously that mutating Kv7.3 to restore three electrostatic contacts between coiled-coil surface residues promotes oligomerization of the Tail subdomain, indicating these interactions are important to coiled-coil formation (Howard *et al.*, 2007). The importance of other electrostatic interactions in Kv7.1 is suggested by a disease mutation, R₅₉₁H, in which a “g”-position Arg residue is changed to His; in Kv7.4, the equivalent Arg is involved in an intermolecular salt bridge with an “e”-position Glu residue (Howard *et al.*, 2007). This mutation disrupts functional channel expression by trapping channels in the ER, leading to LQTS (Grunnet *et al.*, 2005). However, this and three other LQTS-linked mutations in the A-domain Tail still permit normal synthesis and tetramerization of Kv7.1 channels, suggesting their defects arise from trafficking, not assembly (Kanki *et al.*, 2004). Indeed, these mutations do not substantially disrupt oligomerization of Kv7.1 A-domain Tails (Figure 5, 6); in fact, the R₅₉₁H mutation promotes tetramerization relative to wild-type (Figure 5D, 6D). Thus, electrostatic “e/g”-position interactions may be involved in Kv7 coiled-coil stabilization, but the nature of their role is unclear.

Multiple interactions contribute to the oligomerization of A-domain Tails. Thus, equivalent mutations may have different effects in different subtypes depending on their baseline oligomerization propensities. For example, the presence of a Phe (Wild-type) instead of a Leu (F₆₂₂L) at the first coiled-coil “a”-position of Kv7.3 is sufficient to disrupt A-domain Tail oligomerization, whereas the same substitution in Kv7.1 (L₅₉₂F) has little

effect (Figure 2C). We propose that, in Kv7.1, the disruptive effect of an interface Phe is compensated by other stabilizing interactions not present in Kv7.3. This model is supported by size exclusion chromatography: at 50 μ M, the Kv7.1 A-domain Tail is a single oligomeric peak, whereas Kv7.3 F₆₂₂L includes both an oligomer peak and a small monomer peak. Thus, removing the disruptive effect of Phe₆₂₂ increases oligomerization of the Kv7.3 A-domain Tail almost, but not completely, to the level of Kv7.1. We have noted previously that three specific electrostatic interactions in the Kv7.4 coiled-coil structure are possible in Kv7.1, but not in Kv7.3. Mutating Kv7.3 to restore these electrostatic contacts (D₆₃₁S/G₆₃₃E) compensates for the disruptive effect of Phe₆₂₂ (Howard *et al.*, 2007). A triple mutant in which the electrostatic contacts are restored and the interface Phe is replaced with Leu (F₆₂₂L/D₆₃₁S/G₆₃₃E) has almost no trace of monomer at 50 μ M (Figure 2C). Thus, in the case of Kv7.3, hydrophobic and electrostatic interactions can compensate for each other in promoting assembly, with maximal oligomerization observed where both hydrophobic and electrostatic contributions are favorable.

Disrupted oligomerization of the Kv7.3 A-domain Tail correlates with diminished function of homotetrameric Kv7.3 channels relative to other subtypes (Schroeder *et al.*, 1998; Wang *et al.*, 1998). As described above, mutations at predicted hydrophobic and electrostatic contacts enhance oligomerization of Kv7.3 A-domain Tails; therefore, we investigated the ability of these alterations to increase homomeric assembly of full-length Kv7.3 channels. Wild-type and mutant Kv7.3 channels are correctly synthesized in oocytes, as shown by augmentation of Kv7.2 currents (Figure 7D, 7E, 7H), but their currents are close to background levels (Figure 7B, 7C). We are unable to demonstrate

a significant enhancement of homomeric Kv7.3 channel function by single or multiple coiled-coil stabilizing mutations (Figure 7C, 7H). However, this result does not rule out an effect of Kv7.3 mutations on full-length channels. Measuring Kv7.3 function in oocytes is compromised by a combination of inhibitory mechanisms, including pore block and disrupted surface expression, which result in low currents (Etxeberria *et al.*, 2004). Because Kv7.3 currents are often barely above background levels, modulation could be masked by low signal-to-noise ratio. Furthermore, enhancing channel oligomerization may compensate for only one of several inhibitory factors, limiting the net functional effect of assembly mutations.

To assess the functional impact of Kv7.3 A-domain Tail assembly independent of other factors, we created a chimera of Kv7.2 containing the A-domain Tail of Kv7.3 (Kv7.2_{3T}). This channel should be functionally identical to Kv7.2 except for differences in Tail subdomain assembly. Currents recorded from the Kv7.2_{3T} chimera are significantly smaller than wild-type Kv7.2, indicating that the Kv7.3 A-domain Tail inhibits channel function (Figure 7F, 7H). Enhancing Tail assembly via mutations at the hydrophobic interface (F₆₂₂L) restores Kv7.2_{3T} currents approximately to the level of wild-type Kv7.2 (Figure 7H). Additional restoration of surface electrostatic contacts (F₆₆₂L/D₆₃₁S/G₆₃₃E) causes an even more significant increase in chimera currents (Figure 7G, 7H). Thus, disruption of A-domain Tail assembly by noncanonical hydrophobic or electrostatic interactions can inhibit function of full-length channels independent of other channel properties.

Disruption of the Kv7.3 Tail coiled-coil could be a necessary feature of its phenotype. It was recently demonstrated that substitution of Pro at an interface “a”-position, which should further disrupt Kv7.3 coiled-coil formation, does not significantly

affect macroscopic currents or augmentation of heteromer currents (Schwake *et al.*, 2006). This finding supports the hypothesis that the functional Kv7.3 A-domain Tail has a different structure from that of other subtypes: the coiled-coil is disfavored relative to an alternative, probably monomeric conformation, such that further disruption of coiled-coil propensity has no functional impact. Poor oligomerization of this alternate conformation compared to the coiled-coils in other subtypes may cause poor expression of Kv7.3 homotetramers; however, interaction of this motif with other Kv7 subtypes may expose a forward trafficking motif (or mask a retention signal) that promotes function of heterotetramers. Further investigation of Kv7 A-domain Tail structural properties and of the role of specific amino acid interactions in full-length channel function will help elucidate the complex role of this domain in channel oligomerization and binding specificity.

C. Experimental Procedures

i. Sequence Analysis

Prediction of coiled-coil regions in Kv7 channels was carried out with the COILS program (Lupas *et al.*, 1991) (http://www.ch.embnet.org/software/COILS_form.html) version 2.1 using the MTIDK matrix with a window size of 21 residues and no additional weighting of “a”- and “d”-positions.

ii. DNA Constructs

For bacterial expression and purification, DNA fragments of Kv7.1 (residues 583–623) and Kv7.3 (residues 613–653) were amplified by PCR and ligated into the NarI/XhoI sites of a pET27 (Novagen) derived bacterial expression vector (pSV272)

denoted “HMT” (Van Petegem *et al.*, 2004) that contains, in sequence, a hexahistidine tag, maltose binding protein, and a cleavage site for the Tobacco Etch Mosaic Virus (TEV) protease. The Kv7.1 fragment was also ligated into the NheI/HindIII sites of a pET23b (Novagen) derived vector denoted “GBI” that contains, in sequence, the BI domain of protein G and a modified cleavage site for TEV protease.

For oocyte expression, complete Kv7.2 and Kv7.3 cDNAs were ligated in the EcoRI/HindIII or BamHI/XhoI sites, respectively, of a pGEMHE derived oocyte expression vector (Minor *et al.*, 1999). The Kv7.2_{3T} chimera was constructed by engineering a Bsu36I site at the 5' end of the Kv7.2 A-domain Tail sequence and subcloning the Kv7.3 A-domain Tail sequence in the Bsu36I/AclI sites of the altered Kv7.2 construct.

Point mutations were made using mutated oligonucleotide extension (Pfu Turbo Polymerase, Strategene) from plasmid templates harboring the protein of interest, digested with DpnI (New England Biolabs), and transformed into DH5 α cells. All constructs were verified by complete DNA sequencing of the subcloned insert.

iii. Protein Expression and Lysis

HMT or GBI fusion proteins were expressed in *Escherichia coli* (BL21(DE3)pLysS) grown in 2YT media at 37°C and induced at OD_{600nm} = 0.4–0.8 with 0.4 mM IPTG for 4 hr. Cells were harvested by centrifugation at 5000 x g for 20 min at 4°C, and cell pellets were frozen at –20°C. Thawed cell pellets were lysed by sonication in lysis buffer (100 mM Tris pH 7.6, 200 mM KCl, 10% sucrose, 25 mM β -

octylglucoside, 20 µg/ml lysozyme, 25 µg/ml DNaseI, 5 mM MgCl₂, 1 mM PMSF).

Insoluble material was precipitated by centrifugation for 20 min at 12,000 × g at 4°C.

iv. HMT Fusion Protein Purification

For size exclusion and sedimentation equilibrium, the soluble fraction of lysed cells expressing HMT fusion proteins was applied to a 45 ml Poros20MC (Perseptive Biosystems) nickel-charged column, washed in wash buffer (10 mM PO₄²⁻, pH 7.3, 250 mM KCl, 1 mM PMSF), and eluted on a linear gradient to 300 mM imidazole in the same buffer on an ÄKTA-FPLC system (Pharmacia). Imidazole was removed using a Centriprep YM-10 concentrator (Millipore). Fusion proteins were then applied to a 60 ml Amylose (New England Biolabs) column, washed in wash buffer, and eluted in maltose buffer (10 mM PO₄²⁻, pH 7.3, 250 mM KCl, 10 mM maltose). Purified fusion proteins were concentrated in a Centriprep YM-10 and their concentration was determined by absorbance (Edelhoch, 1967).

v. Size Exclusion Chromatography

Samples of 100 µL HMT fusion proteins were loaded on a Superdex200 HR 10/30 column (Amersham Biosciences) equilibrated with high-salt buffer (400 mM KCl, 1 mM EDTA, 10 mM PO₄²⁻, pH 7.3) on an ÄKTA-FPLC system (Pharmacia) at 4°C. Eluates were monitored at 280 nm over a flow rate of 0.3 ml/min. The column was calibrated using six standard protein molecular mass markers (Howard *et al.*, 2007).

vi. Equilibrium Sedimentation

Sedimentation equilibrium experiments were performed at 4°C in a Beckman Optima XL-A analytical ultracentrifuge (Beckman Coulter). Kv7.1 HMT fusion proteins (2–5 μM in 10 mM PO₄²⁻, pH 7.3, 250 mM KCl) were loaded in six-chamber analytical ultracentrifuge cuvettes, using buffer in the adjacent chamber as a blank. The molecular mass was calculated from a single-species exponential fit (Excel) to the distribution of concentration over the radius of the chamber:

$$M = (2RT / ((1-v\rho)\cdot\omega^2)) \cdot (d(\ln(c)) / d(r^2))$$

where M is the molecular weight in g/mol, R is the gas constant (8.314 J(mol•K)⁻¹), T is the temperature in K, v is the partial specific volume of the protein in ml/g, ρ is the density of the solvent in g/mL, ω is the angular velocity of centrifugation in rad/s, and r is the distance in cm from the center of the rotor to a given position in the cell (Laue, 1995). Partial specific volume was calculated from the sum of the volumes of individual residues in the protein. Solvent density was calculated from the components of the buffer. Residuals were calculated as the difference between the measured absorbance value and the predicted value extrapolated from the calculated molecular mass.

vii. Affinity Copurification

For pull-down experiments, the soluble fraction of lysed cells coexpressing HMT and GBI fusion proteins was applied to a TALONspin (Clontech) column containing 500 μl of cobalt-charged resin, washed at least 6 times in wash buffer (50 mM PO₄²⁻, pH 7.0, 300 mM NaCl), and eluted with 150 mM imidazole in the same buffer. Samples were

separated by gel electrophoresis in 15% polyacrylamide with 0.1% SDS and visualized with Coomassie staining (Bio-Rad).

viii. Electrophysiology

Individual stage V–VI oocytes were obtained from anaesthetized frogs and isolated by treatment with collagenase. Synthesis of cRNA was performed with the T7 mMessage mMachine kit (Ambion). Wild-type or mutant Kv7.2, Kv7.3, or Kv7.2_{3T} cRNA (15 ng) was injected into *Xenopus* oocytes; co-injection experiments contained 15 ng total of a 1:1 cRNA mixture. After injection, oocytes were kept at 16° C in ND96 solution (96 mM NaCl, 1 mM MgCl₂, 0.2 mM CaCl₂, 5 mM HEPES, pH 7.4, adjusted with KOH) supplemented with penicillin and streptomycin.

Two or three days after injection, currents were measured at room temperature (21 °C) in two-electrode voltage clamp recordings with a GeneClamp 500B (Axon Instruments) amplifier and pClamp software (Axon Instruments) and digitized at 1 kHz with a Digidata 1332A (Axon Instruments). During recordings, oocytes were perfused with ND96 buffer using a Valvelink 16 (AutoMate Scientific) controller. Voltage protocol for current recordings: from a holding potential of -80 mV, cells were pulsed for 2.5 s to voltages between -80 mV and +40 mV in steps of 15 mV, followed by a 2 s test pulse to -40 mV.

D. References

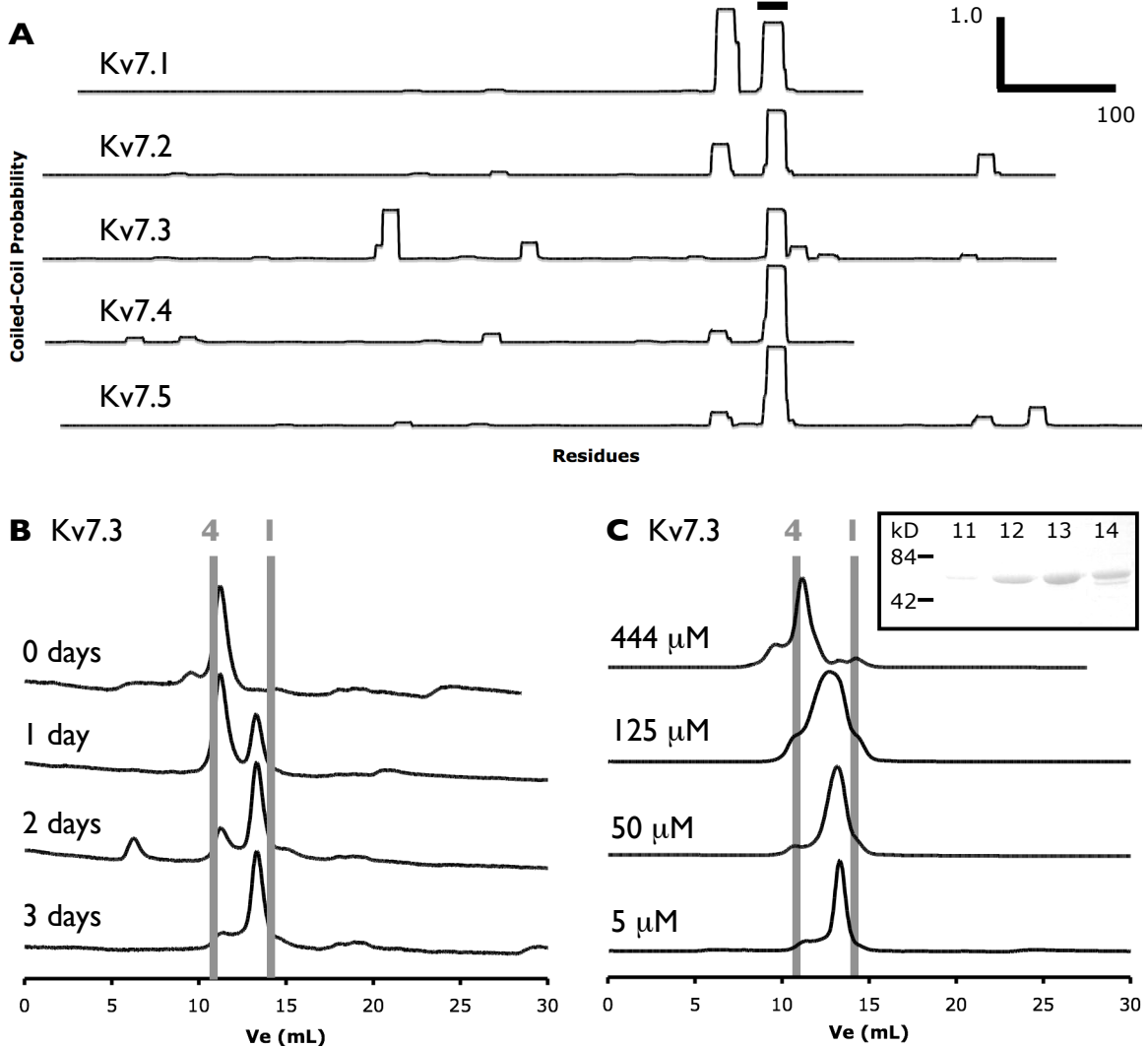
- Conway, J. F. & Parry, D. A. D. S. (1988). Intermediate filament structure: 3. Analysis of sequence homologies. *Int. J. Biol. Macromol*, 10, 79.
- Crick, F. (1953). The Fourier Transform of a Coiled-Coil. *Acta Cryst*, 6, 685-689.
- Edelhoch, H. (1967). Spectroscopic determination of tryptophan and tyrosine in proteins. *Biochemistry*, 6(7), 1948-1954.

- Etxeberria, A., Santana-Castro, I., Regalado, M. P., Aivar, P., & Villarroel, A. (2004). Three mechanisms underlie KCNQ2/3 heteromeric potassium M-channel potentiation. *The Journal of neuroscience : the official journal of the Society for Neuroscience*, 24(41), 9146-9152.
- Gronenborn, A. M., Filpula, D. R., Essig, N. Z., Achari, A., Whitlow, M., Wingfield, P. T. et al. (1991). A novel, highly stable fold of the immunoglobulin binding domain of streptococcal protein G. *Science*, 253(5020), 657-661.
- Grunnet, M., Behr, E. R., Calloe, K., Hofman-Bang, J., Till, J., Christiansen, M. et al. (2005). Functional assessment of compound mutations in the KCNQ1 and KCNH2 genes associated with long QT syndrome. *Heart rhythm : the official journal of the Heart Rhythm Society*, 2(11), 1238-1249.
- Howard, R. J., Clark, K. A., Holton, J. M., & Minor, D. L. (2007). Structural insight into KCNQ (Kv7) channel assembly and channelopathy. *Neuron*, 53(5), 663-675.
- Huth, J. R., Bewley, C. A., Jackson, B. M., Hinnebusch, A. G., Clore, G. M., & Gronenborn, A. M. (1997). Design of an expression system for detecting folded protein domains and mapping macromolecular interactions by NMR. *Protein science : a publication of the Protein Society*, 6(11), 2359-2364.
- Itoh, T., Tanaka, T., Nagai, R., Kikuchi, K., Ogawa, S., Okada, S. et al. (1998). Genomic organization and mutational analysis of KVLQT1, a gene responsible for familial long QT syndrome. *Human genetics*, 103(3), 290-294.
- Jenke, M., Sánchez, A., Monje, F., Stühmer, W., Weseloh, R. M., & Pardo, L. A. (2003). C-terminal domains implicated in the functional surface expression of potassium channels. *The EMBO journal*, 22(3), 395-403.
- Kanki, H., Kupersmidt, S., Yang, T., Wells, S., & Roden, D. M. (2004). A structural requirement for processing the cardiac K⁺ channel KCNQ1. *The Journal of biological chemistry*, 279(32), 33976-33983.
- Laue, T. M. (1995). Sedimentation equilibrium as thermodynamic tool. *Methods in enzymology*, 259, 427-452.
- Le Maire, M., Viel, A., & Møller, J. V. (1989). Size exclusion chromatography and universal calibration of gel columns. *Analytical biochemistry*, 177(1), 50-56.
- Liu, J., Cao, W., & Lu, M. (2002). Core side-chain packing and backbone conformation in Lpp-56 coiled-coil mutants. *Journal of molecular biology*, 318(3), 877-888.
- Liu, J., Zheng, Q., Deng, Y., Kallenbach, N. R., & Lu, M. (2006). Conformational transition between four and five-stranded phenylalanine zippers determined by a local packing interaction. *Journal of molecular biology*, 361(1), 168-179.
- Lupas, A., Van Dyke, M., & Stock, J. (1991). Predicting coiled coils from protein sequences. *Science (New York, N.Y.)*, 252(5009), 1162-1164.
- Lupoglazoff, J. M., Denjoy, I., Villain, E., Fressart, V., Simon, F., Bozio, A. et al. (2004). Long QT syndrome in neonates: conduction disorders associated with HERG mutations and sinus bradycardia with KCNQ1 mutations. *Journal of the American College of Cardiology*, 43(5), 826-830.
- Marx, S. O., Kurokawa, J., Reiken, S., Motoike, H., D'Armiento, J., Marks, A. R. et al. (2002). Requirement of a macromolecular signaling complex for beta adrenergic receptor modulation of the KCNQ1-KCNE1 potassium channel. *Science*, 295(5554), 496-499.
- Mason, J. M. & Arndt, K. M. (2004). Coiled coil domains: stability, specificity, and biological implications. *Chembiochem : a European journal of chemical biology*, 5(2), 170-

- Minor, D. L., Masseling, S. J., Jan, Y. N., & Jan, L. Y. (1999). Transmembrane structure of an inwardly rectifying potassium channel. *Cell*, 96(6), 879-891.
- Neyroud, N., Richard, P., Vignier, N., Donger, C., Denjoy, I., Demay, L. et al. (1999). Genomic organization of the KCNQ1 K⁺ channel gene and identification of C-terminal mutations in the long-QT syndrome. *Circulation research*, 84(3), 290-297.
- Piippo, K., Swan, H., Pasternack, M., Chapman, H., Paavonen, K., Viitasalo, M. et al. (2001). A founder mutation of the potassium channel KCNQ1 in long QT syndrome: implications for estimation of disease prevalence and molecular diagnostics. *Journal of the American College of Cardiology*, 37(2), 562-568.
- Potschka, M. (1987). Universal calibration of gel permeation chromatography and determination of molecular shape in solution. *Analytical biochemistry*, 162(1), 47-64.
- Schroeder, B. C., Kubisch, C., Stein, V., & Jentsch, T. J. (1998). Moderate loss of function of cyclic-AMP-modulated KCNQ2/KCNQ3 K⁺ channels causes epilepsy. *Nature*, 396(6712), 687-690.
- Schwake, M., Athanasiadu, D., Beimgraben, C., Blanz, J., Beck, C., Jentsch, T. J. et al. (2006). Structural determinants of M-type KCNQ (Kv7) K⁺ channel assembly. *The Journal of neuroscience : the official journal of the Society for Neuroscience*, 26(14), 3757-3766.
- Schwake, M., Pusch, M., Kharkovets, T., & Jentsch, T. J. (2000). Surface expression and single channel properties of KCNQ2/KCNQ3, M-type K⁺ channels involved in epilepsy. *The Journal of biological chemistry*, 275(18), 13343-13348.
- Shu, W., Liu, J., Ji, H., & Lu, M. (2000). Core structure of the outer membrane lipoprotein from Escherichia coli at 1.9 Å resolution. *Journal of molecular biology*, 299(4), 1101-1112.
- Splawski, I., Shen, J., Timothy, K. W., Lehmann, M. H., Priori, S., Robinson, J. L. et al. (2000). Spectrum of mutations in long-QT syndrome genes. KVLQT1, HERG, SCN5A, KCNE1, and KCNE2. *Circulation*, 102(10), 1178-1185.
- Van Petegem, F., Clark, K. A., Chatelain, F. C., & Minor, D. L. (2004). Structure of a complex between a voltage-gated calcium channel beta-subunit and an alpha-subunit domain. *Nature*, 429(6992), 671-675.
- Wang, H. S., Pan, Z., Shi, W., Brown, B. S., Wymore, R. S., Cohen, I. S. et al. (1998). KCNQ2 and KCNQ3 potassium channel subunits: molecular correlates of the M-channel. *Science*, 282(5395), 1890-1893.
- Wehling, C., Beimgraben, C., Gelhaus, C., Friedrich, T., Saftig, P., Grötzinger, J. et al. (2007). Self-assembly of the isolated KCNQ2 subunit interaction domain. *FEBS letters*, 581(8), 1594-1598.
- Woolfson, D. N. & Alber, T. (1995). Predicting oligomerization states of coiled coils. *Protein science : a publication of the Protein Society*, 4(8), 1596-1607.

E. Figures

Figure 1. Assembly Properties of Kv7 A-Domain Tails

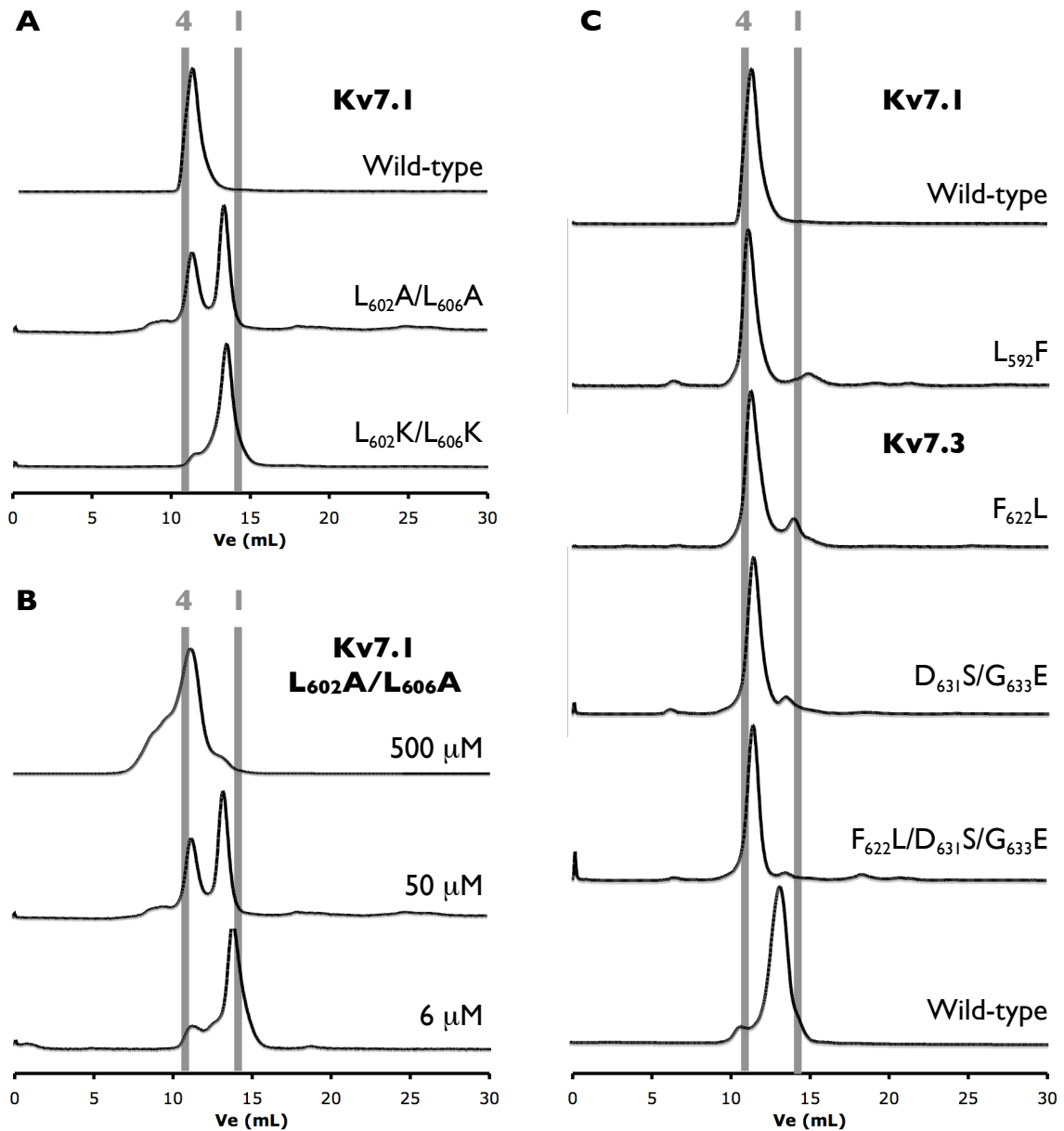


A Coiled-coil propensities of Kv7 channels based on the MultiCoil algorithm (Wolf *et al.*, 1997). A-domain Tails are aligned under the horizontal bar (—). (Inset: axis scales).

B Oligomerization of Kv7.3 A-domain Tails depends on equilibration time. Superdex200 size exclusion chromatography (Amersham Biosciences) of a 1 μ L sample of a fusion protein containing the Kv7.3 A-domain Tail subdomain fused to an HMT tag (van Petegem *et al.*, 2004). From top to bottom, traces represent measurements taken after 0, 1, 2, and 3 days incubating at room temperature following dilution of stock protein. Vertical gray lines indicate predicted elution volumes of tetrameric (4) and monomeric (1) fusion proteins.

C Oligomerization of Kv7.3 A-domain Tails is concentration-dependent. Size exclusion chromatography was performed as described above. From top to bottom, traces represent 444 μ M, 125 μ M, 50 μ M, and 5 μ M samples. All measurements taken after ≥ 3 days equilibration at room temperature. Markers as in **B**. (Inset: SDS-PAGE of fractions from 125 μ M sample. Elution volume of each sample indicated in mL).

Figure 2. Effect of Predicted Interface Mutations on Kv7 A-Domain Tail Oligomerization

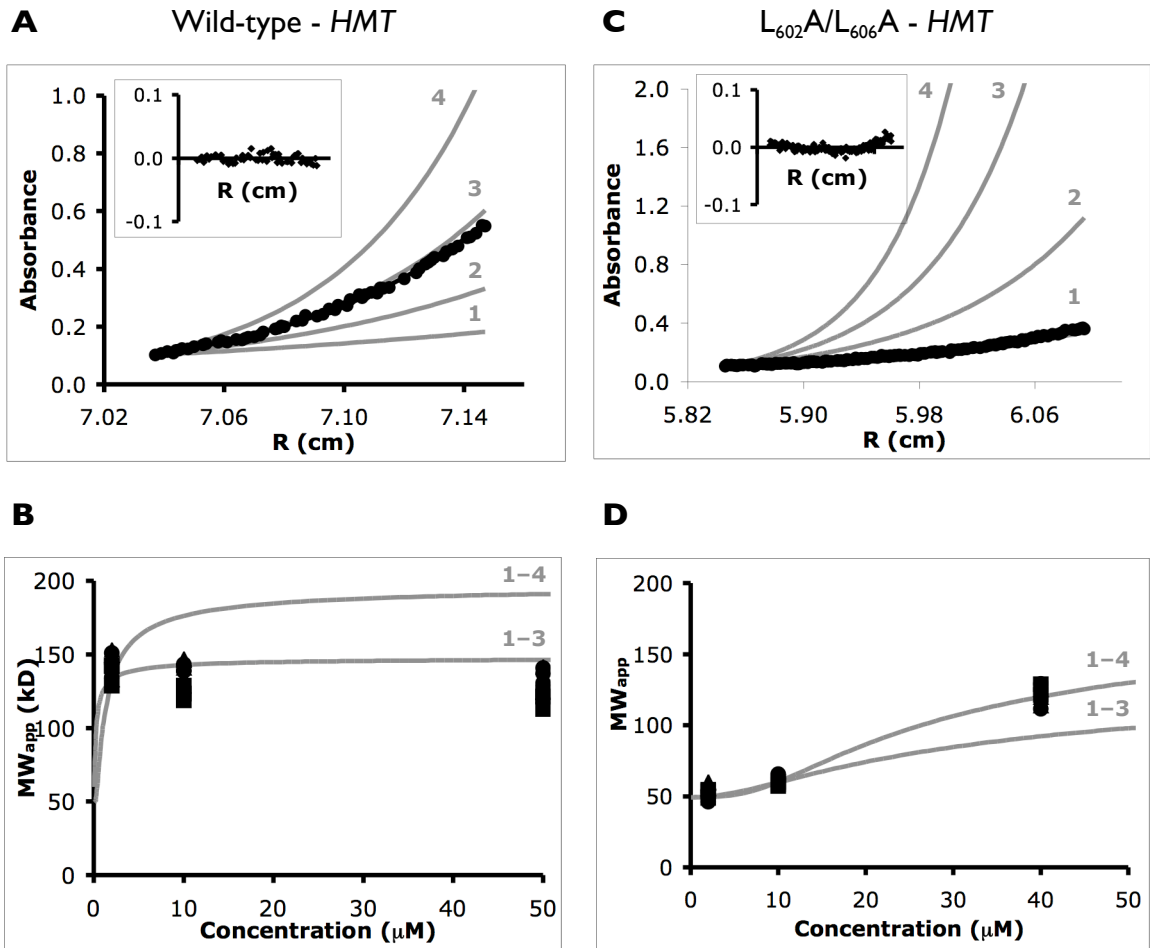


A Stoichiometry of A-domain Tail assembly in 50 μM wild-type and mutant Kv7.1 HMT-fusion proteins shown by Superdex200 (Amersham Biosciences) size exclusion chromatography. From top to bottom, traces represent Kv7.1 wild-type, L₆₀₂A/L₆₀₆A, and L₆₀₂K/L₆₀₆K mutant fusion proteins.

B Assembly of Kv7.1 A-domain Tail L₆₀₂A/L₆₀₆A mutant is concentration-dependent as shown by size exclusion chromatography, described above. From top to bottom, traces represent 500 μM, 50 μM, and 6 μM samples.

C Stoichiometry of 50 μM wild-type and mutant Kv7.3 A-domain Tail HMT-fusion proteins shown by size exclusion chromatography as described above. From top to bottom, traces represent wild-type Kv7.1, Kv7.1 L₅₉₂F, Kv7.3 F₆₂₂L, Kv7.3 D₆₃₁S/G₆₃₃E, Kv7.3 F₆₂₂L/D₆₃₁S/G₆₃₃E, and Kv7.3 wild-type constructs.

Figure 3. Sedimentation Equilibrium of Kv7.1 Wild-Type and Interface Mutant Proteins



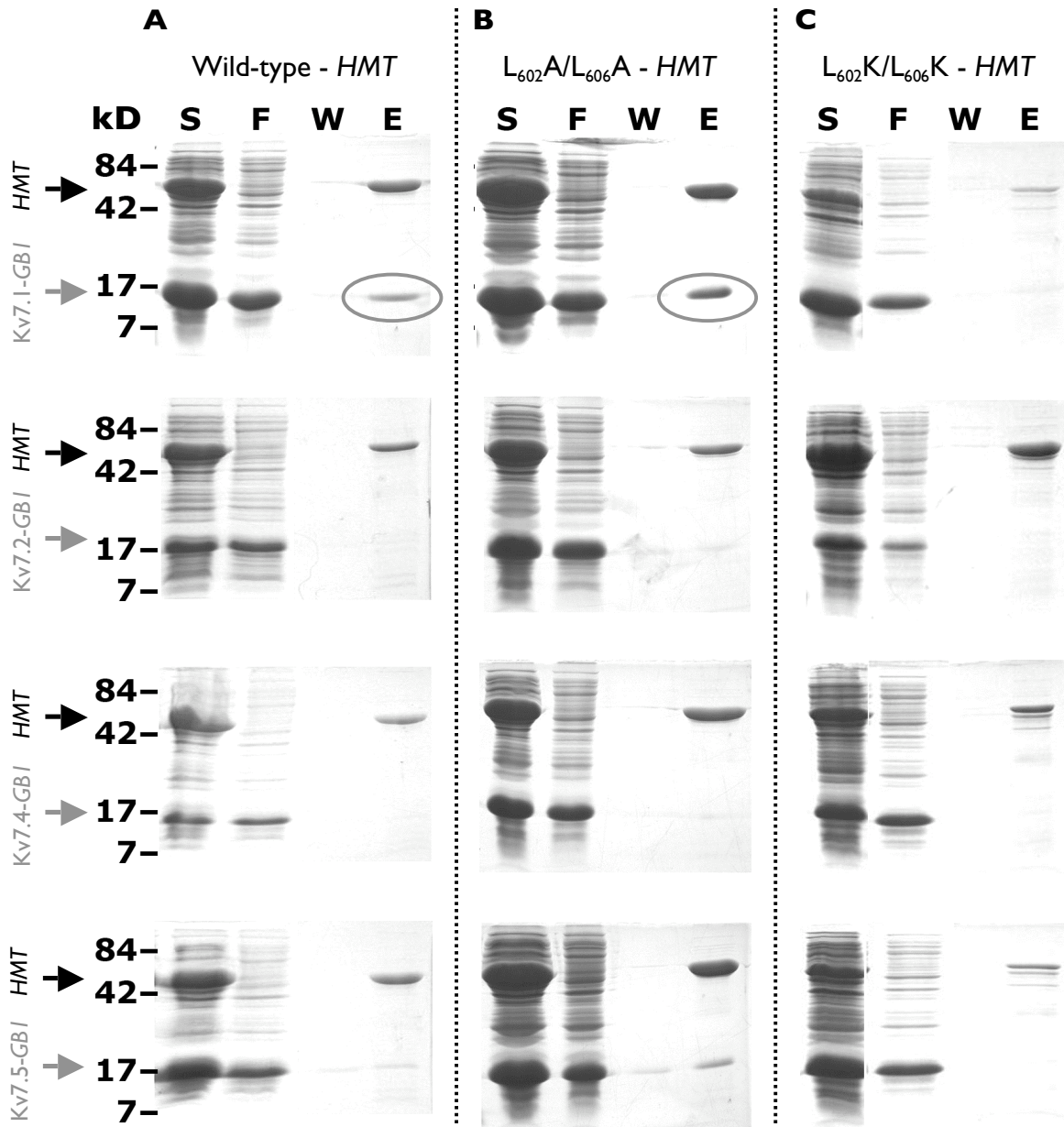
A Equilibrium distribution of 2 μM wild-type Kv7.1 residues 583–623 fused to an HMT affinity tag (van Petegem *et al.*, 2004) (circles) measured by its absorbance at 241 nm is plotted as a function of radial distance at 11,000 rpm at 4°C. Raw data shown relative to predicted curves for tetrameric (4), trimeric (3), dimeric (2), and monomeric (1) species. (Inset: distribution of residuals as a function of radial distance).

B Apparent molecular weight of Kv7.1 at 2 μM, 10 μM, and 50 μM initial concentrations measured by sedimentation equilibrium plotted relative to predicted apparent molecular weights of a monomer-tetramer equilibrium, $K_D = 2 \mu\text{M}$ (1-4), and a monomer-trimer equilibrium, $K_D = 50 \text{ nM}$ (1-3), each adjusted for partial nonideality to fit the measured values. Measurements recorded at 6,000 (▲), 8,000 (●), and 11,000 rpm (■) at 3 wavelengths each.

C Equilibrium distribution of 2 μM Kv7.1 L₆₀₂A/L₆₀₆A mutant measured at 234 nm at 11,300 rpm. (Inset: distribution of residuals versus radial distance).

D Apparent molecular weight of Kv7.1 L₆₀₂A/L₆₀₆A at 2 μM, 10 μM, and 40 μM plotted relative to predicted monomer-tetramer equilibrium, $K_D = 40 \text{ mM}$ (1-4), and monomer-trimer equilibrium, $K_D = 2 \text{ mM}$ (1-3). Measurements recorded at 8,000 (▲), 11,300 (●), and 13,800 rpm (■) at 3 wavelengths each.

Figure 4. Effect of Interface Mutations on Pull-Down of Isolated Kv7.1 A-Domain Tails



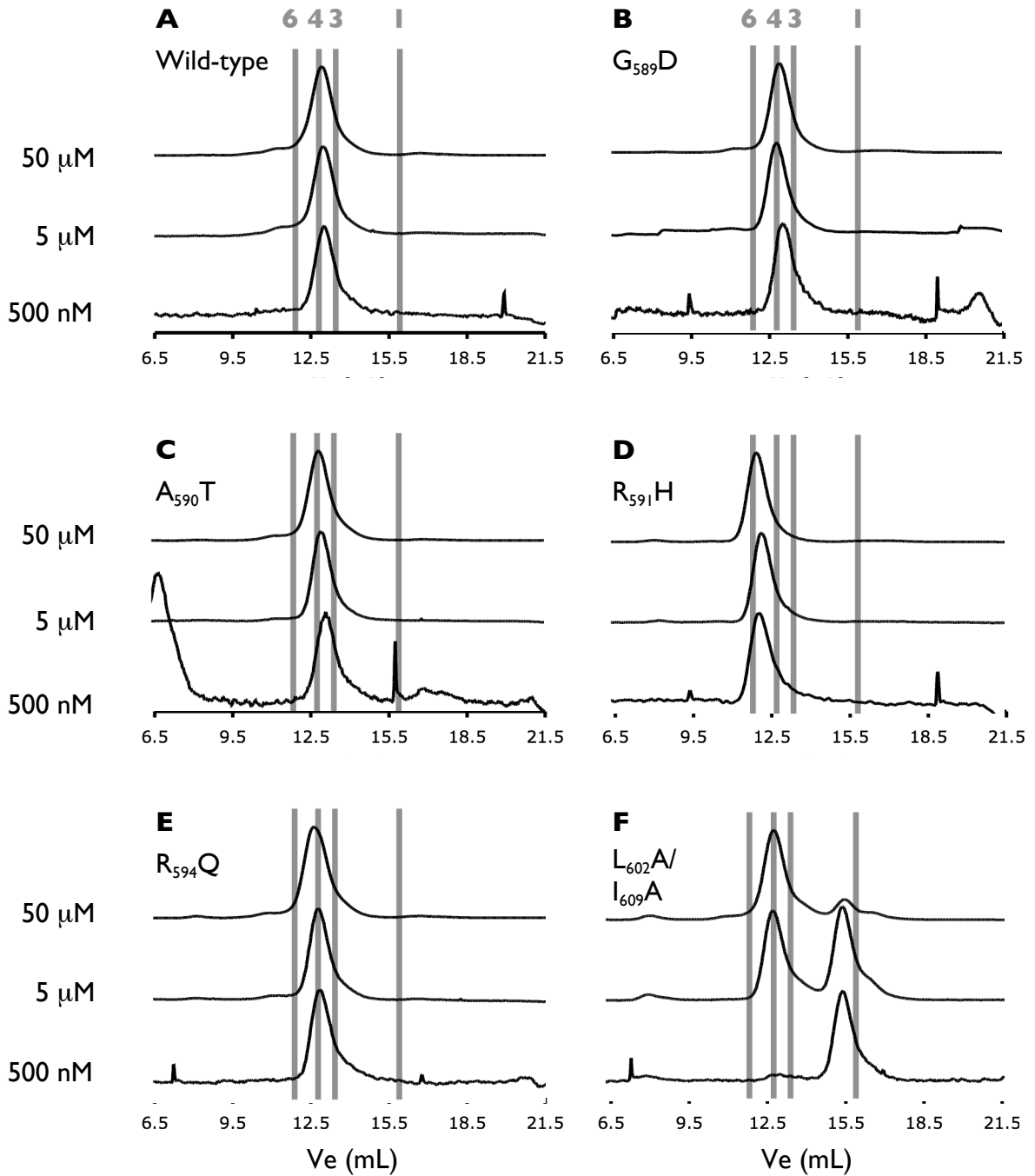
Copurification by Co^{2+} affinity of Kv7.1 wild-type HMT-fusion proteins. Wild-type or mutant Kv7.1 A-domain Tail peptide fused to the HMT tag (black arrows) was coexpressed in *E. coli* with the Kv7.1, Kv7.2, Kv7.4, or Kv7.5 Tail fused to a GBI tag (gray arrows). S, soluble fraction of crude cell lysate; F, flow-through from Co^{2+} affinity column; W, final column wash; E, imidazole elution. Positive copurifications, in which GBI-fusion proteins appear clearly in elution but not in final wash, are circled. Molecular weight standards indicated by kD at left.

A Copurification with wild-type Kv7.1 HMT-fusion protein.

B Copurification with Kv7.1 $\text{L}_{602}\text{A}/\text{L}_{606}\text{A}$ mutant HMT-fusion protein.

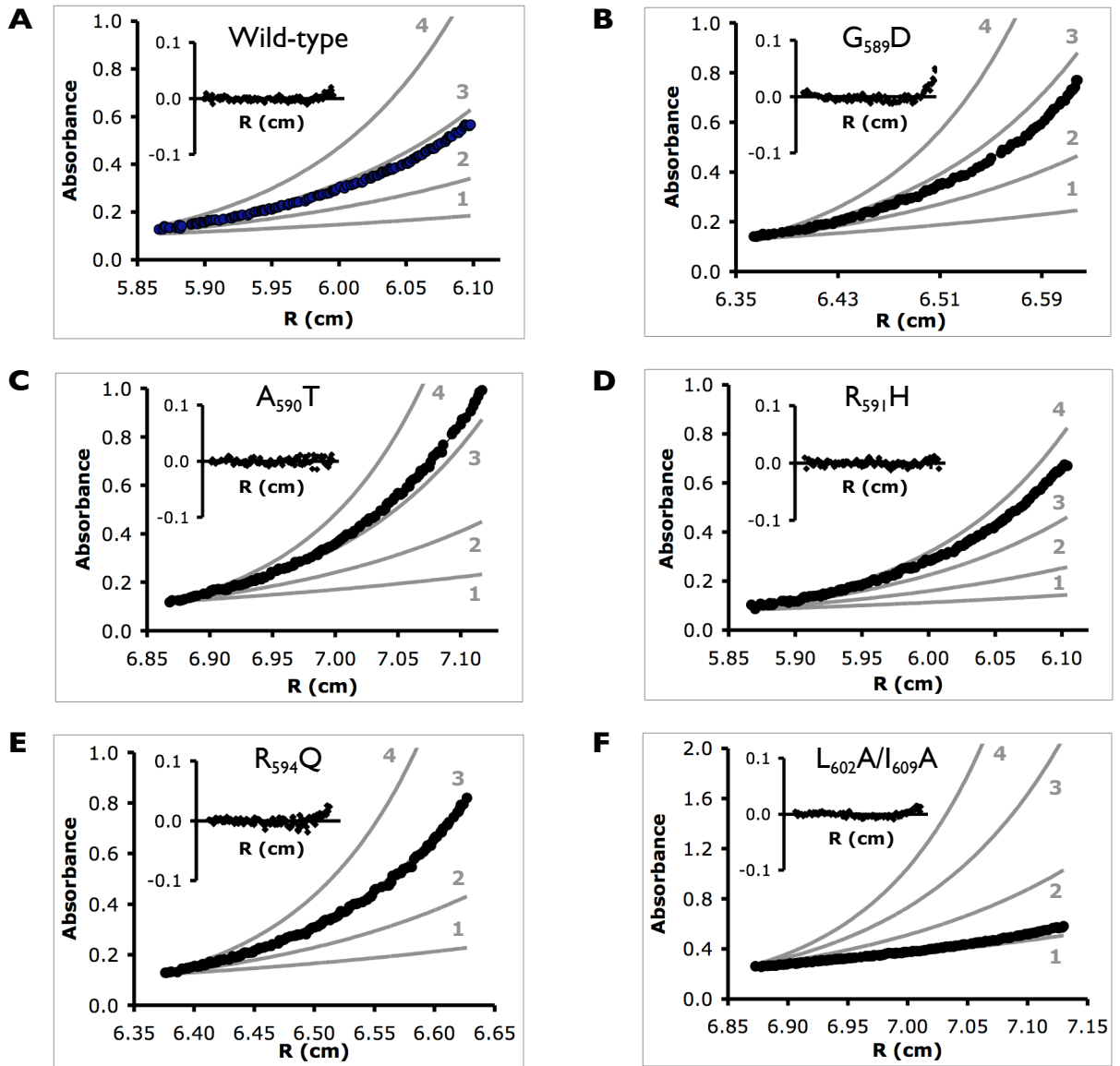
C Copurification with Kv7.1 $\text{L}_{602}\text{K}/\text{L}_{606}\text{K}$ mutant HMT-fusion protein.

Figure 5. Effect of Kv7.1 LQTS Mutations on A-domain Tail Oligomerization



Superdex200 (Amersham Biosciences) size exclusion chromatography of Kv7.1 HMT-fusion proteins. In each chart, top trace was measured at 50 μM initial concentration; middle trace at 5 μM; bottom trace at 500 nM. Vertical gray lines indicate predicted elution volumes of hexamer (6), tetramer (4), trimer (3), and monomer (1) complexes. **A** Wild-type Kv7.1 A-domain Tail HMT-fusion protein; **B** G₅₈₉D; **C** A₅₉₀T; **D** R₅₉₁H; **E** R₅₉₄Q; **F** L₆₀₂A/I₆₀₉A.

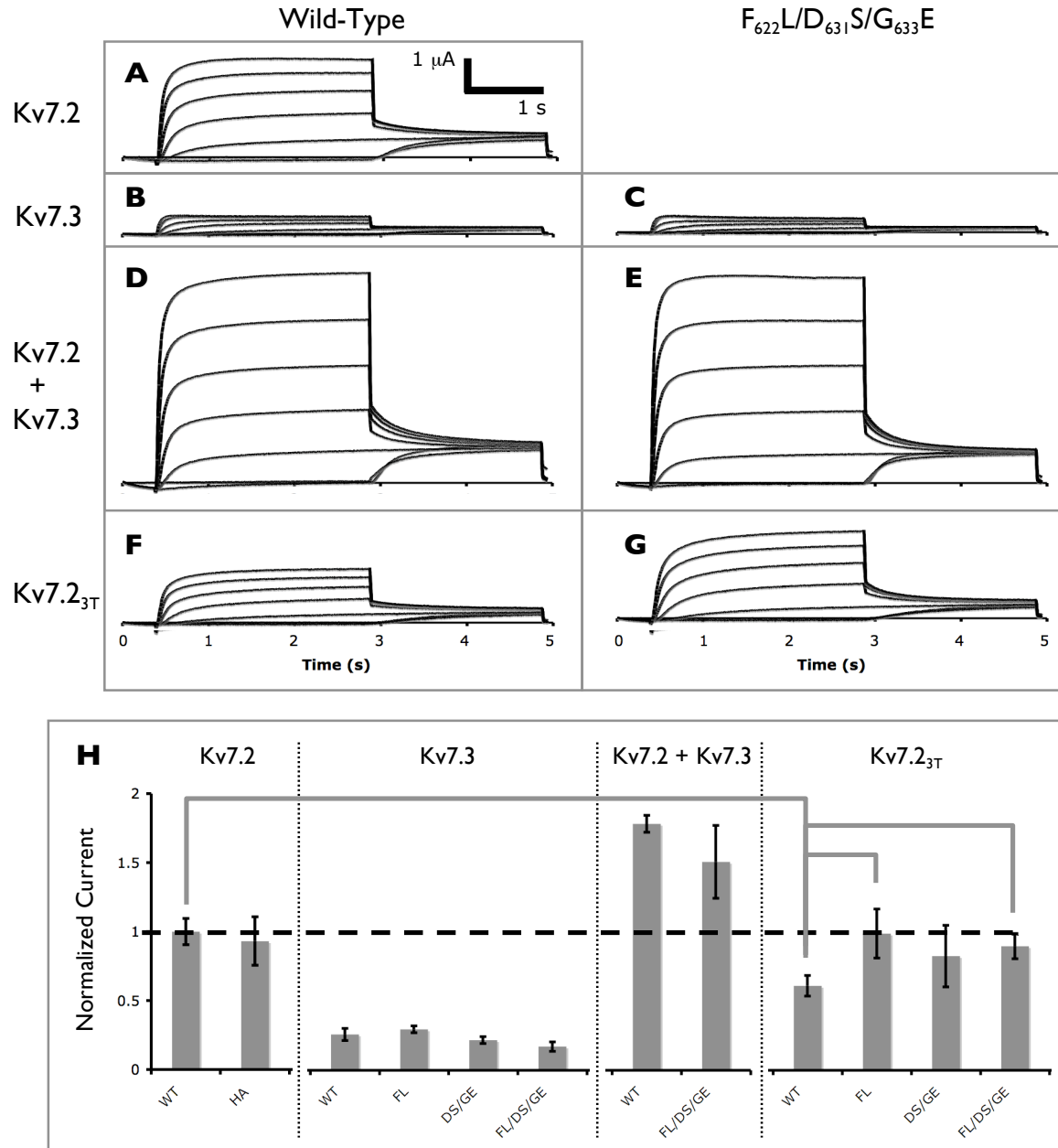
Figure 6. Sedimentation Equilibrium of Kv7.1 A-Domain Tails with LQTS Mutations



Equilibrium distributions of 5 μ M wild-type and mutant Kv7.1 residues 587–623 fused to HMT tags (circles) measured by their absorbances at 285 nm are plotted as functions of radial distance at 8,000 rpm at 4°C. Raw data shown relative to predicted curves for tetrameric (4), trimeric (3), dimeric (2), and monomeric (1) species. (Inset): Distributions of residuals as functions of radial distance.

A Wild-type Kv7.1 A-domain Tail HMT-fusion protein; **B** G₅₈₉D; **C** A₅₉₀T; **D** R₅₉₁H; **E** R₅₉₄Q; **F** L₆₀₂A/I₆₀₉A.

Figure 7. Effect of Interface Mutations on Kv7.2, Kv7.3, and Kv7.2_{3T} Chimera Currents



A–G Example current recordings from oocytes injected with cRNAs of: **A** Kv7.2 (Inset: axes scales), **B** Kv7.3, **C** Kv7.3 $F_{622}L/D_{631}S/G_{633}E$, **D** Kv7.2 + Kv7.3, **E** Kv7.2 + Kv7.3 $F_{622}L/D_{631}S/G_{633}E$, **F** Kv7.2_{3T}, **G** Kv7.2_{3T} $F_{622}L/D_{631}S/G_{633}E$. **H** Mean current amplitudes at the end of a 2.5 s test pulse to +40 mV from oocytes injected with cRNAs as indicated ($n \geq 5$ oocytes for each column). Currents normalized to average Kv7.2 current level, indicated by dashed line. Error bars represent standard error. Gray brackets indicate a subset of statistically significant differences (p-value < 0.05). WT, wild-type; HA, wild-type with extracellular HA tag; FL, $F_{622}L$ mutant channels; DS/GE, $D_{631}S/G_{633}E$ mutant channels; FL/DS/GE, $F_{622}L/D_{631}S/G_{633}E$ mutant channels.

CONCLUSIONS AND FUTURE DIRECTIONS

A. The Kv7 A-Domain Tail in Context

This thesis outlines the biochemical and structural properties of a classic coiled-coil motif found in the C-terminus of voltage-gated Kv7 K⁺ channels. We have solved the structure of this motif, the Tail subdomain of the Kv7 A-domain, from Kv7 subtype 4. Biochemical and structural data indicate the Tail subdomain is a self-assembling oligomer in all Kv7 subtypes, though its assembly affinity varies. By structure-based prediction and mutational analysis, we have demonstrated the role of several critical interface residues in A-domain Tail assembly. We have also begun to characterize the impact of certain interaction sites in the function of full-length Kv7 channels.

Continued investigation of the Kv7 A-domain Tail may prove particularly fruitful with respect to modulation by accessory proteins. The A-domain Tail is located in an extended region of the Kv7 C-terminus that is implicated in regulation by several factors, including PIP₂, CaM, and AKAPs (Zhang *et al.*, 2003; Higashida *et al.*, 2005; Robbins *et al.*, 2006). In some cases, the A-domain Tail may be proximal to a site of interaction, such that proper A-domain assembly could support a correctly folded binding site. In other cases, it may interact directly with modulatory proteins (Marx *et al.*, 2002; Kanki *et al.*, 2004). We have proposed that a cluster of disease-linked mutations in Tail subdomain of Kv7.1 causes arrhythmia by interfering with normal binding of the scaffolding protein yotiao (Howard *et al.*, 2007). Yotiao is a large, multifunctional protein whose structure is poorly characterized (Lin *et al.*, 1998).

Dissecting the Kv7.1-binding domain of yotiao would provide a critical model for AKAP interaction with an ion channel, and could be highly informative as to the impact of phosphorylative regulation on Kv7 channel function and disease. Our group is continuing to pursue the identification and structural characterization of the interaction between yotiao and the Kv7.1 A-domain.

As described in Chapter 3 of this thesis, we have also begun to probe the structural basis for specificity among Kv7 channels, as determined by the A-domain Tail. The precise mechanism by which Kv7.1 selects against coassembly with other subtypes remains to be demonstrated (Maljevich *et al.*, 2003; Schwake *et al.*, 2003). We also hope to resolve the paradoxical low function of Kv7.3 channels with their striking enhancement of function in Kv7.2, Kv7.4, and Kv7.5 channels (Schroeder *et al.*, 1998; Wang *et al.*, 1998; Kubisch *et al.*, 1999; Lerche *et al.*, 2000; Schroeder *et al.*, 2000). We have suggested that disrupted assembly of the Kv7.3 A-domain Tail is involved in one or both of these phenomena. A likely hypothesis is that the Kv7.3 A-domain Tail folds into an alternative conformation that is not favorable to self-assembly, but which interacts with another part of Kv7.2, Kv7.4, or Kv7.5 to promote expression and function. Structural information on the homomeric and heteromeric states of the Kv7.3 A-domain Tail would be extremely informative in exploring this hypothesis.

Our investigations open several avenues to understanding the role of A-domain Tails in Kv7 channel structure and function. Our data provide the first high-resolution image of any part of a Kv7 channel. Our structure is also useful in understanding the Kv7 channel as a whole, as the A-domain is required for efficient channel assembly (Schmitt *et al.*, 2000; Schwake *et al.*, 2000). The Kv7 A-domain Tail may prove, like other coiled coils (Burkhard *et al.*, 2001) and Kv channel assembly domains (Kreusch *et*

al., 1998; Minor et al., 2000), to capable of dynamical regulation; conversely, the relatively tight twisting and canonical interface interactions found in the Kv7.4 Tail superhelix may be a useful model of constitutive coiled-coil assembly. Further elucidation of the structural and functional properties of Kv7 A-domain Tails will provide a basis for understanding Kv7 structure, new options for treatment of channel-related disorders, and a general paradigm for coiled-coil assembly in ion channels.

B. References

- Burkhard, P., Stetefeld, J., & Strelkov, S. V. (2001). Coiled coils: a highly versatile protein folding motif. *Trends in cell biology*, *11*(2), 82-88.
- Higashida, H., Hoshi, N., Zhang, J. S., Yokoyama, S., Hashii, M., Jin, D. et al. (2005). Protein kinase C bound with A-kinase anchoring protein is involved in muscarinic receptor-activated modulation of M-type KCNQ potassium channels. *Neuroscience research*, *51*(3), 231-234.
- Howard, R. J., Clark, K. A., Holton, J. M., & Minor, D. L. (2007). Structural insight into KCNQ (Kv7) channel assembly and channelopathy. *Neuron*, *53*(5), 663-675.
- Kanki, H., Kupersmidt, S., Yang, T., Wells, S., & Roden, D. M. (2004). A structural requirement for processing the cardiac K⁺ channel KCNQ1. *The Journal of biological chemistry*, *279*(32), 33976-33983.
- Kreusch, A., Pfaffinger, P. J., Stevens, C. F., & Choe, S. (1998). Crystal structure of the tetramerization domain of the Shaker potassium channel. *Nature*, *392*(6679), 945-948.
- Kubisch, C., Schroeder, B. C., Friedrich, T., Lütjohann, B., El-Amraoui, A., Marlin, S. et al. (1999). KCNQ4, a novel potassium channel expressed in sensory outer hair cells, is mutated in dominant deafness. *Cell*, *96*(3), 437-446.
- Lerche, C., Scherer, C. R., Seeböhm, G., Derst, C., Wei, A. D., Busch, A. E. et al. (2000). Molecular cloning and functional expression of KCNQ5, a potassium channel subunit that may contribute to neuronal M-current diversity. *The Journal of biological chemistry*, *275*(29), 22395-22400.
- Lin, J. W., Wyszynski, M., Madhavan, R., Sealock, R., Kim, J. U., & Sheng, M. (1998). Yotiao, a novel protein of neuromuscular junction and brain that interacts with specific splice variants of NMDA receptor subunit NR1. *The Journal of neuroscience : the official journal of the Society for Neuroscience*, *18*(6), 2017-2027.
- Maljevic, S., Lerche, C., Seeböhm, G., Alekov, A. K., Busch, A. E., & Lerche, H. (2003). C-terminal interaction of KCNQ2 and KCNQ3 K⁺ channels. *The Journal of physiology*, *548*(Pt 2), 353-360.
- Marx, S. O., Kurokawa, J., Reiken, S., Motoike, H., D'Armiento, J., Marks, A. R. et al. (2002). Requirement of a macromolecular signaling complex for beta adrenergic receptor modulation of the KCNQ1-KCNE1 potassium channel. *Science (New York*,

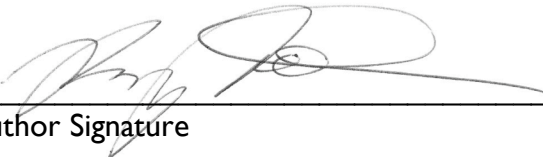
- N.Y.), 295(5554), 496-499.
- Minor, D. L., Lin, Y. F., Mobley, B. C., Avelar, A., Jan, Y. N., Jan, L. Y. et al. (2000). The polar TI interface is linked to conformational changes that open the voltage-gated potassium channel. *Cell*, 102(5), 657-670.
- Robbins, J., Marsh, S. J., & Brown, D. A. (2006). Probing the regulation of M (Kv7) potassium channels in intact neurons with membrane-targeted peptides. *The Journal of neuroscience : the official journal of the Society for Neuroscience*, 26(30), 7950-7961.
- Schmitt, N., Schwarz, M., Peretz, A., Abitbol, I., Attali, B., & Pongs, O. (2000). A recessive C-terminal Jervell and Lange-Nielsen mutation of the KCNQ1 channel impairs subunit assembly. *The EMBO journal*, 19(3), 332-340.
- Schroeder, B. C., Hechenberger, M., Weinreich, F., Kubisch, C., & Jentsch, T. J. (2000). KCNQ5, a novel potassium channel broadly expressed in brain, mediates M-type currents. *The Journal of biological chemistry*, 275(31), 24089-24095.
- Schroeder, B. C., Kubisch, C., Stein, V., & Jentsch, T. J. (1998). Moderate loss of function of cyclic-AMP-modulated KCNQ2/KCNQ3 K⁺ channels causes epilepsy. *Nature*, 396(6712), 687-690.
- Schwake, M., Jentsch, T. J., & Friedrich, T. (2003). A carboxy-terminal domain determines the subunit specificity of KCNQ K⁺ channel assembly. *EMBO reports*, 4(1), 76-81.
- Schwake, M., Pusch, M., Kharkovets, T., & Jentsch, T. J. (2000). Surface expression and single channel properties of KCNQ2/KCNQ3, M-type K⁺ channels involved in epilepsy. *The Journal of biological chemistry*, 275(18), 13343-13348.
- Wang, H. S., Pan, Z., Shi, W., Brown, B. S., Wymore, R. S., Cohen, I. S. et al. (1998). KCNQ2 and KCNQ3 potassium channel subunits: molecular correlates of the M-channel. *Science (New York, NY)*, 282(5395), 1890-1893.
- Zhang, H., Craciun, L. C., Mirshahi, T., Rohács, T., Lopes, C. M., Jin, T. et al. (2003). PIP(2) activates KCNQ channels, and its hydrolysis underlies receptor-mediated inhibition of M currents. *Neuron*, 37(6), 963-975.

Publishing Agreement

It is the policy of the University to encourage the distribution of all theses and dissertations. Copies of all UCSF theses and dissertations will be routed to the library via the Graduate Division. The library will make all theses and dissertations accessible to the public and will preserve these to the best of their abilities, in perpetuity.

Please sign the following statement:

I hereby grant permission to the Graduate Division of the University of California, San Francisco to release copies of my thesis or dissertation to the Campus Library to provide access and preservation, in whole or in part, in perpetuity.



Author Signature

4 Jan 2008

Date

This page must be signed and dated by the author and include the correct pagination.